A STUDY OF THE CARBON-OXYGEN REACTION IN LIQUID STEEL

Thesis submitted

to the University of Glasgow for the

Degree of Doctor of Philosophy

by

WILLIAM M. MILTON, B.Sc., A.R.T.C.

August 1958.

C O N T E N T S.

CHAPTER I.

INTRODUCTION AND PREVIOUS WORK.

INTRODUCTION AND PREVIOUS WORK.

While many chemical reactions are involved in the manufacture of steel those upon which most attention has been focussed are concerned with the elimination of carbon. This is not difficult to understand as, particularly in the open-hearth process, the strong action of the boil promotes heat transfer from the flame, scavenges the bath of troublesome gases, helps to homogenise the metal and slag and, in the basic process, increases the rate of removal of sulphur and phosphorus to the slag. Not surprisingly the work on this subject has been conducted in both laboratory and works, the results of the former, more simple systems being employed in an attempt to elucidate the much more complex state of affairs existing industrially.

Most often the removal of the carbon from a heat determines the duration of the process and, with due regard to quality, economic considerations necessitate the use of scientific knowledge to attain the highest possible rate of carbon elimination. The process is one of oxidation, calling for deoxidation of the final product and, although opinions are varied, there is every reason to believe that the history of the metal, with particular respect to its state of oxidation, will be reflected in the quality of the final product.

It is therefore most important that the factors affecting the rate of carbon removal be known so that they may be employed

to eliminate the carbon at an economic rate and, at the same time, yield a product with the best possible combination of properties.

This study was undertaken with a view to obtaining, from laboratory experiments, some information on the mechanism of the reaction and, from works trials, some proof for any theories or hypotheses resulting from the laboratory tests.

The basic reaction involved in carbon removal may be expressed by the equation.

$$\underline{C} + \underline{O} = CO(g) \qquad \ldots\ldots\ldots\ldots (1)$$

where symbols underlined represent solution in molten iron, the product of the reaction being gaseous carbon monoxide. Strictly speaking carbon dioxide is also present, the quantity, however, decreasing with increasing temperature and carbon content and being small enough to be ignored at steelmaking temperatures except at very low carbon contents.

The equilibrium constant for this reaction is given by.

$$K_1 = \frac{P_{CO}}{[a_C][a_O]}$$

where P_{CO} is the partial pressure of the carbon monoxide, and $[a_C]$ and $[a_O]$ the activities of carbon and oxygen respectively. Since commercial furnaces are operated under nearly constant atmospheric pressure it has become customary to use the expression.

$$m = [\%C][\%O]$$

which is the reciprocal of K_1 when $P_{CO} = 1$, and weight percentages of carbon and oxygen are substituted for activities.

The evaluation of this constant m, both in the laboratory and from works data, has received widespread attention. Vacher and Hamilton(1) melted iron in $CO-CO_2$ atmospheres at 1580°C and 1620°C and obtained m = 0.0025 in both cases in the carbon range 0.01 - 0.94 per cent. That temperature had little effect was substantiated by Phragmen and Kalling(2) who found it to be only

slightly higher at 1700°C than 1550°C. One of the most complete laboratory studies was that carried out by Marshall and Chipman(3) employing pressures up to 20 atmospheres and temperatures within the range 1540°C - 1700°C. These high pressures gave higher concentrations of carbon and oxygen in the metal at equilibrium, thus decreasing the experimental errors in the estimation of these elements, which errors can be considerable with the small quantities present at normal pressures. They confirmed the virtual independence of m upon temperature, expressing their results in the form:

$$\log K_1 = \frac{1860}{T} + 1.643$$

which corresponds to m = 0.0023 and 0.0026 at 1600°C and 1700°C respectively. Thus there is little to be gained in decreased carbon content by increasing the temperature of the reaction except, of course, that the rate of the reaction will increase.

Marshall and Chipman further showed that, even allowing for CO_2 formation, m was not a true constant but increased with carbon content having, for example, a value of 0.0034 at 1% carbon. In addition the "constants" for the reactions:

$$CO_2 + \underline{O} = 2CO \qquad \text{.....(2)}$$

and

$$CO + \underline{O} = CO_2 \qquad \text{.....(3)}$$

which are respectively $\frac{P^2_{CO}}{P_{CO_2}[\%C]}$ and $\frac{P_{CO_2}}{P_{CO}[\%O]}$ were both shown to vary with carbon content and Marshall and Chipman concluded that

the activities of neither carbon nor oxygen were proportional to their weight percentages. The plot of $\frac{P^2_{CO}}{P_{CO_2}}$ against carbon content gave a straight line up to about 0.5% C. but was thereafter a curve which showed that the activity of carbon increased with the carbon content. It has earlier been shown by Chipman and his co-workers(4) that iron-oxygen melts behaved ideally up to oxygen saturation so the deviation, evidenced by the lack of linearity in $\frac{P_{CO_2}}{P_{CO}[\%O]}$ must also be attributed to the presence of carbon. These authors found that the value of the equilibrium constant for equation (2) i.e., $\frac{P^2_{CO}}{P_{CO_2}[\%C]}$ for low carbon contents at 1540°C. was 430. Then at any carbon content

$$K_2 = \frac{P^2_{CO}}{P_{CO_2} f_C [\%C]} = 430 \quad \therefore \quad f_C = \frac{K_2}{430}$$

where f_C is the activity coefficient of carbon.

Their values for f_C lie very close to those of Darken(5) obtained from a theoretical study of the available equilibrium data for the reaction:

$$\underline{C} + 3Fe(liq) = \underline{Fe_3C} \qquad \ldots\ldots\ldots\ldots\ldots(4)$$

The effect of carbon on the activity coefficient of oxygen was similarly derived by Marshall and Chipman from the value of the equilibrium constant for equation (3) at zero carbon content, viz., $K_3 = 1.21$. $\therefore$ at higher carbon concentrations, the activity coefficient of oxygen is given by $f_O = \frac{K_3}{1.21}$. Another set of

f_o values may be obtained from K_1 using the values of f_c already found, the two sets being practically identical.

More recent values of f_c reported by Turkdogan et al(6) are given by the equation: $\log f_c = 0.22[\%C]$. This gives higher values than Chipman and Darken, particularly at higher carbon contents and consequently Turkdogan's values for f_o, in the derivation of which f_c is used, are smaller than those of Marshall and Chipman.

In contrast to Marshall and Chipman, Herasymenko(7) reported from a study of acid open hearth data where "equilibrium" had been attained, that carbon increased the activity of oxygen. Herasymenko claimed this since the plots of $K^o_{Mn} = \frac{[Mn][O]}{(MnO)}$ and $K^o_{Si} = [Si][O]^2$ against carbon content both decreased with increasing carbon. Using data from two heats of Bardenheuer and Thanhaiser(8) in which equilibrium had been attained, Herasymenko calculated K^o_{Mn} and K^o_{Si}, extrapolated to zero carbon and found good agreement with the results of Körber and Oelsen(9) for the pure Fe-Mn-Si-O system. Assuming $f_{Si} = 1$ he then calculated f_{Mn} to be 0.7 and f_o to be 3.4 at 1% carbon. In support of these findings Herasymenko pointed out that carbon increased the activity of sulphur and would therefore be expected to have a similar effect on oxygen on account of their chemical similarity. Other authors have, however, shown the activity coefficient of sulphur in the presence of 1% carbon to be 1.3 and, since carbon monoxide is more stable than the sulphide of carbon,

it is to be expected that f_o would be less than f_s for the same carbon content. Richardson(10) reported that there should be some association between carbon and oxygen atoms when dissolved in liquid iron but not in the case of carbon and sulphur. This seems to cast doubt upon the conclusions of Herasymenko.

A recent paper by Matoba and Banya(11) on the equilibrium between carbon and oxygen in carbon-saturated iron at temperatures from 1300°C to 1600°C. also reported that carbon markedly decreased the activity coefficient of oxygen in molten iron.

The equilibrium value of the constant m has also been derived from open-hearth data by extrapolation of the graph of m against $-\frac{d[C]}{dt}$, the rate of carbon drop, to zero rate of drop. Herty(12) and Schenck, Riess and Brüggemann(13) employing this method both obtained the value 0.0022 for the temperature range 1570°C to 1600°C and found m to increase with carbon content. A similar figure was obtained by McCutcheon and Chipman(14), in a study of the gases evolved from a rimming steel ingot during solidification, from carbon and oxygen analysis of the unsolidified portion of the ingot. The results of Herty and Schenck, Riess and Brüggemann were both inconsistent at high carbon contents and Herty's work was criticised by Sarjant(15) because of his unsatisfactory method of temperature measurement and analysis for metal oxygen content while the work of Schenck et al was criticised by McCance(16) for their failure to take into account the influence of gas oxidation via ferric oxide in the slag and the possible variations in the activity coefficients of carbon and oxygen. Nevertheless the value of 0.0039

at 1% carbon obtained by Schenck and his co-workers is close to that of 0.0034 obtained by Marshall and Chipman.

In evolving a method for the rapid determination of reactive oxygen in open-hearth steel, Mackenzie(17) used a similar equation to Schenck but different velocity constants for the forward and back reactions represented by the equation:

$$(nFe)^{++}O^{--} + C = CO + nFe \qquad \text{.....(5)}$$

since he found Schenck's constants to be unsatisfactory above 0.3% carbon. From this work Mackenzie obtained an equilibrium value of m = 0.0026 for carbon contents 0.07 to 0.7%

Numerous values for the product of carbon and oxygen during carbon removal have been reported in the literature and these are always in excess of the equilibrium value of m. McCutcheon(18), using a bomb sampling method to prevent contamination of the sample by air, found that the product varied from 0.0032 at 0.04%C to 0.0048 at 0.3% C. The range obtained by Fetters and Chipman(19), from a statistical study of data obtained from eight steel companies, was from 0.0033 at 0.05% C to 0.008 at 0.5% C. The average value of that product was expressed in the form:

$$[C][O] = 0.0028 + 0.011\,[C] \qquad \text{.....(6)}$$

Results of other workers show the same trend, namely, that while boiling, the bath contains an excess of carbon and oxygen. The excess of oxygen over that which would be in equilibrium with the carbon present at a carbon monoxide pressure of 1 atmosphere has been referred

to by Larsen(20) as $\Delta[O]$. Although this quantity varied considerably Larsen found it to assume fairly closely defined average values for specific stages of the process. Thus it had the value 0.025 - 0.035% oxygen after ore additions, 0.009 - 0.015% oxygen during a lime boil or in the presence of a bottom boil. In the absence of any such disturbing factors, in the period described by Larsen as steady state conditions, $\Delta[O]$ assumed a value between 0.015 and 0.025% oxygen. Larsen found no relation between $\Delta[O]$ and temperature, slag viscosity, manganese content of slag or metal and only a slight effect of ferrous oxide content of the slag. In fact the only variable to which the differences in $\Delta[O]$ could be attributed was the condition of the hearth, a furnace with a new bottom always giving a lower $\Delta[O]$ than one covered with lime-slag accumulations from a previous heat.

The question of the oxygen content of the bath is a very difficult one. It was originally thought that if the slag and metal were in equilibrium with respect to sulphur, phosphorus and manganese then they would also be in equilibrium with respect to oxygen. Such a view was held by Schenck(21). Fetters and Chipman and Larsen, however, have clearly shown that this is not the case, the latter showing that a simple plot of (ΣFe) or (FeO) against oxygen, i.e. total iron or ferrous oxide in the slag, rarely gave a satisfactory relationship. It has been shown by Taylor and Chipman(22), in a study of oxygen distribution between molten iron and CaO(-MgO)-FeO-SiO_2 slags, that the activity of ferrous oxide in the slag which would determine the metal oxygen content under equilibrium conditions, is by no means a

simple function of its iron content. Turkdogan and Pearson(23) have shown this to be even more true of the complex basic open-hearth slags. Basicity has a pronounced effect on the ferrous oxide activity. Maximum activity and hence maximum oxidising power is obtained from a slag in which the ratio $\frac{CaO}{SiO_2+P_2O_5}$ is such that the amount of lime present (CaO), is exactly that corresponding to ($2CaO.SiO_2+3CaO.P_2O_5$). Increase or decrease of slag basicity beyond this ratio causes a decrease in ferrous oxide activity. This effect of slag basicity has been confirmed by Fetters and Chipman(19) who found that $\frac{[FeO]}{(FeO)}$ decreased with increasing basicity.

It was shown by Larsen(20) and others that the oxygen content of the bath was always higher than that which would be in equilibrium with carbon but much lower than that which would be in equilibrium with the iron oxide of the slag. Several workers, notably Fetters and Chipman(19), Larsen(20) and Fornander(24) have shown that a plot of carbon and corresponding oxygen from open-hearth data gives a band, with fairly narrow limits, which runs parallel to and slightly higher than the carbon-oxygen equilibrium curve. This lends weight to the belief that the oxygen content of the metal is largely controlled by the carbon and that the iron content of the slag is only a secondary factor.

There are considerable differences of opinion regarding the mechanism of carbon removal. Among the earlier workers Feild (25), attempted to derive a rate equation for the elimination of carbon in the open-hearth by equating the oxygen diffusing from the slag to the

bath to that used up in oxidising carbon and metalloids. Among the criticisms levelled at Field's findings were the complexity of his equation and his omission to take account of the necessity for the reactants to diffuse to, and the products to diffuse from, the point of reaction. One of the main sources of disagreement regarding the mechanism has been the rate controlling process. Jette(26) used a similar approach to Field assuming also that the reaction between carbon and oxygen was the rate controlling step. The same assumption was made by Schenck, Riess and Brüggemann(13) who gave the rate of carbon elimination as.

$$\frac{-d[C]}{dt} = k_1 [O][C] - k_2 P_{CO} \qquad \text{.....(7)}$$

where k_1 and k_2 are the velocity constants of the forward and back reactions in equation(1), these constants being independent of temperature but varying with carbon content according to Schenck et al. Assuming the slag to consist of certain compounds of the oxides present (which compounds were dissociated to a greater or lesser extent according to the conditions), the balance being "free" oxide, Schenck(27) estimated the free ferrous oxide content of the slag and calculated the metal oxygen from this, on the further assumption that the contents of ferrous oxide in steel and slag are governed by the partition law.

$$\frac{[FeO]}{(FeO)} = L_{FeO} \qquad \text{.....(8)}$$

where [FeO] is the metal oxide and (FeO) the free ferrous oxide in the slag. Schenck used the constant determined by Körber and Oelsen(28)

for FeO-MnO slags.

$$L_{FeO} = 0.588\ 10^{-4}\ t^{\circ}C - 0.0793 \qquad \text{.....(9)}$$

Schenck's equation, (7) above, then becomes.

$$\frac{-d[C]}{dt} = k_1\ (FeO)\ L_{FeO} - k_2\ P_{co} \qquad \text{.....(10)}$$

From this he constructed a series of curves showing the slag basicity and iron content required for various rates of decarburisation at given carbon contents and temperatures. These curves showed that the rate of carbon elimination increased with carbon content, total iron content of the slag, and temperature, and decreased with increasing slag basicity. Schenck finally stated that the reaction between carbon and oxygen took place mainly in the metal bath at the slag-metal interface, the rate of this reaction controlling the rate of carbon elimination in steelmaking and these two statements form the basis for the main criticism of his theory despite the fact that his calculated rates of carbon drop compare favourably with observed values. If the reaction is a volume zone one, occurring within the metal phase, then it should be extremely rapid at steelmaking temperatures unless the activation energy is very high, e.g., in excess of 100 Kg.cals/gm.mol. Goodeve(29) pointed out that such values are rarely met in ordinary chemical reactions and Vallet(30) has calculated the energy of activation to be of the order of 29 Kg.cals./gm.mol. If, as Schenck suggests, that the inherent rate of this reaction is the controlling factor in the speed of decarburisation then it should be directly related to the excess of reactants present. Many instances when this is not the case

have been quoted both from acid and basic open-hearth practice, e.g., Larsen(20) has quoted a five-fold variation in the rate of carbon drop for the same excess oxygen at the same carbon level. Similar observations were quoted by Körber and Oelsen(31) in laboratory experiments in glazed crucibles, the melt being capable of holding 10-15 times the equilibrium amount of carbon in molten iron containing 0.035% oxygen. This work coupled with the extreme difficulty of initiating bubble formation within a homogeneous phase has led to the largely accepted theory of the hearth acting as a seeding ground for bubble formation. Sims(32), Ranque(33) and Richardson(34) have shown that, within the metal bath, the pressure to initiate bubble formation would require to be in excess of 60 atmospheres to overcome the surface tension forces. The hearth, as Larsen(20) pointed out, provides a source of crevices or gas filled pockets too small to permit the entry of molten metal, yet large enough to permit the entry of carbon monoxide, forming bubbles of considerably larger diameters which, when they become detached, are well able to withstand the restricting forces due to surface tension. Thus, while the pressure exerted on a bubble of 1 micron (1×10^{-3} m.m.) diameter due to surface tension forces is 60 atmospheres, that exerted on one of 1 m.m. diameter is only 0.06 atmospheres according to the equation:

$$P = \frac{2T \times 9.87 \times 10^{-7}}{r}$$ where

P = pressure in atmospheres.
T = surface tension in dynes/cm^2
r = bubble radius in cms.

Larsen's theory of carbon removal therefore involves the diffusion of oxygen across the slag-metal interface into the upper

layers of the metal from whence it is transported by convection and turbulence to the hearth where the initial bubbles are formed.

A similar theory has been proposed and considerably expanded by Vallet(30) whose final equation for the rate of carbon removal is:

$$\frac{-d[C]}{dt} = K_1' S[C] \times \Delta[O] \qquad \ldots\ldots\ldots\ldots\ldots\ldots\ldots\ldots(11)$$

where K_1' = a constant incorporating k_1 of equation (1) and other numerical constants.

$= Ae^{-E/RT}$ where A = a constant, E = activation energy of decarburisation reaction, R = perfect gas constant, and T = absolute temperature.

S = total surface area of bubbles in bath at time t.

$K_1' S$ is equivalent to the velocity constant of Schenck.

This equation differs from that of Schenck in two notable respects. Firstly the constant K_1' depends upon the temperature but is independent of the carbon content whereas the constants in the equation derived by Schenck were independent of temperature but varied with carbon content. Secondly Vallet has now introduced a new term, S, which may vary throughout the heat as well as from heat to heat. Thus an increase in $\Delta[O]$ by the addition of ore, for example, can also bring about an increase in S since smaller cavities can enter into the picture and promote the formation of bubbles.

The theory of the hearth acting as a promoter of bubbles is almost universally accepted but there is still not full agreement on either the reason for the necessity of excess oxygen in the bath or on what constitutes the rate controlling step in the process. There can be little doubt that $\Delta[O]$ is real although it has been suggested that it may be attributed to

inaccuracies in sampling and analyses. The mass of evidence in favour of the existence of $\Delta[O]$ supplied by Brower and Larsen(20),(35),(36), could hardly be attributed to such errors. The necessity for the existence of excess oxygen to maintain a boil is shown by the calculation of Richardson of the minimum [C][O] product necessary in order that the hearth crevices may act as sources of bubbles. He showed, for example, that [C][O] would require to be twice its equilibrium value for a crevice of 0.008 cm. diameter and a bath depth of 16" before bubble formation could occur. In a review of steelmaking reactions, Carter(38) states that this cannot be regarded as an entirely satisfactory explanation of $\Delta[O]$ since, while it explains why excess oxygen is required for the maintenance of a boil, it also indicates that, if the furnace bottom remains unaltered during the refining period, the minimum $\Delta[O]$ required to maintain a boil should decrease as the carbon increases which is not in accordance with the findings of Larsen that $\Delta[O]$ is independent of the carbon content.

Many attempts have been made to explain the observed values of $\Delta[O]$, the best resulting from consideration of the rate processes in carbon removal in which the steps are diffusion of oxygen from slag to metal, reaction between carbon and oxygen, bubble formation and growth of bubbles. Darken(39),(40), looked upon carbon removal as a typical steady state problem with two slow steps controlling the overall speed, the two slow steps being the diffusion of oxygen through a "dead" film of metal adjacent to the slag and through a similar film adjacent to the carbon monoxide bubbles. He deduced as a result of this the following expression for the rate of carbon removal.

$$-\frac{d[C]}{dt} = \frac{D.\Delta[O]'.12}{\ell.\Delta\ell.16}$$

where D is the diffusivity of oxygen, ℓ and $\Delta\ell$ are the bath depth and film thickness respectively and $\Delta[O]'$ is the excess oxygen of the slag over the bath. As uncertainty exists as to the true value of D, and there is no direct method available for measuring $\Delta\ell$, this expression cannot be applied quantitatively to carbon removal in the open hearth.

Similarly as the quantity S cannot be effectively measured, the theory of Vallet cannot be easily applied in practice. In this respect few equations can better that of Mackenzie(17) which may be used to calculate [O] from carbon drop or vice versa.

$$\frac{-d[C]}{dt} = 1.9\,[C][O] - 0.005\ (\%\ /\ \text{minute}) \qquad (13)$$

This has the advantage of being based on no hypothesis of the mechanism of the reaction and appeared to represent reasonably accurately what was obtained in practice.

From the above considerations of the mechanism of the reaction the most likely factors affecting its speed are those controlling the rate of supply of oxygen to the hearth together with the condition of the hearth itself. The former involves the transfer of oxygen through the slag and across the slag-metal interface. Factors affecting the movement of oxygen through the slag are likely to be slag viscosity and composition. The transfer of oxygen across the slag-metal interface has been shown by Chipman(41) to be endothermic, indicating the importance of heat transfer through the slag. The carbon-oxygen reaction itself is exothermic so the transfer of oxygen to the metal phase is the more important consideration.

Very little data on the viscosity of open-hearth slags are available although Rait, McMillan and Hay(42) have shown that silica additions to $MnO-SiO_2$ and $CaO-SiO_2$ slags increase the viscosity and fluorspar additions produce a decrease in viscosity.

The viscosity of the slag too must have an important bearing on the transfer of oxygen from the gas phase which is a very important source of oxygen, possibly the only source during steady state conditions as defined by Larsen. This oxidation may occur indirectly by the oxidation of ferrous oxide in the slag to ferric oxide, at the slag-gas interface and transference of this ferric oxide by convection currents during boiling to the slag-metal interface where it is reduced to ferrous oxide according to the equation.

$$(Fe_2O_3) + \underline{Fe} = 3(FeO).$$

This was suggested by McCance(43) and discussed in detail by Hay, Ferguson and White(44) who showed gas oxidation to be affected by slag composition, basic slags having a higher Fe_2O_3/FeO ratio than acid.

Direct gas oxidation, whereby the metal particles are actually thrown through the slag into the gas atmosphere during the boiling action, was first suggested by Whiteley and Hallimond(45) who found the metal particles in acid open-hearth slags were always lower in carbon content than the bath and in addition they absorbed ferrous oxide and transported it to the slag. Fitterer(46), investigating the feasibility of this metal particle theory, found the slag to contain about 1% of these metal particles which represented about 60 lb. of metal. Fitterer calculated that if this weight of metal passed through the slag 3 times per second then the entire reduction of carbon could be accounted for by dilution

alone and he believed that replacement at this rate was not unreasonable. No analyses for ferrous oxide content were made and therefore no estimate of the contribution to oxygen content of the bath could be made.

Like slag viscosities there is little information available about the effect of the hearth on the rate of carbon elimination. Brower and Larsen(35) have reported more rapid rates of elimination with new bottoms than with those covered with lime-slag accumulations from a previous heat. This is in contradiction to the results of Bradley and his co-workers (47), who found the boil to be less vigorous in a new basic-hearth and attributed the more rapid rates attainable with old hearths to the presence of ferrous oxide left after the previous heat.

It will be appreciated that with so many factors involved it is not surprising that no simple formula can predict carbon drop under all conditions. In the present study it is proposed to examine in the first place the rate of carbon removal in iron-carbon alloys with no slag covering and then to determine the effect of slags of varying ferrous oxide activities. Finally, it is proposed to study the factors affecting the rates of carbon removal obtained under steelmaking conditions.

CHAPTER 2.

EXPERIMENTAL PROCEDURE.

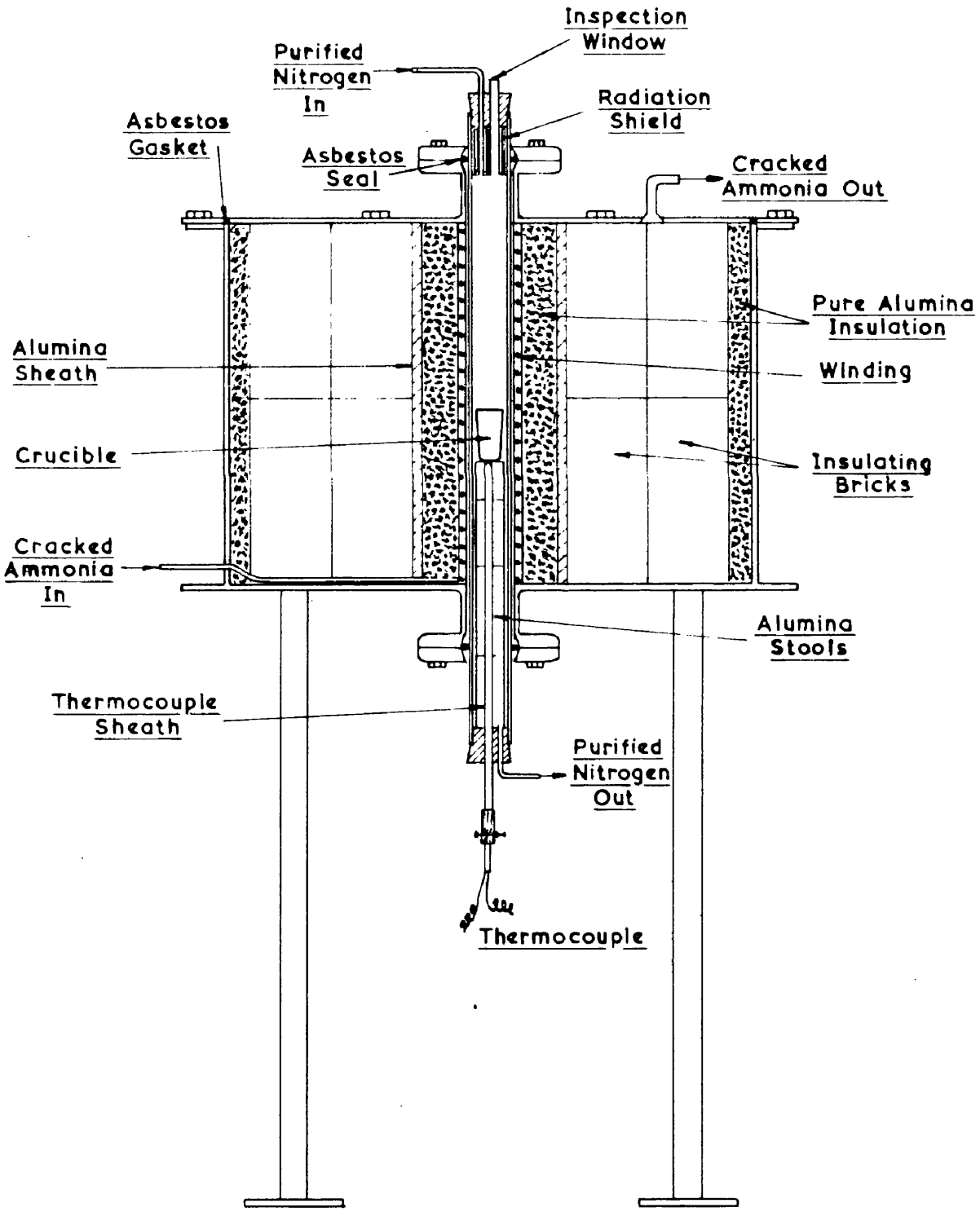

FIGURE 1.
SCALE 1"=10"

EXPERIMENTAL PROCEDURE.

Introduction.

It was proposed in the first place to investigate the effect of the type of crucible and the state of the walls on the rate of carbon drop in the presence of different slags.

However, earlier workers(48) in a study of sulphur pick up by molten iron-carbon alloys contained in magnesia crucibles under atmospheres of nitrogen and sulphur dioxide reported carbon loss in excess of the oxygen supplied by sulphur dioxide. They concluded that the loss must have come about as a result of reaction between the alloys and the crucibles as has also been indicated by Morgan and Kitchener(49).

The initial work in this study therefore was carried out without any slag additions in order to substantiate or refute these findings.

Furnace.

The runs were carried out in a conventional molybdenum furnace, shown in Figure 1, fitted with a 2 inches internal diameter furnace tube. The furnace case was gas tight, the cover being held in position by 8 bolts screwed down on an asbestos tape gasket. The furnace tube was held top and bottom by screwed metal glands packed with asbestos rope. The winding was protected by the passage of cracked ammonia through the sealed casing and the atmosphere of purified nitrogen within the furnace proper was obtained by passing commercially prepared nitrogen successively over iron turnings, copper, ferro-chromium and magnesium contained in combustion tubes in a wire-wound core furnace heated to around 600°C.

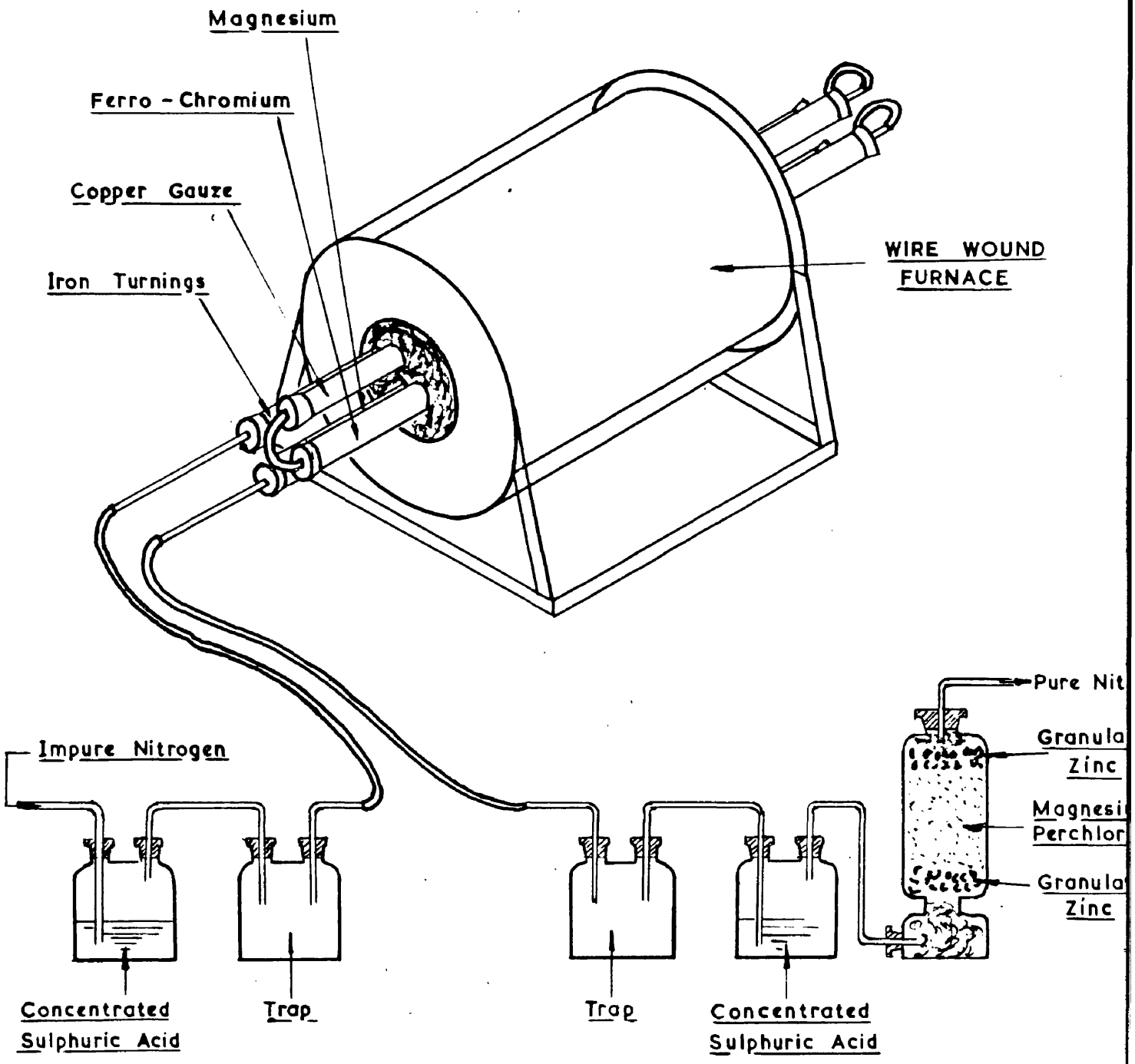

FIGURE 2

SCALE 1" ≡ 1'-0"

This purification train is shown in Figure 2. This arrangement was employed for all the work with magnesia, alundum, alumina and 1 inch diameter magnesite brick crucibles. The furnace was, wherever possible, flushed out overnight with nitrogen before heating was commenced. Where this was not possible, a rapid stream of nitrogen was passed for five minutes and then turned down to its normal rate.

Crucibles Used.

Magnesia slip-cast crucibles. These were prepared using fused magnesia ground for at least 17 hours in a rubber-lined ball mill loaded with magnesia balls. This magnesia was suspended in alcohol which was dried by the Grignard method, made up to the consistency of a very thick cream, allowed to stand for 12 hours in an airtight jar, stirred and poured into Plaster of Paris moulds, the crucible wall thickness being determined by the time in the mould.

Alundum and pure alumina crucibles. These were similarly prepared using alundum cement and fused alumina respectively, ground in a ball mill and suspended initially for 24 hours in 10% hydrochloric acid. The supernatant liquid was then poured off and the slip made to the consistency of a thick cream by the addition of water.

Magnesite brick crucibles. These were prepared by drilling 1 inch holes in fired magnesite bricks, the wall thickness being reduced by buffing to about 0.2 inch.

By firing crucibles, thus manufactured, to different temperatures, a range of surface finishes was obtained and the series was completed, in the case of the alumina crucibles, by the inclusion of a crucible

with a very smooth wall supplied by the Thermal Syndicate.

The effect of the state of the walls and the bases of the crucibles on the ease of bubble formation could be further varied by the addition to the bases of graded material of similar composition to the crucibles, this material being sintered into position before any metal was added. This was done with magnesia and magnesite brick as reported later.

Charge.

Metal charges consisted either of ingot material prepared by melting suitable proportions of Armco Iron and graphite in a refractory crucible or of weighed crucibles drilled out of Armco Iron into which were packed weighed amounts of carbon to give the desired analyses.

Temperature Measurement.

This was accomplished by Pt./Pt.Rh. thermocouples connected by suitable compensating leads to Cambridge potentiometers. For use in the molybdenum furnace the couple, in a protecting sheath, entered the bottom of the furnace tube and impinged on the base of the crucible. The accuracy of the couples was checked periodically by the determination of gold and palladium points.

Sampling and Analyses.

Metal samples were obtained by sucking into silica tubes connected to a rubber bulb. The standard procedure adopted was to immerse the tube to the bottom of the crucible and immediately plunge the sample into water when withdrawn. As mentioned later the touching of the base of the crucible with the silica tube almost invariably initiated bubble formation

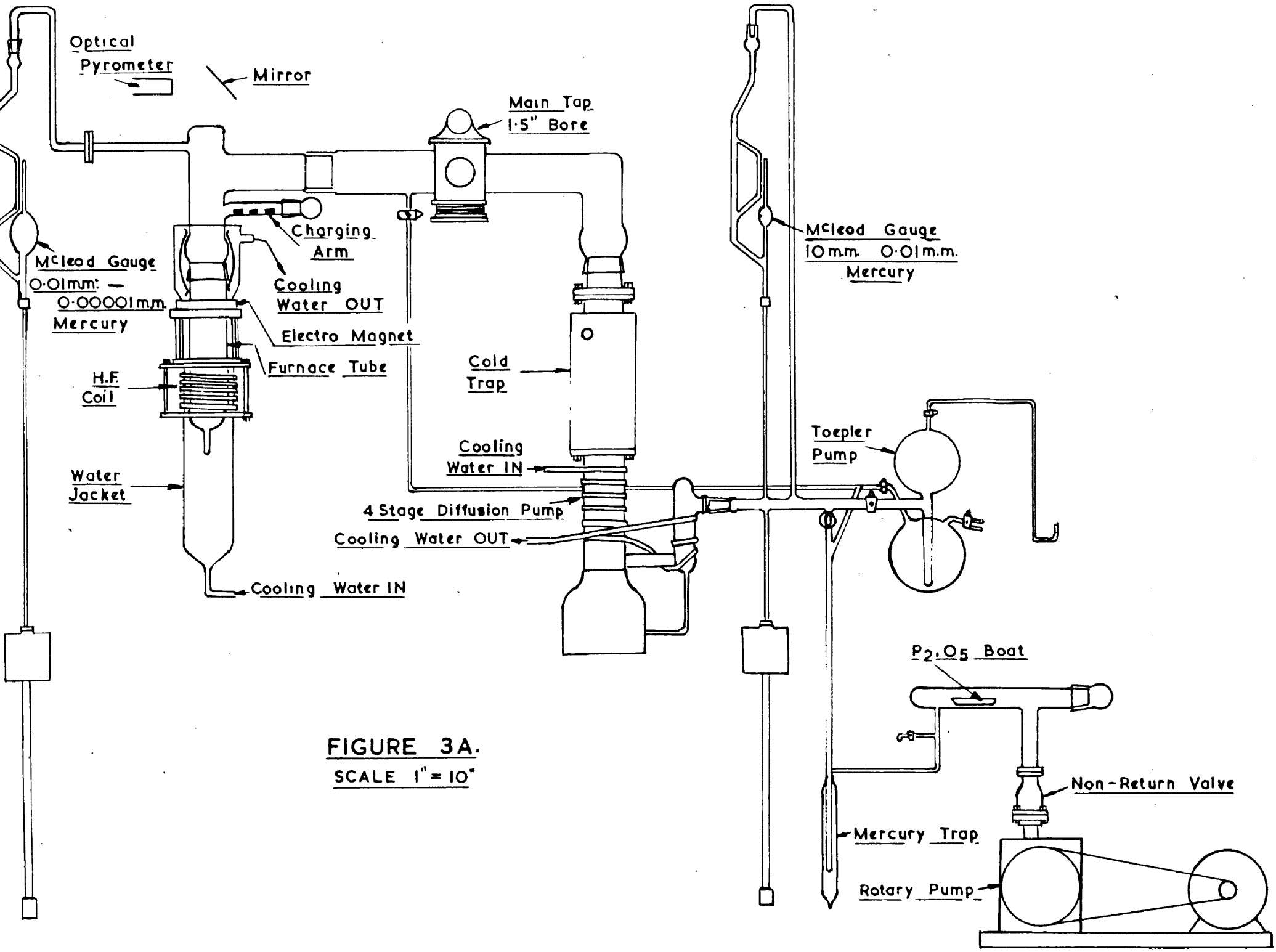

FIGURE 3A.
SCALE 1" = 10"

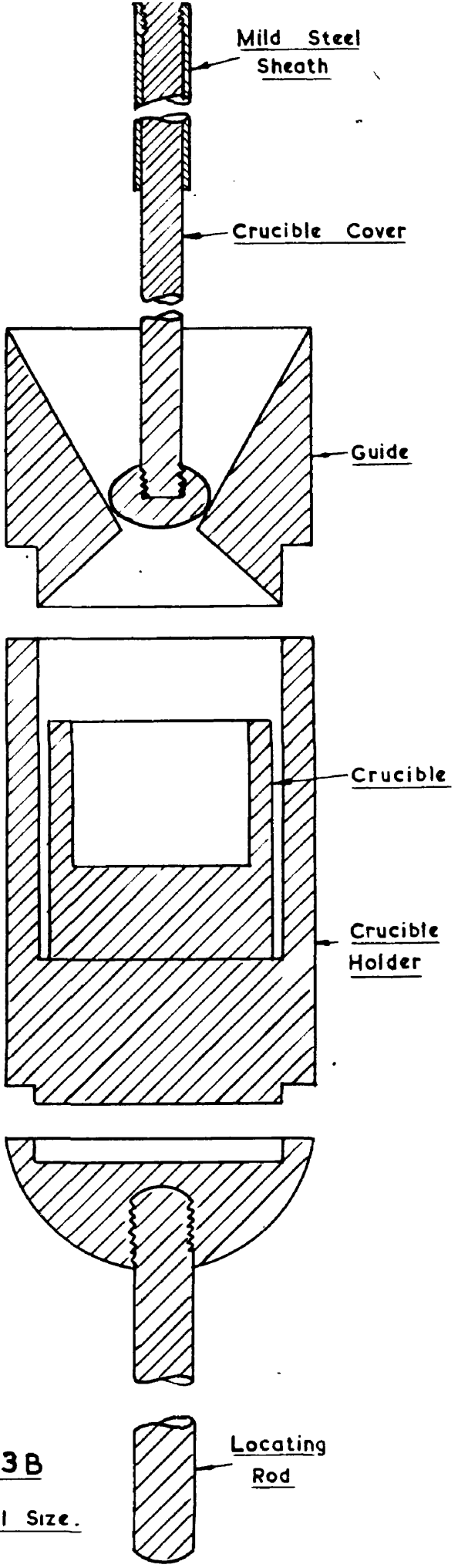

FIGURE 3B

SCALE. Full Size.

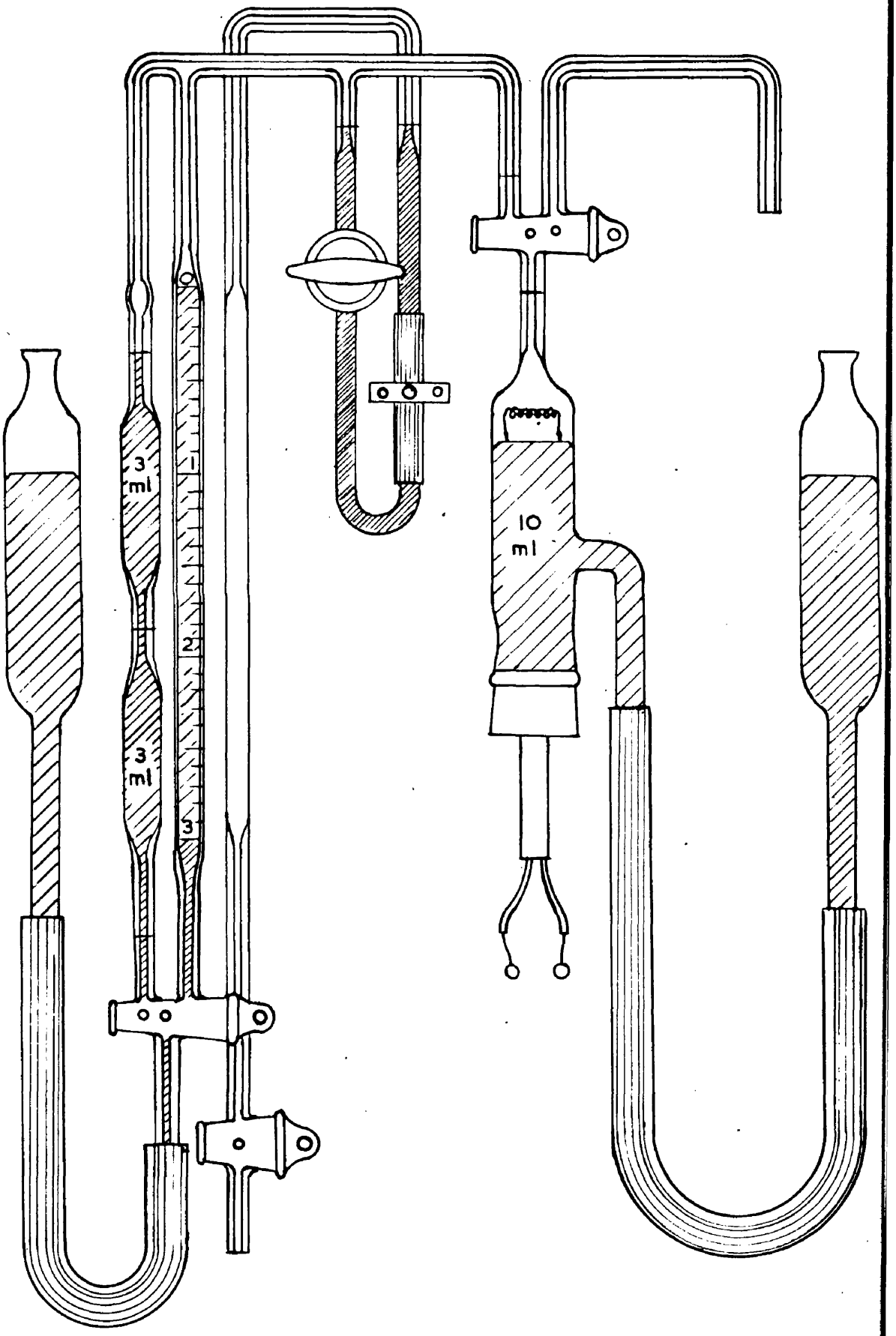

FIGURE. 4A.

SCALE 1" ≅ 2"

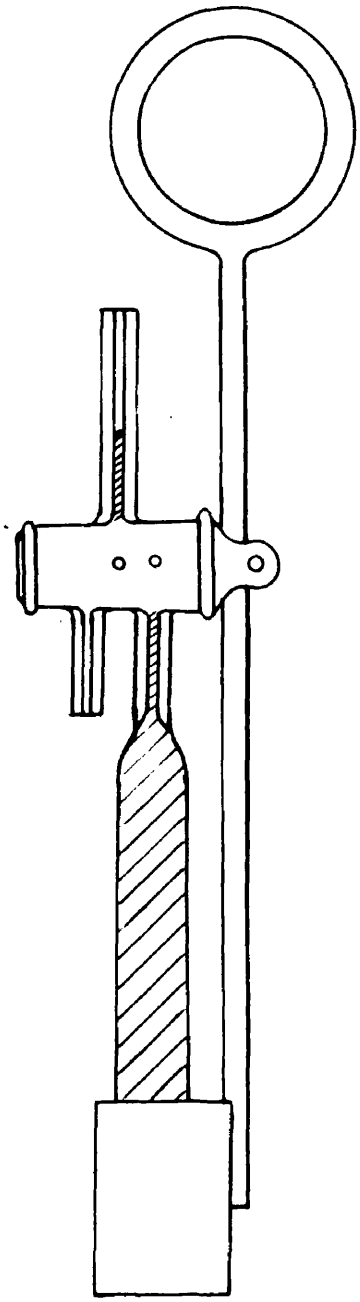

FIGURE 4B

SCALE 1" ≡ 2"

and when this had ceased the sample was drawn. If the sample were sucked up during this momentary period of gas evolution it was blown and gave bad duplicate results for oxygen content.

Carbon analyses were carried out by the usual combustion method. Oxygen analyses were obtained by the vacuum fusion method. The unit, shown in Figure 3A, is essentially the same as that described by Sloman in Special Report No.9 of the Iron and Steel Institute. The four stage mercury diffusion pump employed was an Edwards 2M4 model, fitted with a 2 inches diameter cold trap charged with solid carbon dioxide to prevent mercury vapour diffusing out of the pump into the system, and backed by an Edwards 1S 150 "Speedivac" Rotary High Vacuum Pump. The large spring loaded two-way tap between the furnace tube and the diffusion pump had a bore of 1.5 inches. The crucible assembly constructed from Acheson graphite is shown in Figure 3B.

The analysis of the gas obtained by Vacuum fusion and collected over mercury was carried out in the Sleigh Gas Analysis Unit shown in Figure 4A. This unit, designed primarily for mine gas analysis, was found to be eminently suited to the small quantities of gas evolved from the metal samples of 2-4 grammes weight. The sampling tube and holder used to transfer the tube from the Toepler Pump to the Sleigh apparatus are shown in Figure 4B.

In the earlier heats when the sampling technique had not been fully developed, the sizes of the samples drawn often did not permit the oxygen content to be determined. These runs were, however, repeated later to enable oxygen analyses to be shown with corresponding carbon contents.

CHAPTER 3.

METAL-CRUCIBLE EXPERIMENTS.

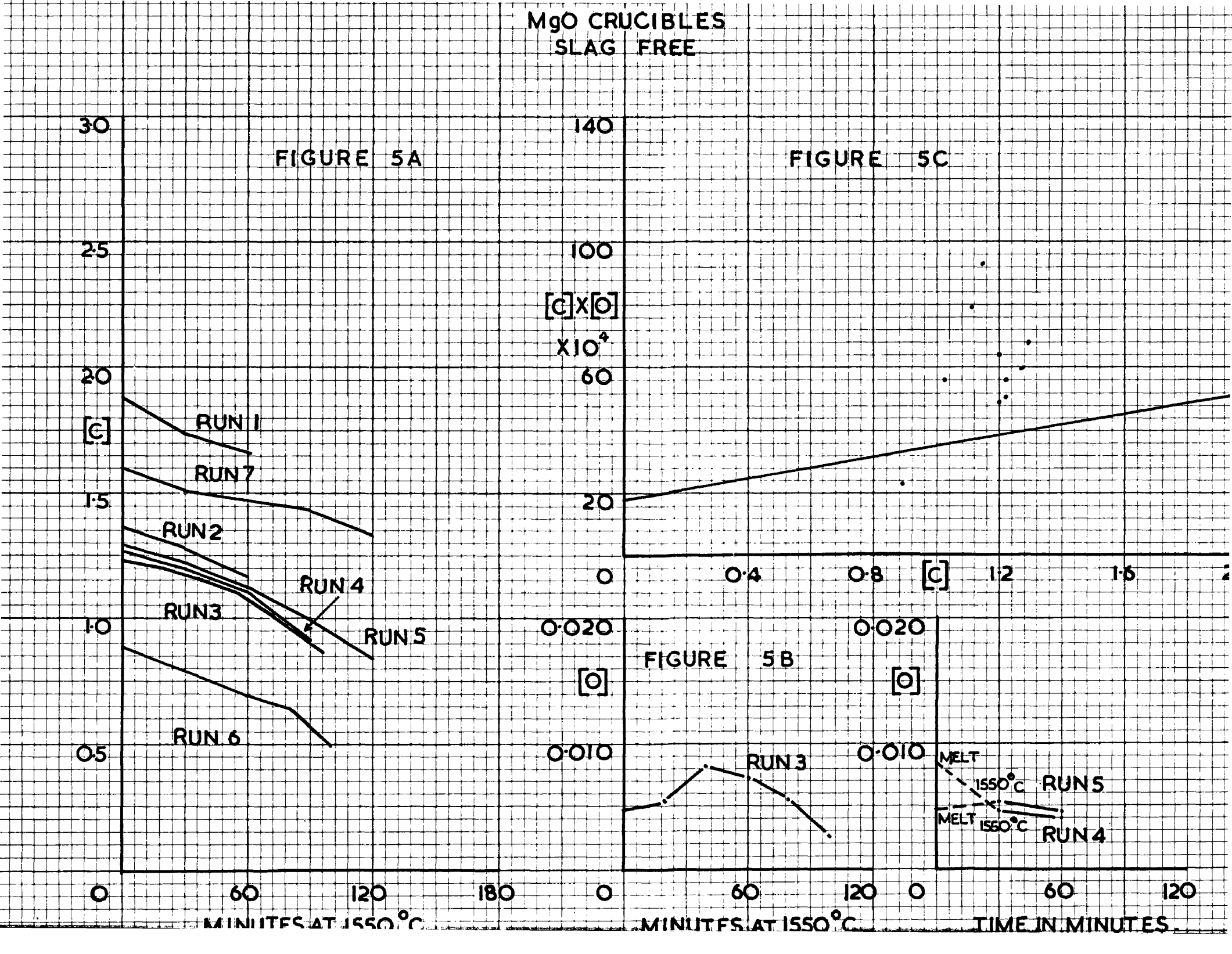
MgO CRUCIBLES
SLAG FREE
FIGURE 5A
FIGURE 5C
FIGURE 5B
[C]
RUN 1
RUN 7
RUN 2
RUN 4
RUN 3
RUN 5
RUN 6
[C]X[O]
X10⁴
[O]
MELT
1550°C
RUN 5
MELT
1550°C
RUN 4
MINUTES AT 1550°C
MINUTES AT 1550°C
TIME IN MINUTES

METAL-CRUCIBLE EXPERIMENTS.

Experiments in Slip-Cast Magnesia Crucibles.

Several runs were first carried out in magnesia slip-cast crucibles, prefired to 1600°C,in the molybdenum furnace. The graphs of carbon content against time for these runs, Nos. 1, 2, 3, 4 and 5, all conducted at 1550°C, are given in Figure 5A along with the graph for Run 6, carried out at 1600°C, to determine the effect of temperature. The oxygen contents where available are given in Figure 5B.

To determine the effect of roughening the base of the crucible by the addition of crushed and graded magnesia, heat No.7 was carried out in which 0.5 gm. -22 to +30 mesh magnesia was added to the base of the crucible and sintered into position before charging. The results of heat 7 are also graphed in Figure 5A. The analyses for all magnesia crucible runs are reported in Table I.

Discussion of Results of Magnesia Experiments.

In all the runs listed above a carbon loss was measured, the rate being fairly constant and not being noticeably affected by the addition of rougher material to the crucible base in Heat 7.

A possible source of oxidation leading to loss of carbon is by means of the air initially filling the furnace tube if this were not properly expelled. The capacity of the tubes employed would permit of their containing some 360 cubic centimeters of oxygen if no air were displaced. This quantity of oxygen is sufficient to remove approximately 0.2 gm. carbon from 100 gms. metal while the quantity actually removed often far exceeded this. Furthermore, purified nitrogen was always

TABLE I.

Reaction between Molten Iron and Magnesia Crucibles.

Heat No.	Crucible Type.	Charge.	Carbon and Oxygen Contents.	1	2	3	4	5	6
1	MgO	Fe-C Alloy [C]=2.17	[C]	1.985	1.884	1.731	1.668		
			T		0	36	66		
2	MgO	Fe-C Alloy [C]=1.844	[C]	1.461	1.355	1.265	1.153		
			T		0	30	60		
3	MgO	Armco Iron + C [C]=1.464	[C]	1.228	1.200	1.156	1.108	1.025	0.884
			[O]	0.0046	0.0053	0.0081	0.0071	0.0054	0.0027
			m	0.0056	0.0064	0.0094	0.0079	0.0056	0.0024
			T	0	20	40	60	80	100
4	MgO	Armco Iron + C [C]=1.495	[C]	1.377	1.262*	1.197	1.091	0.911	
			[O]	0.0084	0.0047	0.0040			
			m	0.0115	0.0059	0.0049			
			T		0	30	60		
5	MgO	Armco Iron + C [C]=1.474	[C]	1.371	1.287*	1.209	1.110	0.979	0.826
			[O]	0.0048	0.0053	0.0041			
			m	0.0065	0.0068	0.0050			
			T		0	30	60	90	120
6	MgO	Fe-C Alloy [C]=1.165	[C]	0.878	0.692	0.638	0.496		
			T	0	60**	80	100		
7	MgO + 0.5 gm. -22 to +30 mesh MgO	Fe-C Alloy [C]=1.748	[C]	1.685	1.60	1.505	1.428	1.330	
			T		0	30	90	120	

T = time in minutes at 1550°C.
* Melt out samples, not 1550°C.
** At 1600°C.

passed for some minutes at a rate approaching 1000 cubic centimeters/minute which alone would have replaced the furnace atmosphere several times over. The rate was then reduced to 180-200 cubic centimeters/minute and maintained at this in most cases for 12 hours before heating began. Repeated analyses of the nitrogen yielded no oxygen from this source. Analyses of exit gases from the furnace tube during heating showed these contained no oxygen so that air leakage into the system appears most improbable.

There remains the possibility of air being introduced when the furnace bung was removed to permit sampling but, as can be seen from the carbon drop curves, there is no noticeable increase in the rate of carbon elimination where sampling is more frequent. It is also possible that the air still left in the sampling tube when immersed in the metal charge is being expanded and forced out through the metal. At the worst this could only account for 0.003 gm. carbon each time which is a negligible quantity.

Figure 5A shows typical carbon drop curves for iron-carbon alloys contained in magnesia crucibles, Run 6 alone being at 1600°C, the remainder at 1550°C. While there are differences in these curves, the rate of carbon elimination is fairly constant over the normal duration of a run. The oxygen contents of the metal samples which were usually of the order of 0.004-0.005% do show some interesting fluctuations. As already stated the sampling tube was always lowered into the melt until it made contact with the crucible base. This invariably led to the evolution of gas, especially when first sampling a slag-free run, suggesting that supersaturation had existed and this was relieved by the sampling tube initiating bubble formation. This may be because (a) the fresh surface

of the silica tube is causing nucleation or (b) the touching of the base of the crucible may be sufficient to cause a "break" in the magnesia surface allowing bubble formation to take place. Whatever the real explanation, the action of the silica tube would appear to be very close to that achieved by the permanent immersion of a glass rod in a beaker of boiling liquid. In this case the point of contact between the rod and the beaker is a continuous source of bubbles. The evolution of gas caused by the silica tube was not of the same degree throughout different runs or even in the same run. Had this been the case it could have been due to the expansion of the air in the sampling tube. The effect was very momentary although, once started, it often resulted in perceptible bubble formation continuing for several minutes after the sample had been withdrawn but this only at the rate of perhaps one or two very small bubbles bursting on the surface of the melt every few seconds. At the end of this period no further gas would be perceptibly evolved until the metal was next disturbed during sampling.

The drawing of the melt sample in Run 4 led to the evolution of a much larger quantity of gas than from the second sample, while more gas was evolved during the drawing of the second sample in Run 5 than in the first one from that run. These observations are reflected in the oxygen analyses, there being more oxygen in 4(1) than in (2) and more in 5(2) than in (1). Whereas in a short time this observable evolution caused by sampling appeared tocease it is probable that gas evolution continued at a slow rate all the time. Otherwise it has to be concluded that carbon loss only occurred through the agency of gas

evolved during sampling. This state of affairs would necessitate the evolution of some 1230 cubic centimeters of carbon monoxide for the removal of 0.1% carbon from 100 grammes metal and the quantity observed to be evolved was certainly not of this magnitude. It must then be assumed that carbon monoxide was being continually removed from the surface of the melt, lack of diffusion causing supersaturation and preventing this surface reaction from going to completion, thereby leaving the metal receptive to any agency initiating bubble formation.

It might be expected that, if carbon loss were due to reaction with the crucible, the rate of loss should be constant throughout. However, it increased with time in all cases, inferring that, as the run progressed, conditions became more suited to the removal of carbon. As all crucibles were prefired to 1550°C-1600°C there should be little alteration in the state of the walls during the run and even if there were this would be expected rather to decrease the rate of carbon elimination. By removal of metal samples the ratio of surface area in contact with the crucible walls to the bulk of the metal is reduced. Furthermore, the ferrostatic head is being constantly reduced and the reduction of this would make the removal of the carbon monoxide by the surface reaction easier and it is suggested that the action is certainly between the crucible and the alloy with the following net effect.

$$MgO = Mg(vap.) + \underline{O} \quad \ldots\ldots\ldots (1)$$

$$\underline{C} + \underline{O} = CO \quad \ldots\ldots\ldots (2)$$

The first equation represents the pick up of oxygen by the molten alloy by the reaction of the molten iron with the crucible. Lack of diffusion

enables this oxygen to build up to the extent of saturation in the melt.

The first equation involves two steps, the reduction of the magnesia and the solution of the oxygen so released by the alloy contained in the crucible. The change in free energy for this reaction is given by:

$$\Delta G = +143,440 - 45.46\ T$$

At 1550°C this gives thelogarithm of the equilibrium constant of the reaction as

$$\log_{10} K = \underline{-7.25}$$

and the equilibrium constant represented by:

$$K = P_{Mg}\ [\%O]$$

then has the value $K = 5.62 \times 10^{-8}$.

Considering an oxygen content of 0.01% this gives P_{Mg} as 5.62×10^{-6} which implies that the reaction is possible provided that the solubility limit of magnesium in iron-carbon alloys corresponds to a fugacity lower than this figure. Philbrook(50) gave the solubility limit of calcium in carbon saturated alloys as less than 10^{-5} so it seems that the above limit for the solubility of magnesium is quite a probable one. The mechanism of reaction depicted by equations (1) and (2) is therefore thermodynamically possible, the magnesium vapour escaping in the gas stream wherever the solubility limit is exceeded, causing a continuous removal of carbon from the melt.

Experiments in slip-cast Alundum and Alumina Crucibles.

An investigation of the possibility of similar reactions taking place when the crucible material was alumina formed the second part of

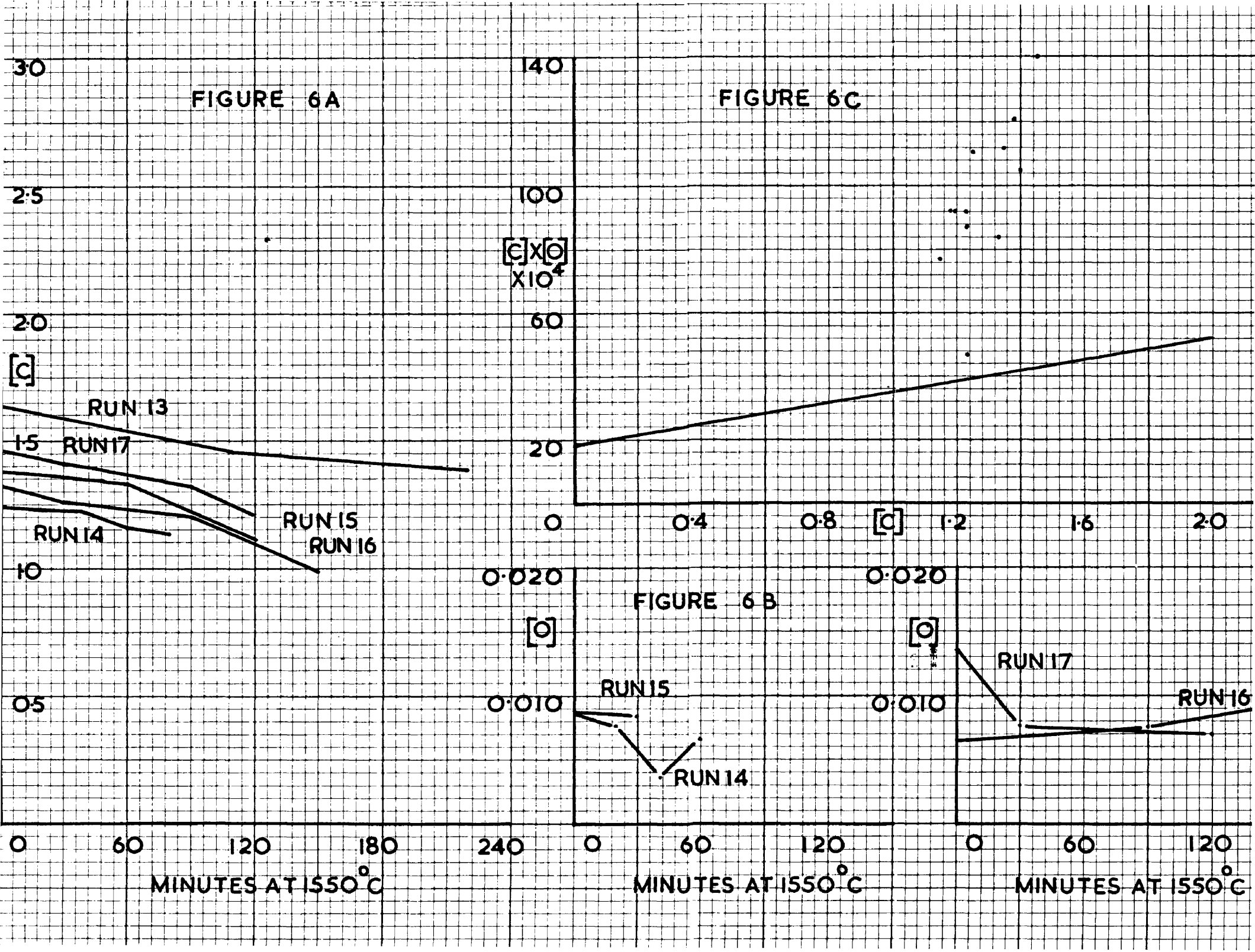
FIGURE 6A
3·0
2·5
2·0
[C]
1·5
1·0
0·5
RUN 13
RUN 17
RUN 15
RUN 16
RUN 14
0
60
120
180
240
MINUTES AT 1550°C
FIGURE 6C
140
100
[C]x[O] X10⁴
60
20
0
0·4
0·8
[C]
1·2
1·6
2·0
FIGURE 6B
0·020
[O]
0·010
RUN 15
RUN 14
0
60
120
MINUTES AT 1550°C
0·020
[O]
0·010
RUN 17
RUN 16
0
60
120
MINUTES AT 1550°C

this study. Four runs, numbers 8, 9, 10 and 11 were carried out in alundum slip-cast crucibles and sampled only at the beginning and end of the run. The crucibles for 8 and 9 were prefired to 1200°C while those for runs 10 and 11 were prefired to 1600°C. Runs 12, 13, 14, 15 and 16 were carried out in pure alumina, the first from an aerated slip fired to 1200°C and the remainder from good dense slips fired to 1600°C. In run 17 a Thermal Syndicate crucible, (T.S.530), with a very smooth wall, was used. A working temperature of 1550°C was adopted throughout.

The analyses of the samples drawn in the above runs are given in Tables II and III and the results of heats 13 to 17 inclusive are graphed in Figures 6A and 6B.

Discussion of Results in Alumina Crucibles.

There were more variables to be considered in these heats than in those carried out in magnesia crucibles, the two main ones being the chemical purity of the alumina and the physical state of the crucible walls. As with the magnesia crucibles a carbon loss was observed in all cases but this varied from heat to heat.

The experimental set up was exactly similar to that employed with the magnesia runs so the arguments put forward against the possibility of either oxygen in the furnace atmosphere or air infiltration during the runs being responsible for the carbon loss are still valid. It is probable therefore that crucible action is again responsible for the carbon loss.

TABLE 11.

Reaction between Molten Iron and Alumina Type Crucibles.

Heat No.	Crucible and Firing Temp. °C.	Charge.	Sample Analysis			Weight of Carbon lost(gms.)	Duration of Melt (Mins.at 1550°C)	Carbon loss per hour(gms.)
8	Alundum 1200	Fe-C Alloy [C]=1.980	[C]		1.608*	0.435	106	0.246
			[Al]		0.036			
9	Alundum 1200	Fe-C Alloy [C]=1.570	[C]		1.153*	0.427	155	0.165
10	Alundum 1600	Fe-C Alloy [C]=1.557	[C]		1.292*	0.263	145	0.109
			[Al]		0.20			
11	Alundum 1600	Fe-C Alloy [C]=1.745	[C]		1.351*	0.383	210	0.110
			[Al]		0.25			
12	Al_2O_3 1200	Fe-C Alloy [C]=1.685	[C]	Tr.	Tr.	0.927	525	0.106
			[Al]	0.084	0.124			
			[O]	0.110	0.122			
13	Al_2O_3 1600	Fe-C Alloy [C]=1.830	[C]	1.625	1.456 1.396	0.224	260	0.052
			[Al]	0.101	0.036 0.018			

* Denotes sample at end of heat.

TABLE III.

Reaction between Molten Iron and Alumina Crucibles.

Heat No.	Crucible	Charge		Carbon and Oxygen Contents. 1	2	3	4	5	6
14	Al_2O_3	Armco	[C]	1.244	1.230	1.226	1.152	1.137	
		Iron	[O]	0.0089	0.0075	0.0038	0.0067		
		+ C	m	0.0111	0.0092	0.0047	0.0077		
		[C]=1.497	[Al]				0.036	0.044	
			T	0	20	40	60	80	
15	Al_2O_3	Armco	[C]	1.478	1.379	1.351	1.334	1.229	1.112
		Iron	[O]	0.0108	0.0088	0.0083			
		+ C	m		0.0121	0.0112			
		[C]=1.559	[Al]	0.032		0.092	0.044	0.116	0.132
			T	0	0	30	60	90	120
16	Al_2O_3	Fe-C	[C]	1.472	1.332	1.268	1.197	0.995	
		Alloy	[O]	0.0032	0.0064		0.0077	0.0092	
			m		0.0085		0.0092	0.0092	
		[C]=1.522	T		0	30	90	150	
17	Al_2O_3	Fe-C	[C]	1.469	1.452	1.406	1.323	1.224	
	Thermal	Alloy	[O]	0.0122	0.0137	0.0074		0.0071	
	Syndicate	[C]=1.540	m		0.0199	0.0104		0.0087	
	530		T		0	30	90	120	

T = time in minutes at 1550°C.

During runs conducted in the alundum (impure alumina containing alumino-silicates) crucibles, the rates of carbon loss varied from 0.246 gm./hour in run 8 to 0.109 gm/hour in run 10. The only difference between these two heats was, as shown in Table II, that the crucible for run 8 was fired to 1200°C while that for run 10 was fired to 1600°C.

Runs 12 and 13 were both carried out in pure alumina crucibles, but the slips varied in density and the crucible for run 12 was fired to 1200°C while that for run 13 was fired to 1600°C. The two rates of carbon removal are 0.106 gm./hour and 0.052 gm/hour respectively. The results of heat 12 show that it is possible to produce a pure alumina crucible capable of removing carbon at a rate comparable with the impure ones used in runs 10 and 11 by reducing the density of the slip and prefiring to a lower temperature.

Run 12 was rather unique in respect of the oxygen and aluminium contents of the metal samples. It has always been assumed that since aluminium is a strong deoxidiser its presence in quantity would be associated with low oxygen contents. Nevertheless the two samples drawn in heat 12 had oxygen contents of 0.110% and 0.122% with corresponding soluble aluminium contents of 0.084% and 0.124%. Whereas in any case only soluble aluminium was estimated, microexamination failed to reveal any aluminous inclusions which could explain these high aluminium contents. In their work on the aluminium-oxygen equilibrium in liquid iron Gokcen and Chipman(51) found that aluminium strongly reduced the activity coefficient of oxygen and similarly oxygen reduced that of aluminium,

FIGURE 7

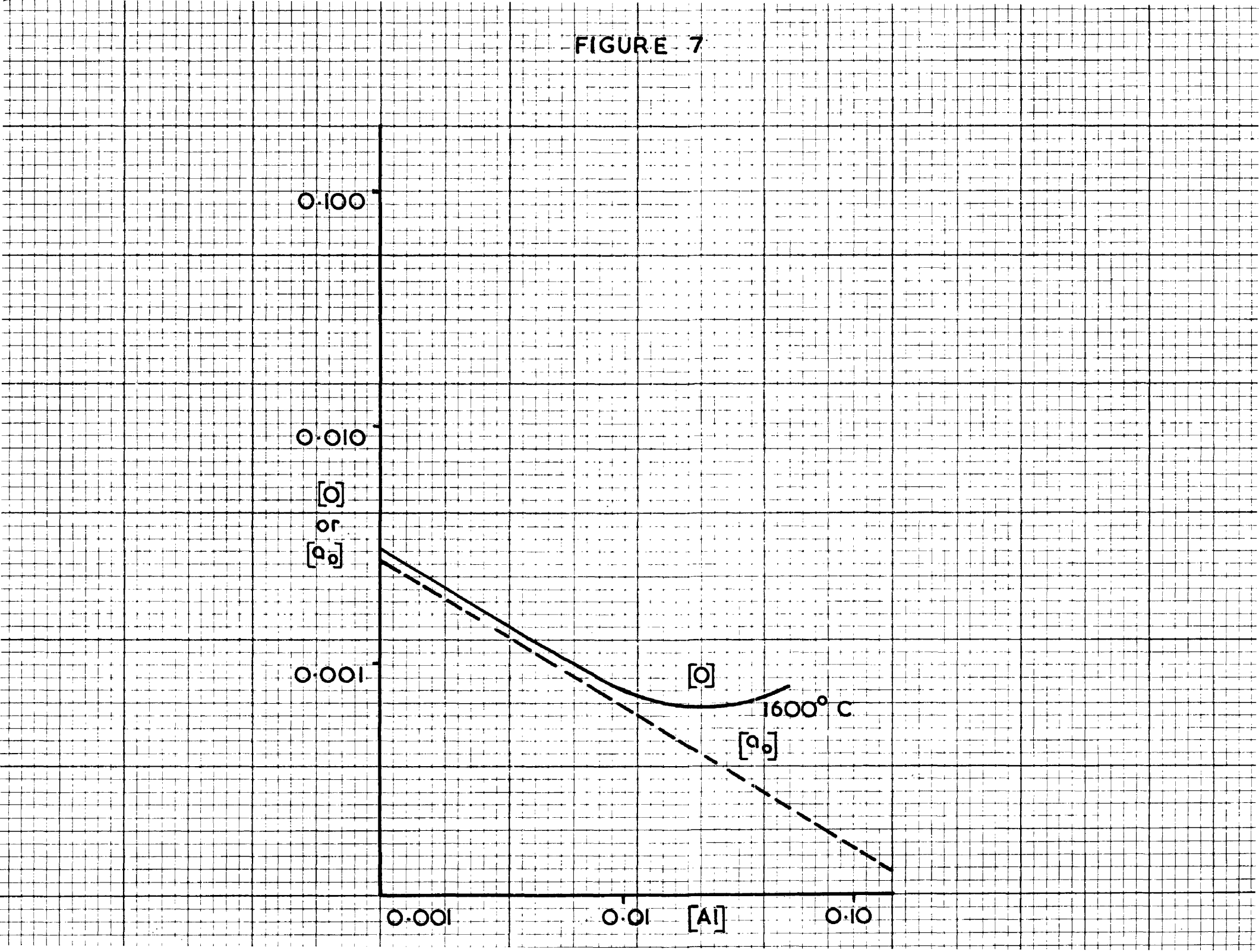

the effect diminishing with increasing temperature. Their results for 1600°C are reproduced in Figure 7 showing that beyond about 0.04% aluminium the percent oxygen rises quite steeply. While the oxygen contentsin the present study seem considerably higher than those of Gokcen and Chipman, the values of these workers were considerably lower than those of Wentrup and Hieber(52) and Hilty and Crafts(53).

If the net reaction responsible for the removal of carbon is given by the equation:

$$Al_2O_3 + 3\underline{C} = 2\underline{Al} + 3CO.$$

the alumina being the pure material or that from the alumino-silicates present in the alundum crucibles, then, aluminium being soluble in iron-carbon alloys it would be expected to increase as the reaction proceeded to the right with the loss of carbon. It might also be expected that higher aluminium contents and greater carbon losses would result from the alundum crucibles since pure alumina is a chemically inert substance and should be slower to react. It will be seen from Table II that, whereas this is not wholly true since the final metal sample from heat 8 had a relatively low aluminium content, the highest aluminium values were in fact recorded for runs 10 and 11. The results shown in Tables II and III also show that, while the soluble aluminium in heat 13 decreased as the reaction proceeded, the values obtained in heats 12,14 and 15, with the exception of 15(4), all increased with decreasing carbon. These discrepancies make it difficult to formulate a reasonable hypothesis but whatever this may be the presence of soluble aluminium in the metal must be taken as indicative of reaction between the crucible and the alloy.

While aluminium is present in the alloys after reaction with the crucible this is not in stoichiometric amounts in accordance with the equation

$$Al_2O_3 + 3\underline{C} = 2\underline{Al} + 3CO \quad \text{.....(1)}$$

This suggests two possibilities, either

(a) some other reaction is also responsible for the removal of carbon with the formation of an aluminium compound which is not going into solution in the metal, or

(b) the aluminium in solution is reacting further to form a volatile compound.

There is considerable evidence in the literature to suggest the possible formation of gaseous suboxides of alumina. Beletski and Rapoport(54) report on the formation of a lower oxide of aluminium in the reduction by carbon of alumina mixed with silica, and from X-ray data this oxide was shown to be close to Al_2O. Hoch and Johnston(55) have described the formation of both Al_2O and AlO by interaction of aluminium and alumina at temperatures as low as 1000°C. Brewer and Searcy(56) have also reported on the formation of these two gaseous oxides of aluminium.

It seems probable then that several reactions are proceeding simultaneously, that expressed by equation(1) being responsible for the soluble aluminium in the metal while the rest of the carbon is removed by a reaction expressed by the equation

$$Al_2O_3 + 2\underline{C} = Al_2O + 2CO \quad \text{.....(2)}$$

It may even be that equation (1) represents the removal of the carbon while a reaction of the form

$$4\underline{Al} + Al_2O_3 = 3Al_2O(vap.)$$

explains the absence of stoichiometric proportions of aluminium in the decarburised alloy. In both cases the volatile suboxide formed may be carried away from the reaction chamber in the stream of purified nitrogen or deposited elsewhere in the furnace.

To avoid the spurious results obtained in the earlier runs discussed above only high purity, high fired alumina crucibles were used in the later slag-metal runs. Restricting the discussion to these crucibles it will be seen in Figure 6B and from Table III, that there are quite large differences in oxygen contents in the heats 14, 15, 16 and 17. Two types of charge were used with different initial oxygen contents, Armco iron with added carbon and an iron-carbon alloy. The variations in oxygen levels from run to run and between successive samples in the same run are of interest. In the runs employing Armco Iron and carbon as charge material, 14 and 15, the crucibles for which were slip-cast alumina fired at 1600°C. the melt oxygen was around 0.009 - 0.01% whereas in the two employing an iron-carbon alloy, Run 16 in a similar pure slip-cast alumina crucible melted out at 0.0032% oxygen and 17 in the Thermal Syndicate crucible melted out at 0.0122% oxygen. This large difference seems likely to be related to the smooth walls of the crucible used in Run 17 not permitting the easy formation of bubbles. Certainly, it was observed, during the drawing of the second sample, that more gas was evolved than had ever before been observed. The state

MAGNESITE BRICK CRUCIBLES
SLAG FREE

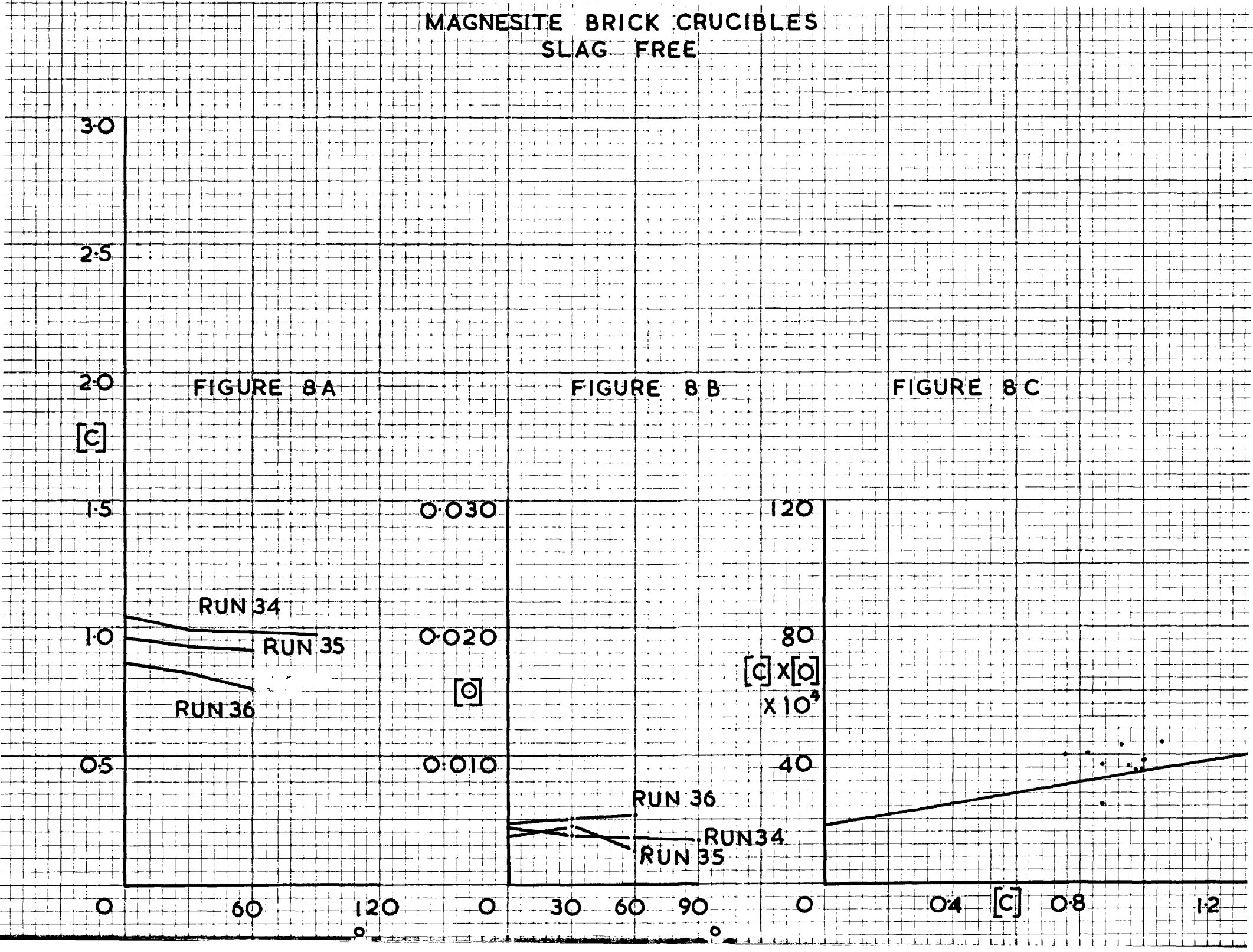

of supersaturation was such that this release of gas was brought about by the simple insertion of the silica sampling tube in the melt. In agreement with this observation is the 50% reduction in the oxygen content from 17(2) to 17(3), the oxygen figures for (1) and (2) being the highest recorded for slag-free runs conducted in dense crucibles.

It will be seen from Figure 6A that generally in these pure, well fired crucibles, the rate of carbon loss is fairly regular from run to run, being, as with magnesia crucibles, greater towards the end of the run when the depth of metal is reduced. The evolution of gas on sampling substantiates the theories put forward for the existence of supersaturation in magnesia crucibles, and the findings of run 17 lend considerable weight to these arguments.

Experiments in Magnesite Brick Crucibles.

Since it was proposed to use magnesite brick crucibles later in this study in slag-metal experiments, it was necessary to obtain data about the carbon loss resulting from reaction of these with iron-carbon-alloys. Therefore in all experiments in these crucibles at least two samples were drawn at the working temperature before any slag additions were made. Graded magnesite was sintered to the bases of the crucibles in two heats to determine whether or not this affected the rate of carbon removal. The carbon and oxygen contents for the samples drawn in heats 34, 35 and 36 prior to slag additions are given in Figures 8A and 8B respectively and reported in Table IV as typical of those obtained in magnesite crucibles. Heats 35 and 36 had graded magnesite added.

Discussion of Results in Magnesite Brick Crucibles.

In all cases there was a carbon loss similar to that obtained in the pure alumina crucibles and a little less than that in magnesia. As the runs were not over such an extended period of time the effect of reducing the ferrostatic head was not noticed.

The addition of graded magnesite did not materially affect the rate of carbon removal. This is not really surprising since the pores in the graded magnesite would be no different from the pores in the crucibles themselves and the pores formed between adjacent pieces of graded magnesite would be too large to be of any value in aiding nucleation.

The oxygen analyses were very steady around the 0.004% level and, although bubbles were evolved during sampling as with the other two types of crucible, the evolution was least of all in the case of magnesite.

TABLE IV.

Heat No.	Crucible Type	Charge		Carbon and oxygen contents. 1	2	3	4	5
34	Magnesite Brick.	Armco Iron + C [C]=1.167	[C]	1.134	1.047	0.9982	0.9926	0.9817
			[O]	0.0041	0.0042	0.0038	0.0035	0.0034
			m		0.0044	0.0038	0.0035	0.0033
			T		0	30	60	90
35	Magnesite Brick and graded magnesite	Armco Iron + C [C]=1.143	[C]	1.014	0.954	0.927	0.916	
			[O]	0.0061	0.0039	0.0046	0.0027	
			m		0.0037	0.0043	0.0025	
			T		0	30	60	
36	Magnesite brick and graded magnesite	Armco Iron + C [C]=1.155	[C]	0.938	0.862	0.817	0.753	
			[O]	0.0040	0.0044	0.0050	0.0053	
			m		0.0038	0.0041	0.0040	
			T		0	30	60	

T = time in minutes at 1550°C.

Conclusions on Experiments on Crucible Reactions.

Carbon loss due to reaction of the iron-carbon alloys with the crucibles has been found in the three cases investigated.

In magnesia the reaction has been expressed by the equations

$$MgO = Mg + \underline{O} \quad \ldots\ldots\ldots\ldots\ldots (1)$$

$$\underline{C} + \underline{O} = CO \quad \ldots\ldots\ldots\ldots\ldots (2)$$

and these have been shown to be thermodynamically possible if the solubility limit of magnesium in iron carbon alloys corresponds to a fugacity of less than 5.62×10^{-6} atm.

The carbon loss in alumina crucibles has been shown to be due mainly to the reduction of alumina to aluminium but it has been shown at the same time that side reactions are possible leading to the formation of a lower oxide of aluminium. The results of heat 12, in one sample from which 0.122% oxygen and 0.124% aluminium were found with only a trace of carbon, are particularly interesting and would warrant further work but as this was not the main object of this research, time did not permit going further into these investigations.

Geller(57) has reported similar loss of carbon when iron-carbon alloys were melted in silica crucibles. He attributed this to the reduction of the silica by the carbon either directly or through the formation firstly of ferrous oxide. The silicon so formed is soluble in the metal and was determined by analysis but a sub oxide of silicon, SiO, is known to exist and this may also be formed in a similar fashion to the lower oxide of aluminium in the alumina crucible reactions.

This reduction of silica by carbon has of course a practical significance in the acid open-hearth furnace where the hearth and banks are formed with silica. This reaction was referred to by Herasymenko(7) as the one likely to occur when the rate of transfer of oxygen from the slag was not rapid enough to satisfy the carbon reaction.

The difficulty of forming bubbles of carbon monoxide has been demonstrated by the existence of supersaturation in all cases, this being greatestin alumina and least in magnesite brick crucibles. This super-saturation effect which was relieved by the sampling rod is clearly shown by the plot of the carbon-oxygen product, m, in Figures 5C, 6C and 8C where the equilibrium curve of m against carbon is also given. In this respect it is interesting to compare the results of the present work with those of Turkdogan et al(6) who studied decarburisation under air and oxygen/argon atmospheres. They used a high frequency induction furnace under which conditions of melting there is a considerable stirring action. Samples drawn during the heats revealed no supersaturation. It is therefore reasonable to conclude that most of the carbon removal is by loss of carbon monoxide to the gas from the surface, the continued renewal of the latter in induction heating preventing supersaturation taking place.

CHAPTER 4.

SLAG-METAL EXPERIMENTS.

SLAG-METAL EXPERIMENTS.

The main aim of the present work was to study the removal of carbon in the presence of iron-containing slags. The existence of a reaction between the various types of crucibles used and the iron-carbon alloys contained in them having been confirmed, a number of experiments was carried out to examine the effect of slags of varying iron oxide activity on the rate of carbon removal. It was borne in mind that any quantitative study would have to incorporate an allowance for this crucible action.

Experimental Procedure.

The molybdenum furnace was again used as a melting unit, the three crucible types magnesia, pure alumina and magnesite brick being employed to hold the alloys.

Metal charges in all cases consisted of weighed crucibles, drilled out of Armco iron, into which were packed weighed amounts of carbon to give the desired analysis.

The slags used were pure ferrous oxide, prepared by heating ferrous oxalate in vacuo, fayalite prepared from stoichiometric amounts of this ferrous oxide and pure silica and various works slags of basic and acid open-hearth origin with a range of ferrous oxide activities. These slags were crushed and ground in an agate mortar, pelletised in a press and the pellets weighed. Pure iron wire was then attached to the pellets and bent in the form of a hook enabling the slag to be lowered directly on to the surface of the molten charge by means of a platinum wire.

FIGURE 9

FeO ADDITIONS

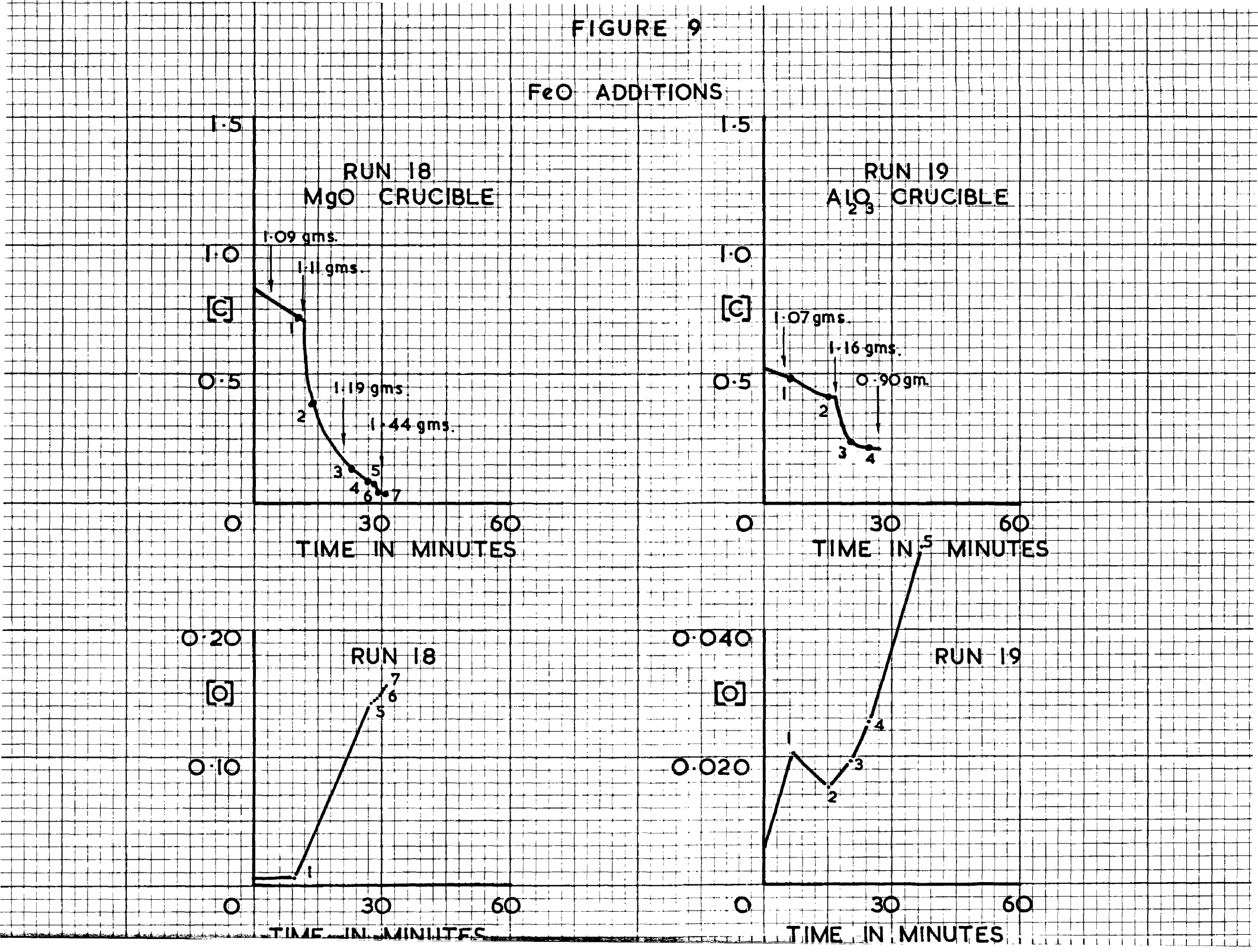

Occasionally the metal samples drawn were too small to allow both carbon and oxygen to be determined and in such cases only carbon was determined. At the same time if the samples were in any way imperfect, for example if they contained blowholes, they were not used for oxygen determination.

The first experiments, heats 18 and 19, were carried out in magnesia and alumina crucibles respectively using the pure ferrous oxide as slag additions. As expected from the work of Dancy(58) on the reduction of pure ferrous oxide and pure magnetite by carbon in molten pig iron, the reaction was very vigorous, throwing particles of metal and presumably slag up the furnace tube to a height of 18 inches above the metal bath. The carbon drop curves for these heats together with the time and quantity of ferrous oxide additions and the oxygen curves are given in Figure 9 and the analyses, along with all those for laboratory slag-metal heats, are tabulated in Table V.

A fayalite slag was employed in heats 20 and 21, again in magnesia and alumina crucibles respectively and the graphs for these are given in Figure 10. The effects produced by the fayalite were similar to those produced by the pure ferrous oxide except that in the magnesia crucible, after the initial vigorous reaction which occurred after each slag addition, a much slower gas evolution rate, about 1 bubble every few seconds, was perceptible for almost an hour after the addition had been made.

TABLE V.

Laboratory Slag Metal Experiments.

Heat No. Fig. No.	Crucible Type.	Slag		Metal Sample Analysis. Before Slag Additions.	1	2	3	4	5	6	7
18	MgO	FeO	[C]	0.829 ↓	0.676 ↓	0.398 ↓	0.136 ↓	0.082	0.071	0.044	0.036
9			[O]	0.0034	0.0036	-	-	-	0.141	0.147	0.158
			m	0.0028	0.0024	-	-	-	0.0100	0.0065	0.0057
19	Al_2O_3	FeO	[C]	0.503 ↓	0.480	0.408 ↓	0.246	0.221 ↓	Tr.	Tr.	Tr.
9			[O]	0.0059	0.0204	0.0151	0.0189	0.0259	0.0527	*	-
			m	0.0030	0.0098	0.0061	0.0047	0.0057	-		
20	MgO	$2FeO.SiO_2$	[C]	1.230 ↓	0.955	0.738 ↓	0.625	0.319 ↓	0.147		
10			[O]	0.0046	0.0048	0.0085	0.0043	0.0079	-		
			[Si]	0.02	0.08	0.11	0.09	0.26	0.06		
			m	0.0057	0.0046	0.0063	0.0028	0.0025	-		
21	Al_2O_3	$2FeO.SiO_2$	[C]	1.323 ↓	1.314 ↓	1.289 ↓	1.200	1.030 ↓	0.941	0.745	0.578
10			[O]	0.0033	0.0177	0.0239	0.0397	0.0038	0.0130	0.0044	0.0031
			[Si]	Tr.	0.04	0.02	0.02	0.02	0.06	0.04	0.04
			m	0.0043	0.0232	0.0309	0.0476	0.0039	0.0122	0.0033	0.0018
22	MgO	E230	[C]	1.047 ↓	0.892 ↓	0.725	0.595 ↓	0.502	0.477		
11			[O]	0.0055	0.0065	0.0081	0.0102	-	0.0279		
			[Si]	0.02	0.11	0.11	0.12	0.02	0.02		
			[Mn]	0.04	0.27	0.33	0.36	0.19	0.17		
			m	0.0057	0.0057	0.0059	0.0061	-	0.0133		
23	Al_2O_3	E230	[C]	1.276 ↓	1.189 ↓	1.172 ↓	1.069	0.973	0.965	0.954	
11			[O]	0.0017	0.0048	0.0035	0.0085	0.0061	0.0049	0.0046	
			[Si]	0.02	0.02	0.03	0.06	0.07	0.07	0.07	
			[Mn]	0.04	0.06	0.07	0.10	0.10	0.11	0.12	
			m	0.0022	0.0057	0.0041	0.0091	0.0060	0.0047	0.0044	
24	MgO	C161	[C]	1.205 ↓	1.117 ↓	0.944	0.900	0.813	0.783	0.682	
			[O]	0.0087	0.0096	0.0105	0.0073	-	0.0038	-	
			[Si]	0.01	0.06	0.13	0.13	0.13	0.13	0.13	

TABLE V. (Cont'd)

Heat No. Fig. No.	Crucible Type.	Slag.		Metal Sample Analysis. Before Slag Additions	1	2	3	4	5	6	7
25 12	MgO	M251 (4)	[C]		1.091	1.025	0.982 ↓	0.845	0.720 ↓	0.524	0.251
			[O]		0.0050	0.0033	0.0057	0.0087	0.0035	-	0.0061
			[Si]		Nil	Nil	Nil	Nil	Nil	Nil	Nil
			[Mn]		0.04	0.05	0.04	0.13	0.15	0.26	0.30
			[P]				0.008	0.044	0.060	0.054	0.110
			m		0.0055	0.0034	0.0056	0.0074	0.0024	-	0.0015
26 13	MgO + Graded MgO	E230	[C]	1.208 ↓	0.930 ↓	0.771					
			[O]	0.0034	0.0036	0.0075					
			[Si]	Tr.	0.07	0.09					
			[Mn]	0.04	0.20	0.22					
			m	0.0041	0.0033	0.0058					

Heat No. Fig. No.	Crucible Type.	Slag.		Metal Sample Analysis. 1	2	3	4	5	6	7
27 14	Magnesite	M251 (4)	[C]	0.638 ↓	0.480	0.300				
			[O]	0.0069	0.0152	0.0083				
			[Si]	Nil	Nil	Nil				
			[Mn]	0.04	0.16	0.16				
			[P]	0.0111	0.045	0.076				
			m	0.0044	0.0073	0.0025				
28 14	Magnesite	M251 (4)	[C]	0.769 ↓	0.398	0.256				
			[O]	0.0077	0.0102	0.0118				
			[Si]	Nil	Nil	Nil				
			[Mn]	0.04	0.15	0.22				
			[P]	0.008	0.076	0.096				
			m	0.0059	0.0041	0.0030				

TABLE V. (Cont'd).

Heat No. / Fig. No.	Crucible Type	Slag	Metal Sample Analysis.	1	2	3	4	5	6	7
29 / 15	Magnesite	M251 (4)	[C]	1.134	1.047	0.998	0.993	0.982 ↓	0.764	0.649
			[O]	0.0041	0.0042	0.0038	0.0035	0.0034	0.0119	0.0088
			[Si]	Nil	Nil	Nil	Nil	Nil	Nil	Nil
			[Mn]	0.05	0.05	0.04	0.04	0.05	0.23	0.22
			[P]					0.008	0.048	0.079
			m	0.0046	0.0044	0.0038	0.0035	0.0033	0.0091	0.0057
31 / 15	Magnesite + Graded Magnesite.	M251 (4)	[C]	0.938	0.862	0.817	0.753 ↓	0.556	0.371	0.256
			[O]	0.0040	0.0044	0.0042	0.0053	0.0157	0.0101	0.0042
			[Si]	Nil	Nil	Nil	Nil	Nil	Nil	Nil
			[Mn]	0.05	0.05	0.05	0.04	0.19	0.16	0.17
			[P]				0.0095	0.035	0.045	0.060
			m	0.0038	0.0038	0.0034	0.0040	0.0087	0.0040	0.0011

Heat No. / Fig. No.	Crucible Type	Slag	Metal Sample Analysis. Before Slag Additions.	1	2	3	4	5	6	7
32 / 17	Magnesite	M251 (4)	[C]	0.605 ↓	0.267	0.191	0.147	0.115	Tr.	
			[O]	0.0144	0.0178	0.0075	0.0210	0.0267	0.0195	
			[Si]	Nil	Nil	Nil	Nil	Nil	Nil	
			[Mn]	0.04	0.24	0.26	0.27	0.24	0.23	
			[P]	0.008	0.064	0.064	0.064	0.104	0.064	
			m	0.0087	0.0048	0.0014	0.0031	0.0031	-	
33 / 17	Magnesite	M251 (4)	[C]	0.329 ↓	0.671	0.627 ↓	0.458 ↓	0.344 ↓	0.196	0.180	0.147
			[O]	0.0077	0.0117	0.0055	0.0113	0.0179	0.0125	0.0087	0.0097
			[Si]	Nil	Nil	Nil	Nil	Nil	Tr.	Nil	Nil
			[Mn]	0.04	0.11	0.11	0.17	0.20	0.24	0.26	0.26
			[P]	0.011	0.036	0.040	0.104	0.048	0.060	0.064	0.064
			m	0.0064	0.0079	0.0034	0.0052	0.0063	0.0025	0.0016	0.0015

TABLE V. (Cont'd).

Heat No. Fig. No.	Crucible Type.	Slag	Metal Sample Analysis. Before Slag Additions.	1	2	3	4	5	6	7
34 18	Magnesite	M251 (4) + FeO	[C] 0.982 ↓	0.802 ↓	0.655 ↓	0.425	0.240			
			[O] 0.0054	0.0181	0.0126	0.0460	0.0161			
			[Si] Tr.	Tr.	Tr.	0.05	0.05			
			[Mn] 0.05	0.16	0.23	0.23	0.24			
			[P] 0.008	0.038	0.044	0.040	0.060			
			m 0.0053	0.0145	0.0083	0.0196	0.0039			
35 13	Magnesite	M251 (4) + FeO	[C] 0.954 ↓	0.840 ↓	0.605 ↓	0.398 ↓	0.229	0.169	0.125	
			[O] 0.0039	0.0106	0.0200	0.0058	0.0370	0.026	0.0088	
			[Si] Nil	Nil	Nil	Nil	Nil	Nil	Nil	
			[Mn] 0.05	0.07	0.13	0.17	0.19	0.19	0.18	
			[P] 0.0095	0.022	-	0.036	0.036	0.040	0.056	
			m 0.0037	0.0089	0.0120	0.0023	0.0085	0.0044	0.0011	
36 19	Magnesite	M251 (4) + FeO	[C] 1.15 6 ↓	0.911 ↓	0.693	0.666 ↓	0.513	0.491	0.480	
			[O] 0.0024	0.0131	0.0100	0.0155	0.0165	0.0143	0.0096	
			[Si] 0.03	0.03	Tr.	-	0.03	0.03	Tr.	
			[Mn] 0.05	0.12	0.15	0.16	0.18	0.17	0.17	
			[P] 0.008	0.036	0.035	0.045	-	0.048	0.052	
			m 0.0028	0.0119	0.0069	0.0103	0.0085	0.0070	0.0046	

Arrowheads indicate times of slag additions.

* Very high.

FIGURE 10
FAYALITE ADDITIONS

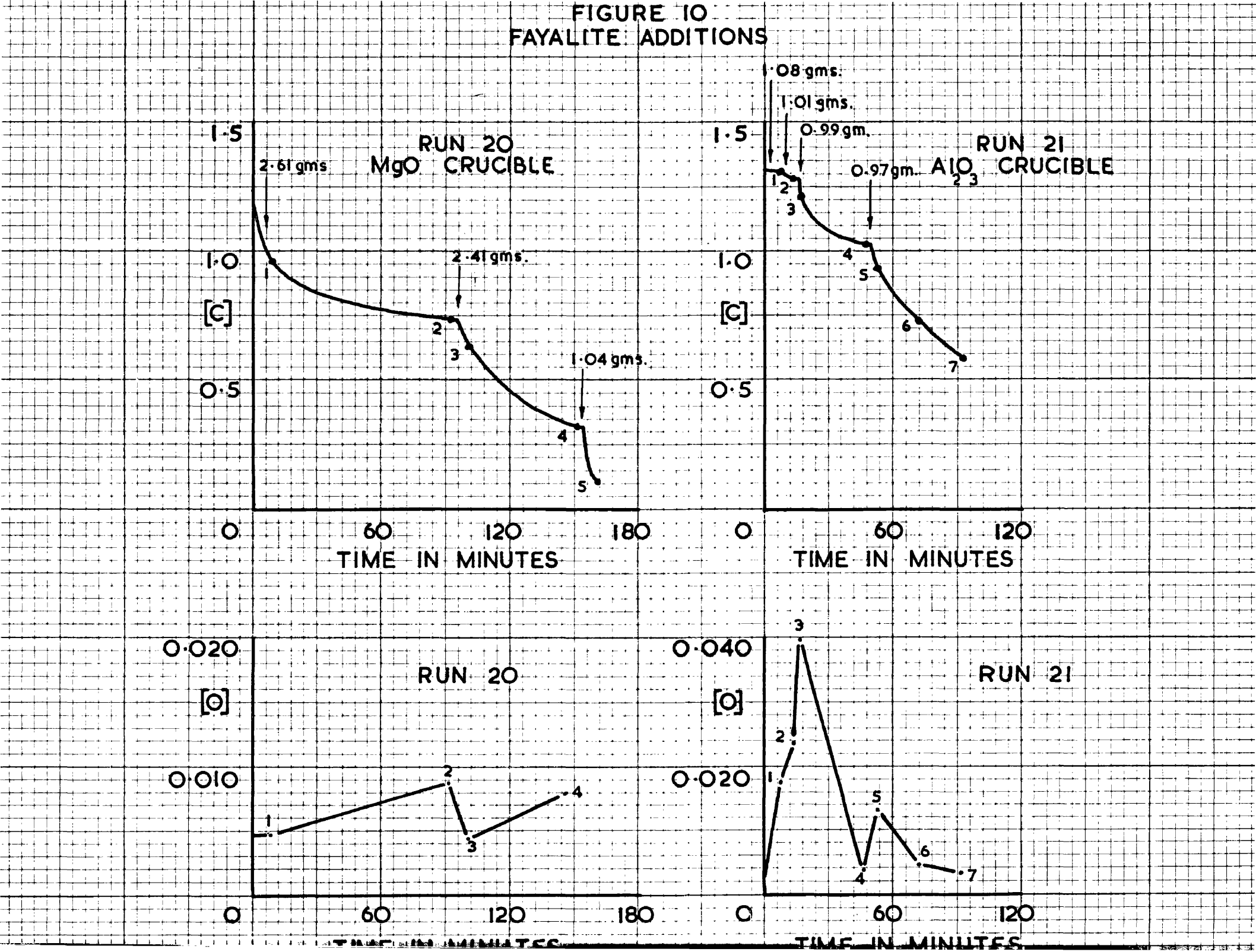

FIGURE 11

E 230 A.O.H. SLAG ADDITIONS

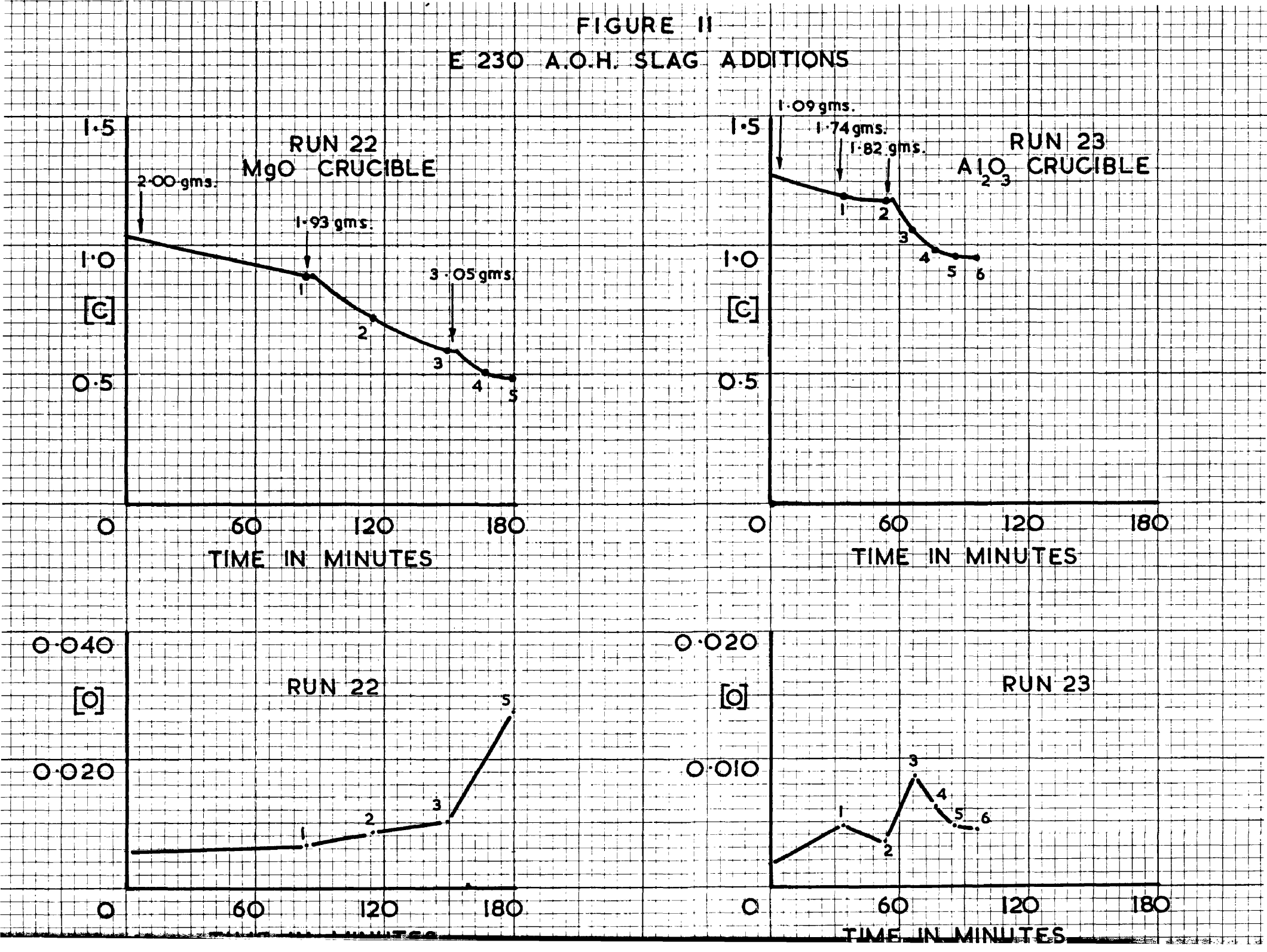

The next two runs, 22 and 23, were to compare the rate of carbon removal under an acid open hearth steelmaking slag with the rates obtained under the ferrous oxide and fayalite slags. The ferrous oxide activity of this slag (E230) as of the other slags employed (listed in Table VI) was calculated from the work of Turkdogan and Pearson(23). In these two runs, graphed in Figure 11, the first slag addition caused a fair reaction, although much less than with either pure ferrous oxide or fayalite, and bubbles continued to rise at a slow rate through the melt and burst on the surface for about an hour after the initial vigorous reaction had ceased.

Another acid open hearth slag, C161 Table VI, of lower ferrous oxide activity than the E230 melt slag was used in heat 24 in which a magnesia crucible was again employed. With this slag not even the initial "spurting", evident in heats 22 and 23, was observed, the reaction being a slow, regular one continuing apparently until the effect of the addition had worked itself out. The carbon and oxygen curves are plotted in Figure 12.

The series of slags was completed with a basic open hearth slag, M251(4) Table VI, with a ferrous oxide activity slightly greater than E.230. This slag was used in heat 25, the results of which are also graphed in Figure 12. On first melting a fair reaction resulted but no metal was thrown up into the atmosphere above the melt. After this short initial period the effect of the slag was very similar to that of the acid open hearth slags although perceptible reaction ceased about 80 minutes after the additions.

TABLE VI.

Analysis of Slags used in Slag-Metal Experiments.

Slag	SiO_2	Al_2O_3	Cr_2O_3	Fe_2O_3	FeO	MnO	CaO	MgO	P_2O_5	S	^aFeO
E230	48.6	1.53	Tr.	0.41	29.02	18.87	1.89	Tr.	Nil	Nil	0.23
C161	48.82	2.77	1.23	2.68	12.36	21.95	8.23	Tr.	Nil	Nil	0.14
M251(4)	11.7	Nil	Nil	Nil	12.7*	5.45	50.0	7.9	9.9	0.306	0.3

* ($\leq$FeO)

FIGURE 12

MgO CRUCIBLES

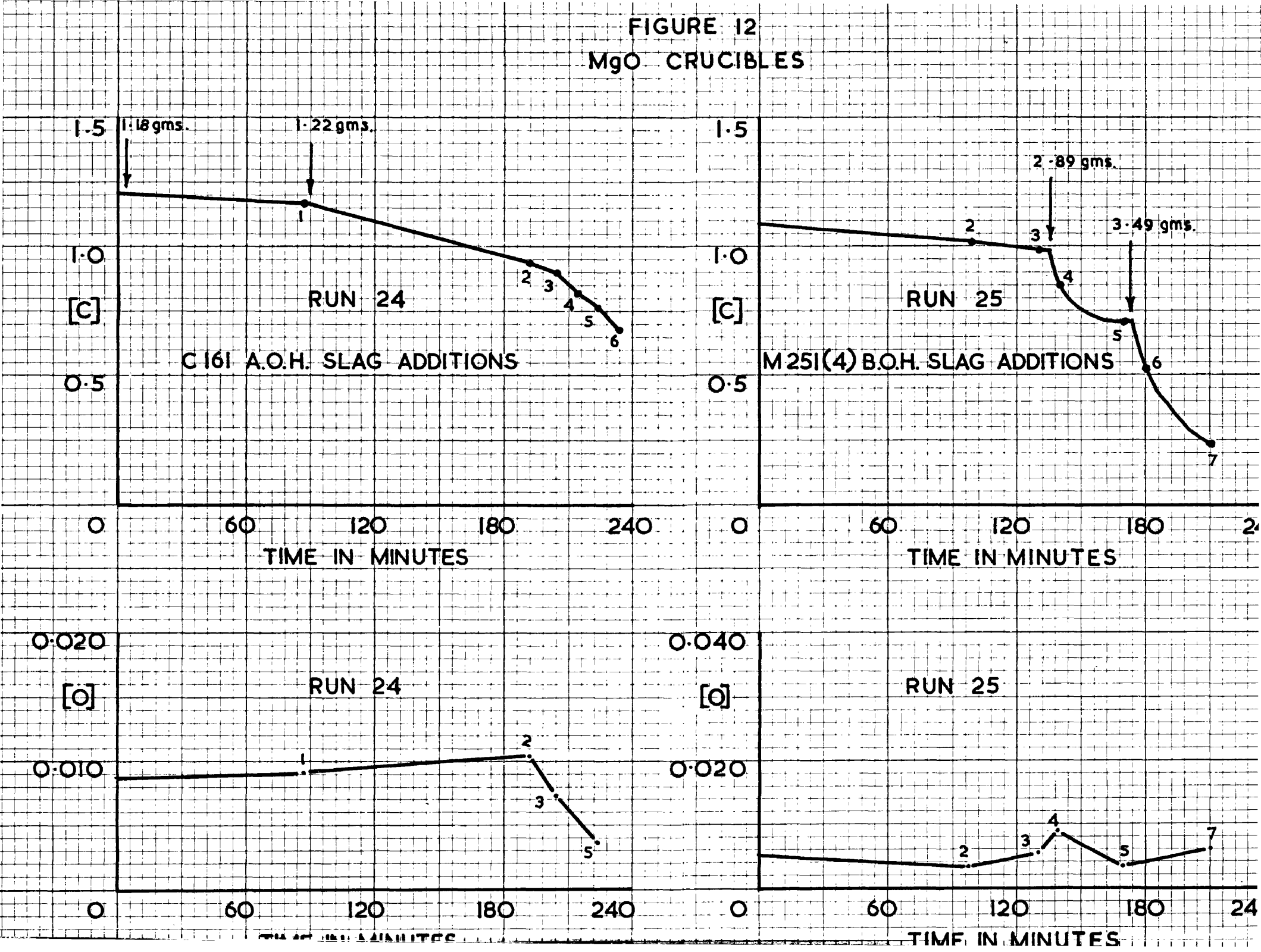

Heat 26 was a repeat of heat 22 with the addition of graded magnesia to the base of the crucible to determine whether or not this would affect the rate of carbon removal. The carbon drop curve is plotted alongside that of heat 22 in Figure 13.

Magnesite brick was next employed as crucible material. Two heats, 27 and 28, were carried out, the addition of slag M251(4) being made immediately the melt was sampled after the working temperature had been reached. Two samples only were drawn in each case after the slag addition, the first at the end of the apparent reaction and the second 30 minutes later with the results shown in Figure 14. The next three heats, 29, 30 and 31 have already been reported since the earlier parts were used to determine the extent of crucible action in magnesite brick crucibles. Graded magnesite was added to the bases of the crucibles in 30 and 31 and in all three cases the slag additions were made some considerable time after reaching the working temperature. Heats 29 and 31 are graphed in Figure 15, heat 30 being omitted since the slag addition was improperly made.

The initial rate of carbon removal following slag additions to these runs was not unlike that achieved by the same slag in a magnesia crucible (heat 25) but up to this point no success had been met with in obtaining slag samples. The slags appeared to form only thin films on the metal surface after reaction had ceased, the major part of the remaining slag being at the periphery of the metal bath. It was felt that larger slag bulks might afford a better opportunity of maintaining a continuous slag covering on the metal and so increase the chance of

FIGURE 13

E 230 A.O.H. SLAG ADDITIONS

MgO CRUCIBLES

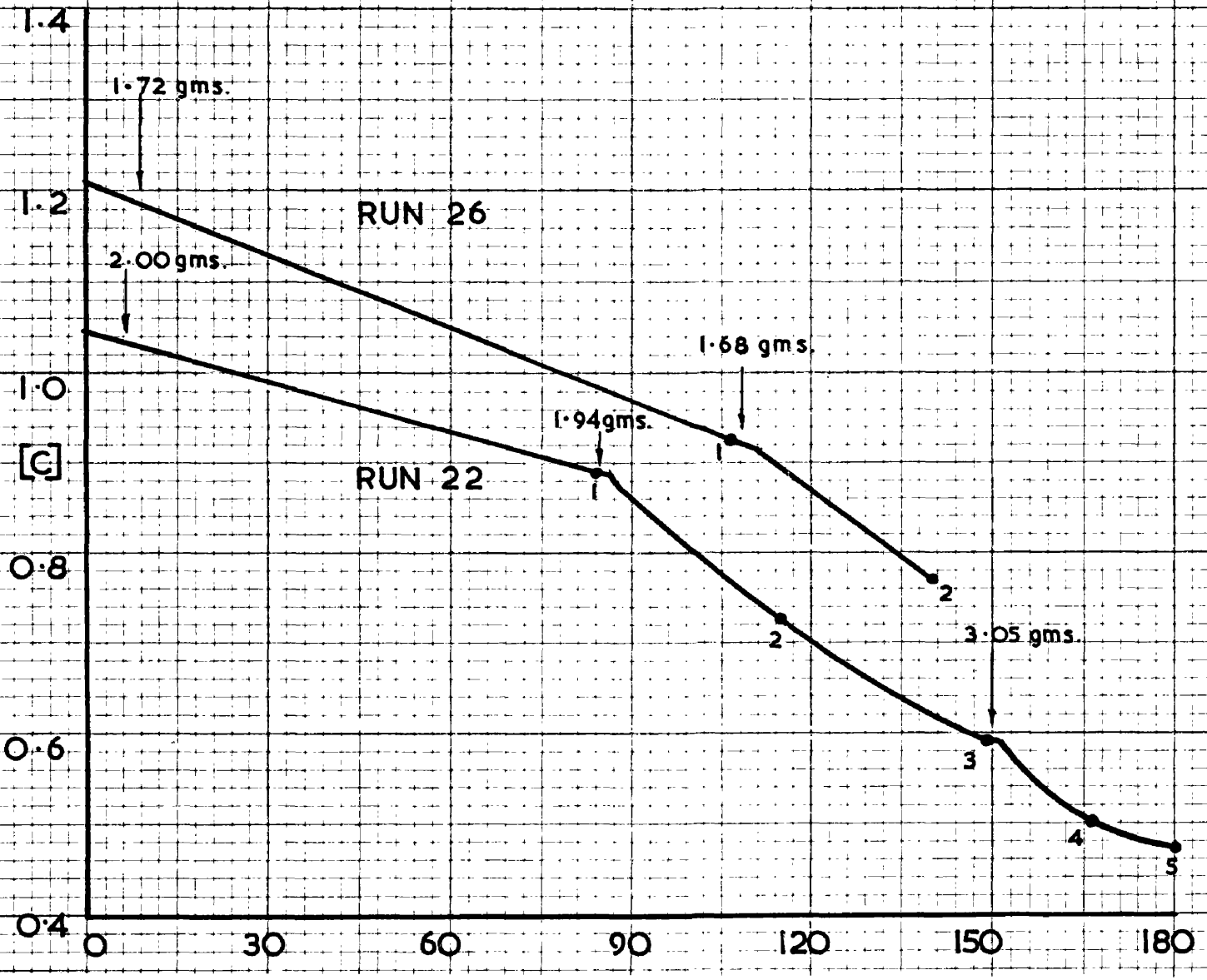

FIGURE 14
MAGNESITE CRUCIBLES
M 251 (4) B.O.H. SLAG ADDITIONS

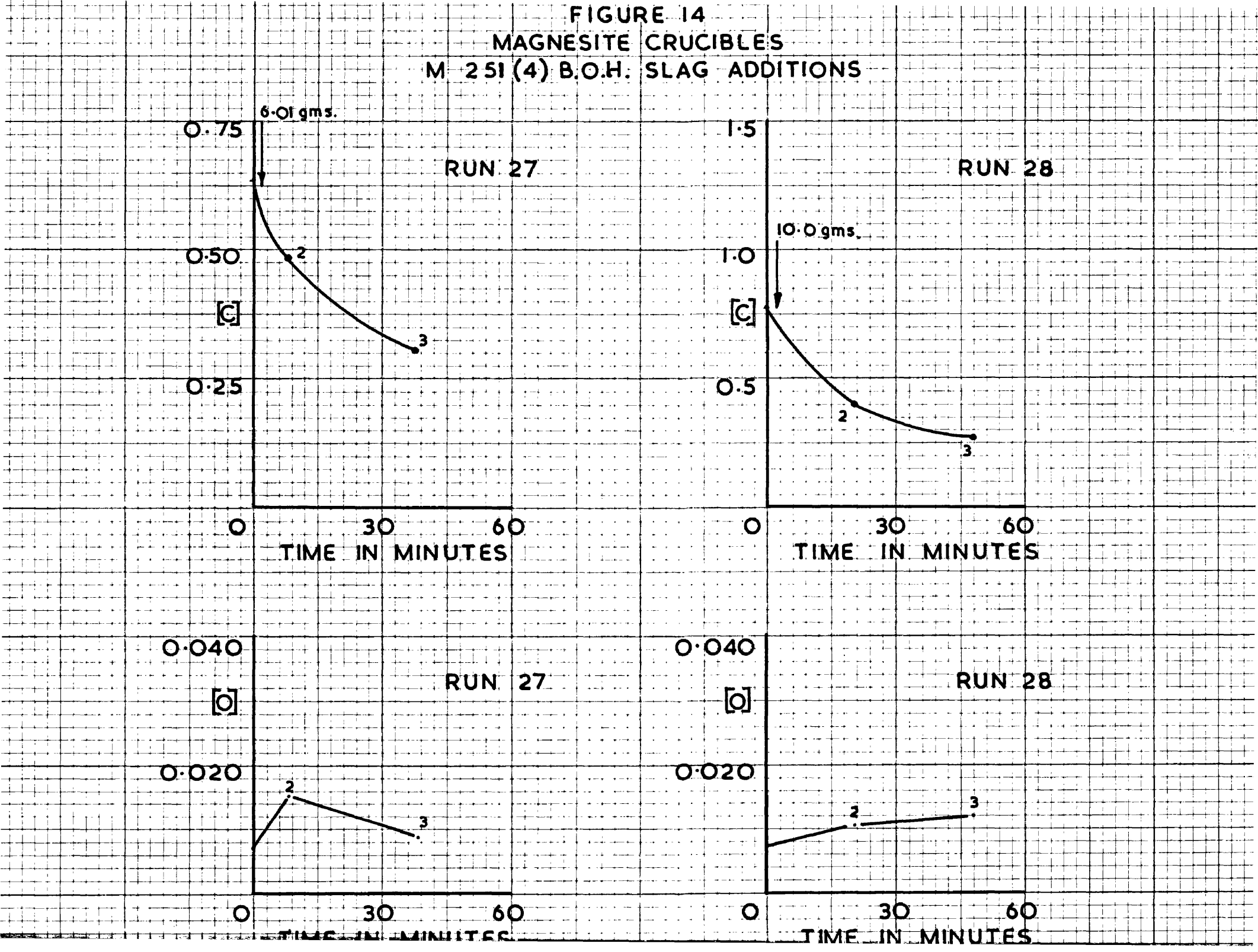

FIGURE 15
MAGNESITE CRUCIBLES
M 251 (4) B.O.H. SLAG
ADDITIONS

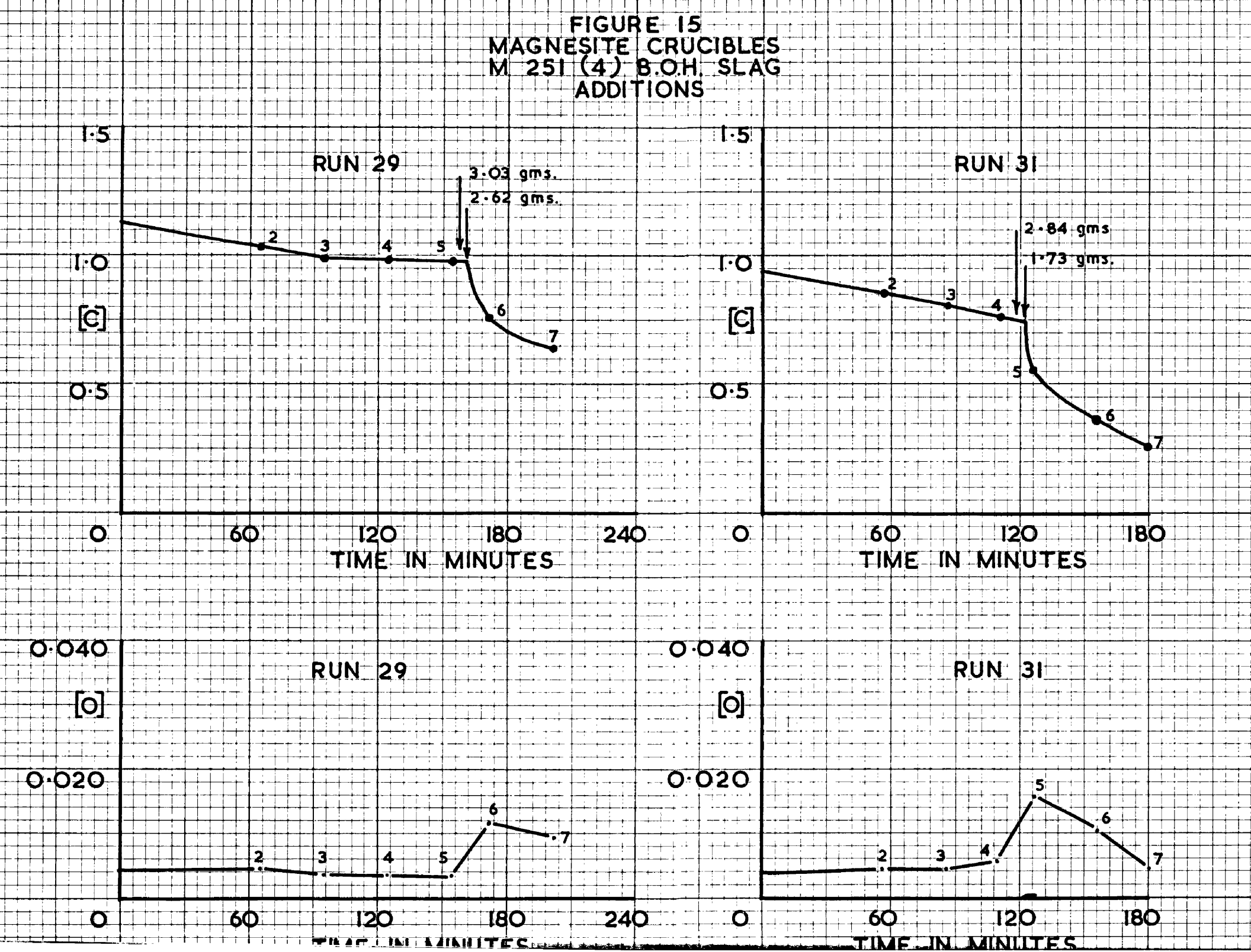

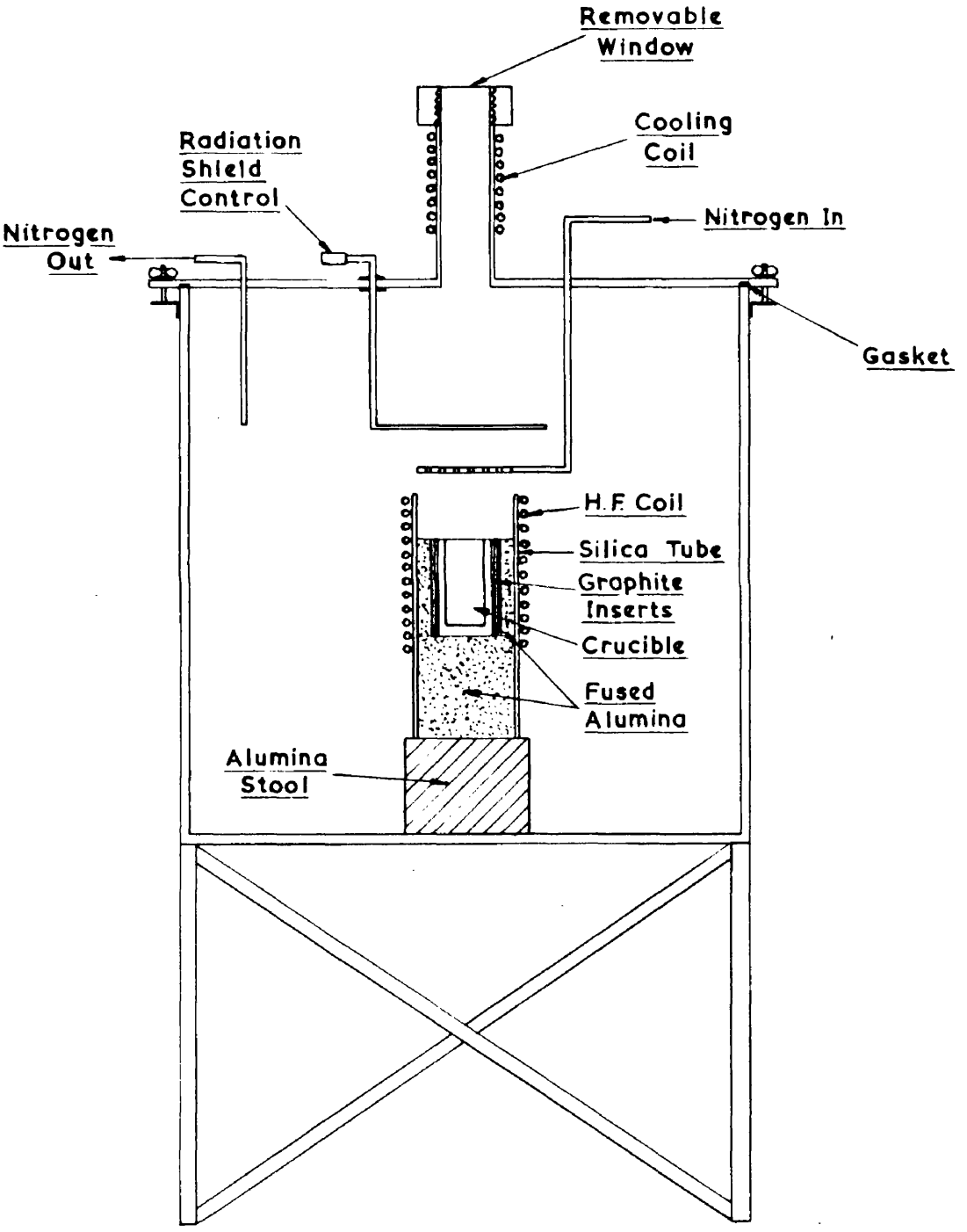

FIGURE 16.
SCALE 1"= 9"

obtaining slag samples. Slip cast crucibles of dimensions larger than 1" internal diameter are difficult to manufacture whereas magnesite ones can be readily drilled out of bricks. Due to the similar results obtained above with magnesite crucibles these were adopted for this next section of the work. Crucibles of 2" internal diameter with a wall thickness of 0.4-0.5 inch were prepared. These could not be accommodated in the molybdenum furnace and a high frequency furnace was used. This, shown in Figure 16 consisted simply of a 5 inches diameter copper coil with a suitable number of turns, set in a 24 inches square case constructed from dense asbestos sheet and fitted with a screw-down lid provided with a recess containing a gasket. Also located in the lid were an inlet and outlet for controlled atmosphere and an inspection window, screwed on to a length of copper tube centrally situated on the lid, the tube being water cooled. The window could be removed for the purpose of making additions or taking temperature readings by immersion thermocouple and was protected from direct radiation by a shield which could be swung out over the crucible. The coil ends were set in a high grade insulating material in one side of the furnace from where they were connected to a high frequency supply by flexible leads. A silica tube was fixed centrally within the coil, fused alumina poured in to the desired depth and the magnesite crucible embedded centrally within the silica tube. Graphite strips, to aid heating, were then fitted round the crucible and the annulus between these and the silica tube packed with fused alumina.

In this arrangement the metal charge melted in a very short time but the high frequency currents had no direct effect upon the pelletised

FIGURE 17
MAGNESITE CRUCIBLES
M 251 (4) B.O.H. SLAG
ADDITIONS

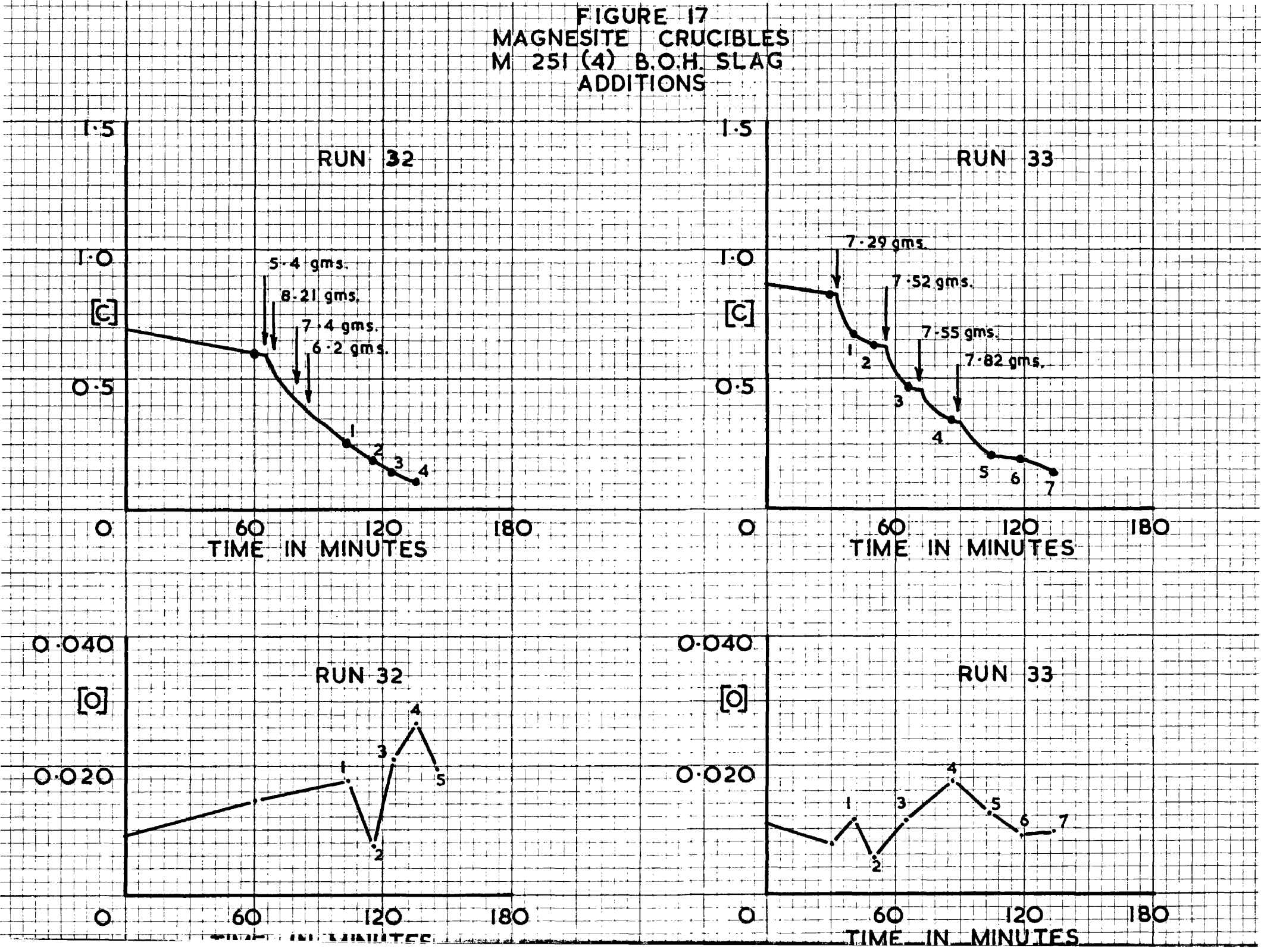

slag additions, which were only heated by conduction from the metal and radiation from the graphite strips. The slag additions appeared to melt only where in physical contact with the metal. It was disappointing and, at first, rather strange that the high frequency method of heating should prove so inadequate for obtaining suitable slag samples since this method of heating had been used with great success by several workers(59-61) studying slag/metal equilibria. Similarly Balajiva, Quarrel and Vajragupta(62) obtained satisfactory slag samples when using electric arc melting. However, in these cases the metal involved was iron rather than iron-carbon alloys. There can be little doubt that carbon removal changed the composition of the slag in contact with the metal so rapidly that a viscous layer was formed which inhibited further reaction or melting. Consequently the furnace had reluctantly to be abandoned.

Still aiming to get information about changing slag composition it was decided to revert to the molybdenum furnace with 1" diameter magnesite brick crucibles and to use larger slag additions.

Heat 32 was carried out in this manner employing, as in all future runs, the basic open-hearth slag M251(4). The additions in this heat graphed in Figure 17 were made over too short a time interval with the result that the metal surface chilled for about 30 minutes. Run 33 was a duplicate run with similar additions but these were spaced out over a longer time. The carbon drop and oxygen curves for this heat are also plotted in Figure 17.

FIGURE 18
MAGNESITE CRUCIBLES
M 251 (4) B.O.H. SLAG
+ FeO ADDITIONS

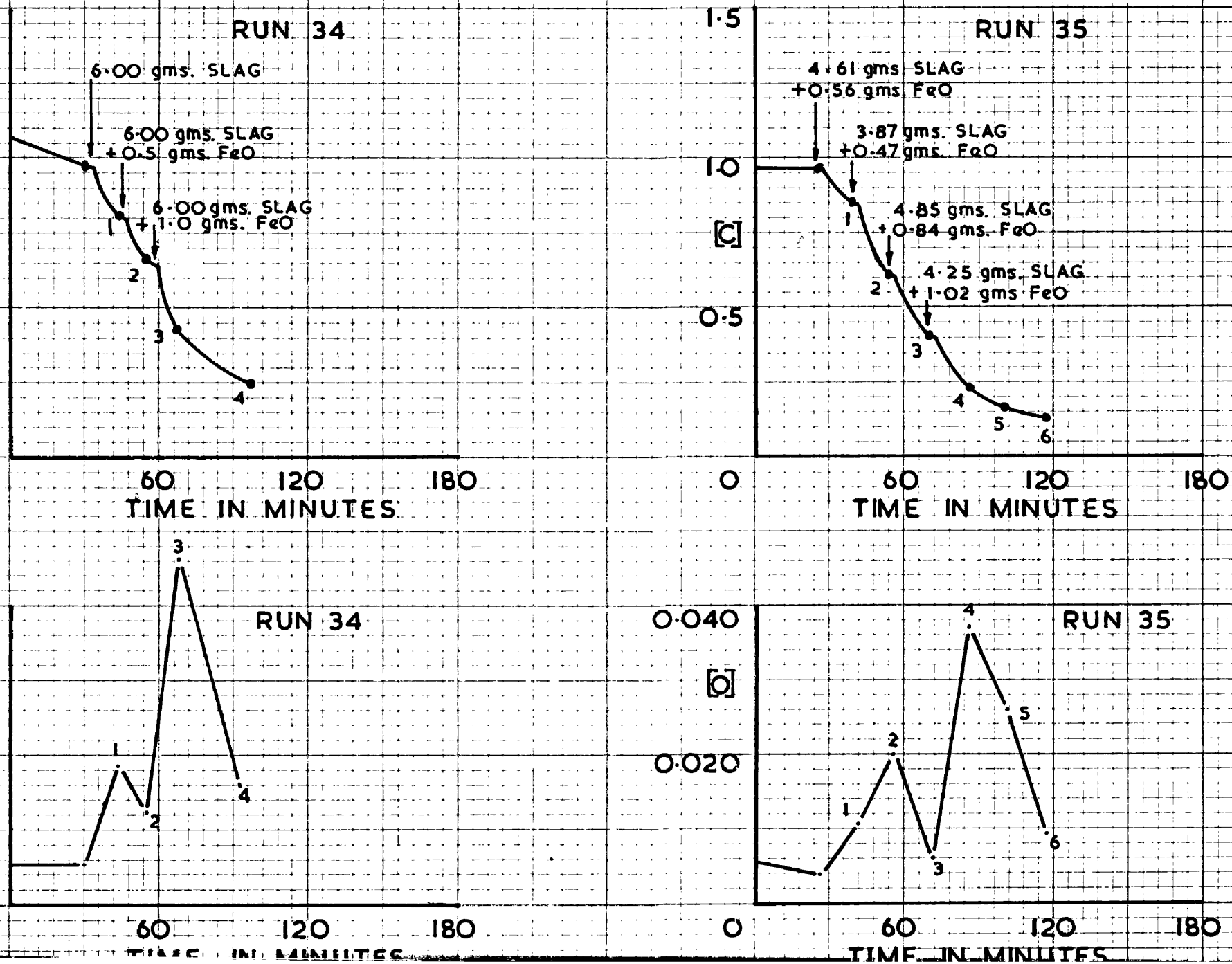

FIGURE 19
MAGNESITE CRUCIBLE
M 251 (4) B.O.H. SLAG
+ FeO ADDITIONS

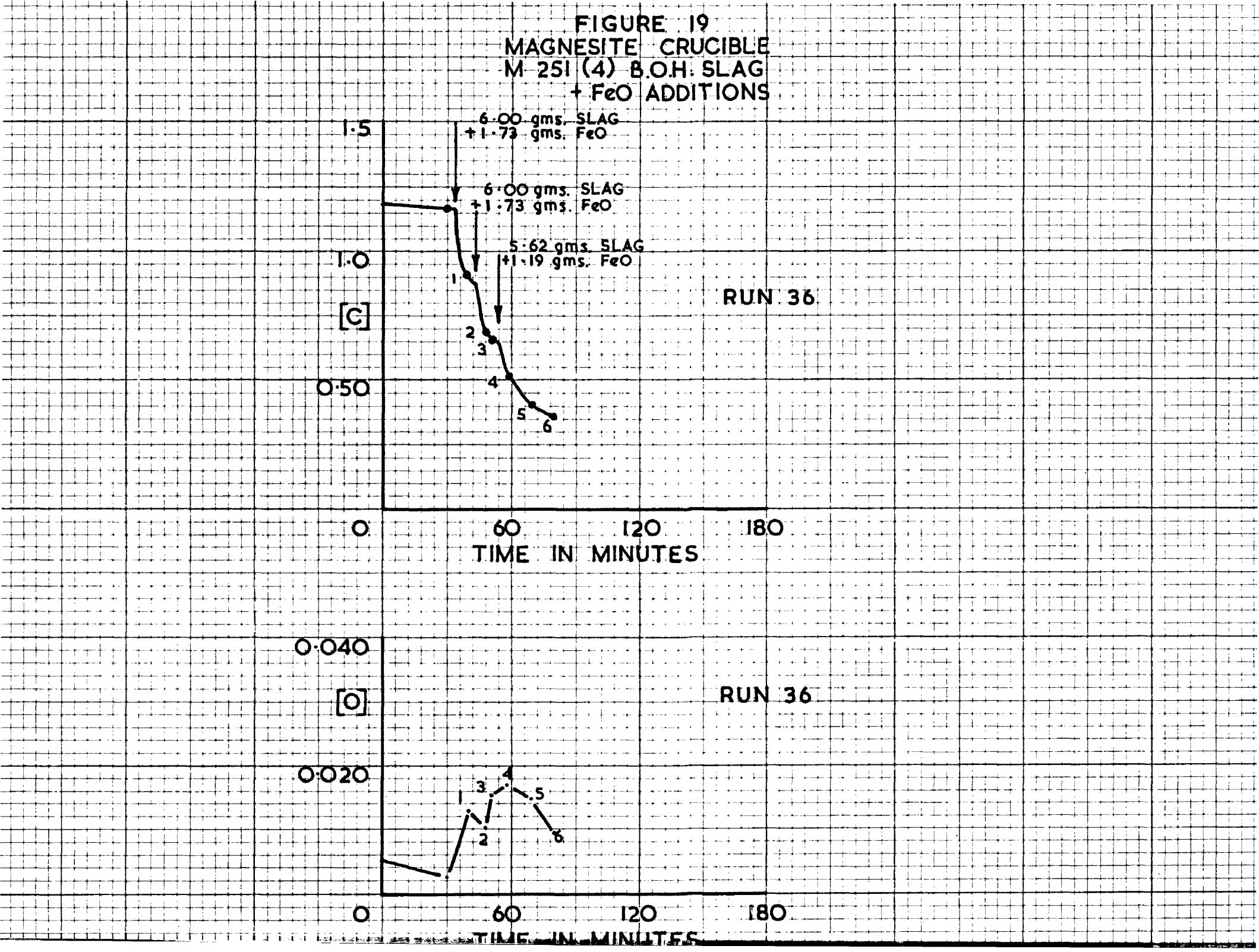

After the reaction had ceased in these two runs, the slag remaining while in greater quantity than in previous heats, appeared to be quite viscous and crusty, presumably due to changes in composition brought about by reaction with the metal and crucible, this viscous nature making it impossible to obtain slag samples as desired.

In an effort to improve upon this, quantities of ferrous oxide were intimately mixed with the slag additions made to subsequent runs. It was felt that these additions would help to maintain the fluidity of the slag but they did nothing to improve the condition of the slag for sampling. The results of these runs (34, 35 and 36) are shown in Figs. 18 and 19.

FIGURE 20
MgO CRUCIBLES
VARIOUS SLAG ADDITIONS

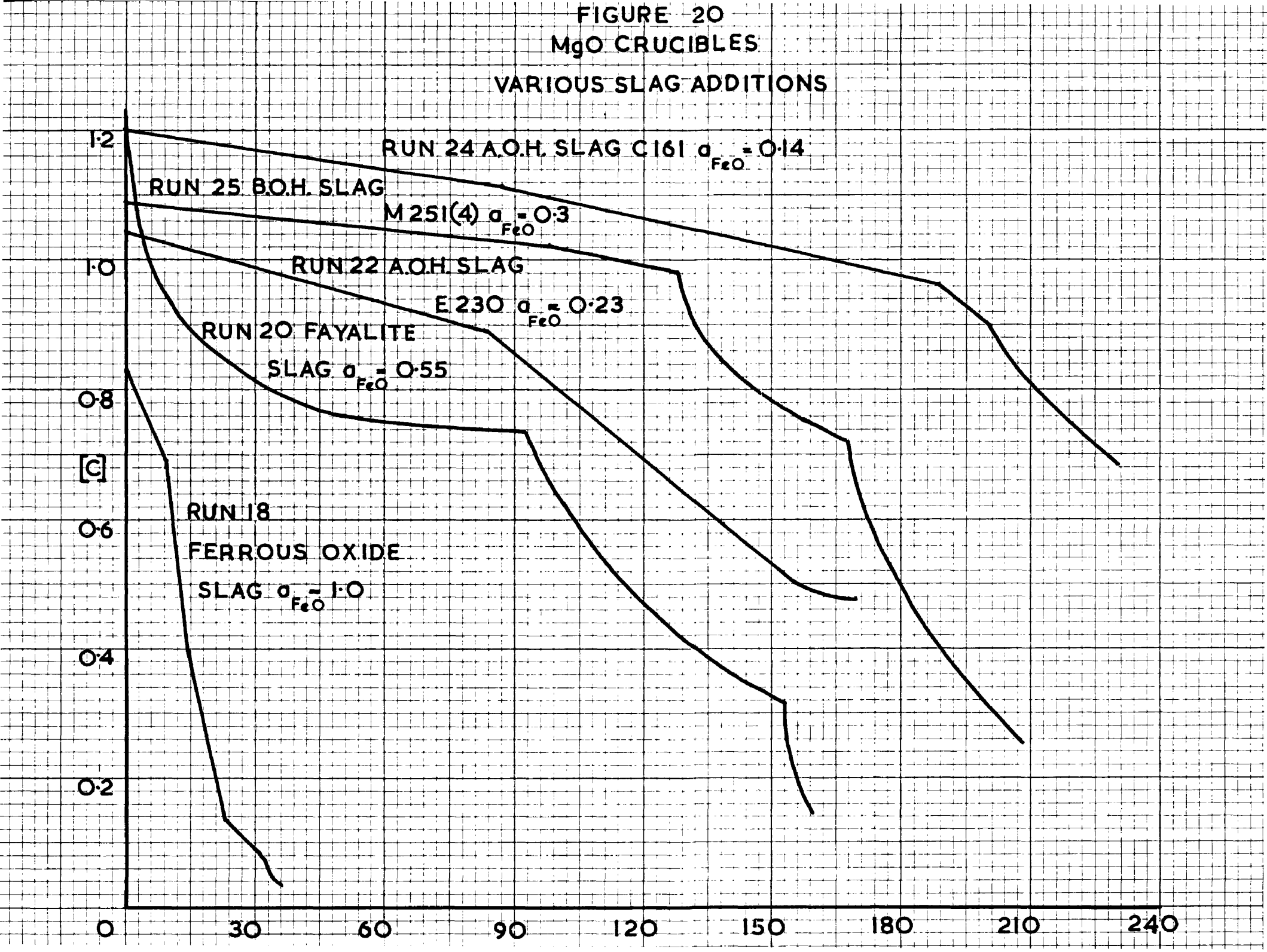

DISCUSSION OF RESULTS FROM LABORATORY SLAG-METAL EXPERIMENTS.

While the conclusions from the laboratory slag-metal work are largely qualitative several points are firmly established.

(a) The slag of highest ferrous oxide activity gave the highest rate of carbon elimination.

In Figure 20 are replotted the carbon drop curves in magnesia crucibles for the five slags employed, i.e., pure ferrous oxide, fayalite, the basic open hearth slag M251(4) and the two acid open hearth slags E230 and C161. The list above places the slags in order of decreasing ferrous oxide activity and it will be seen from Figure 20 that the rate of carbon elimination decreases in the same manner being greatest with the pure ferrous oxide and least with the acid slag C161. The ferrous oxide activity of the slag may thus be looked upon as the power of the slag to supply the metal beneath it with the oxygen necessary for carbon removal. However, since it was not possible to obtain slag samples it is difficult to analyse the results quantitatively as the changing composition of the slag must have considerable influence on the ferrous oxide activity. For example, the fayalite slag will soon become one saturated with silica for which the ferrous oxide activity according to the equation of Schuhmann and Ensio(63)

$$\log a_{FeO} = \frac{300}{T} - 0.590$$

is 0.375 at 1550°C.

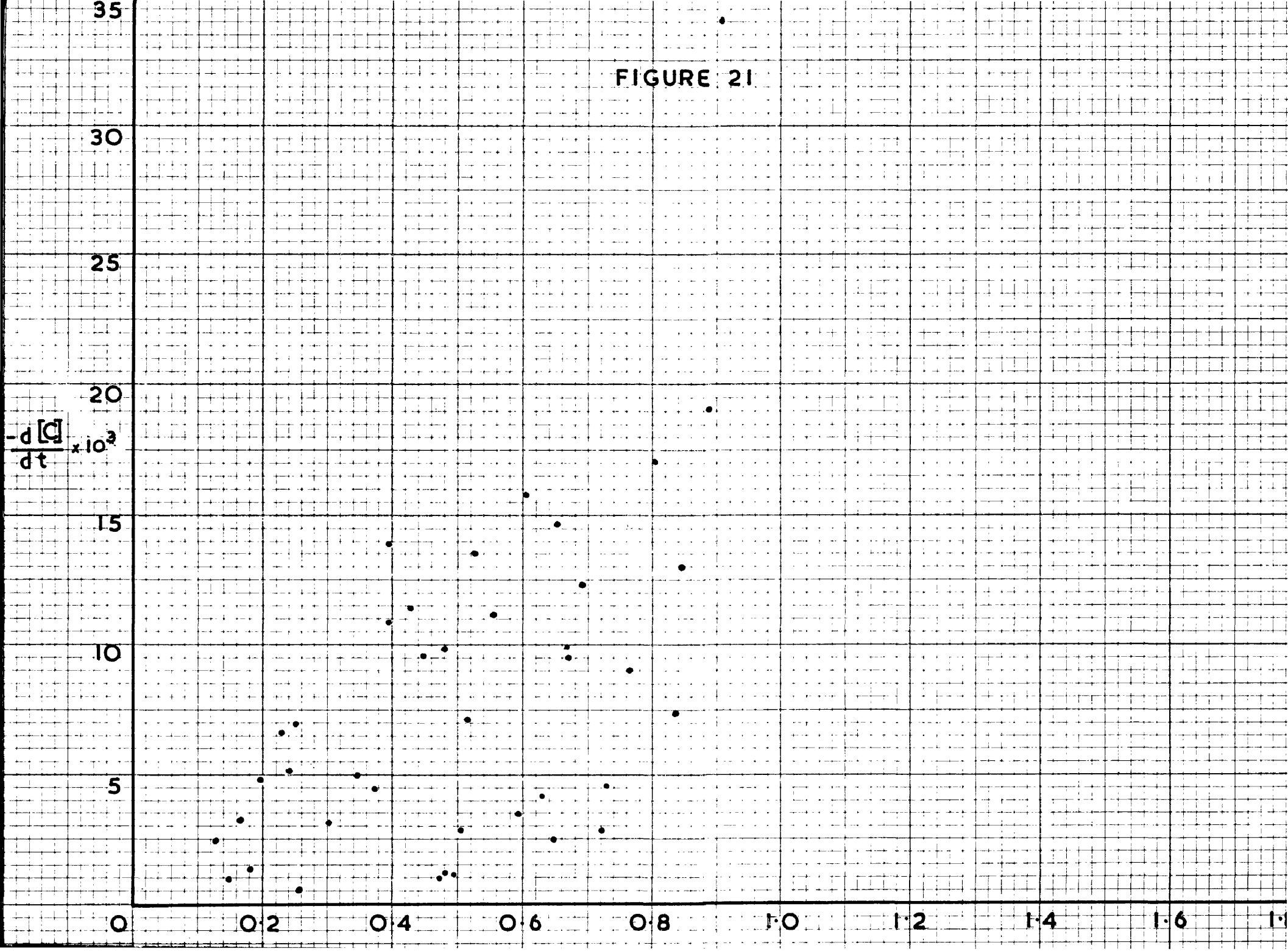

FIGURE 21

(b) The rate of carbon elimination immediately following a slag addition was always greater than when the metal had been under that addition for some time. Thus the rates of carbon removal, carbon and oxygen contents for the three samples following the last slag addition to heats 33 and 36 are :

Sample Number	Carbon %	Oxygen %	$\frac{-d[C]}{dt}$ %/minute.
33(5)	0.196	0.0125	0.0048
33(6)	0.180	0.0087	0.0014
33(7)	0.147	0.0097	0.0010
36(4)	0.513	0.0165	0.0072
36(5)	0.491	0.0143	0.0012
36(6)	0.480	0.0096	0.0012

and for samples drawn earlier in the heats 25, 33 and 36 are

25(4)	0.845	0.0087	0.0129
25(5)	0.720	0.0035	0.0029
33(1)	0.671	0.0117	0.0095
33(2)	0.627	0.0055	0.0043
36(2)	0.693	0.0100	0.0123
36(3)	0.666	0.0155	0.0099

Although higher rates of carbon removal were obtained at higher carbon contents it is obvious from the above data that there can be no quantitative relationship between carbon content and rate of carbon removal. This is clearly illustrated by the scatter in Figure 21 where $-\frac{d[C]}{dt}$ is plotted against carbon content for all the laboratory slag-metal runs employing open hearth slags.

(c) The supersaturation effect noticed in the slag-free runs was again in evidence, there being always an evolution of gas when the silica sampling tube touched the base of the crucible. The effect was less

FIGURE 22

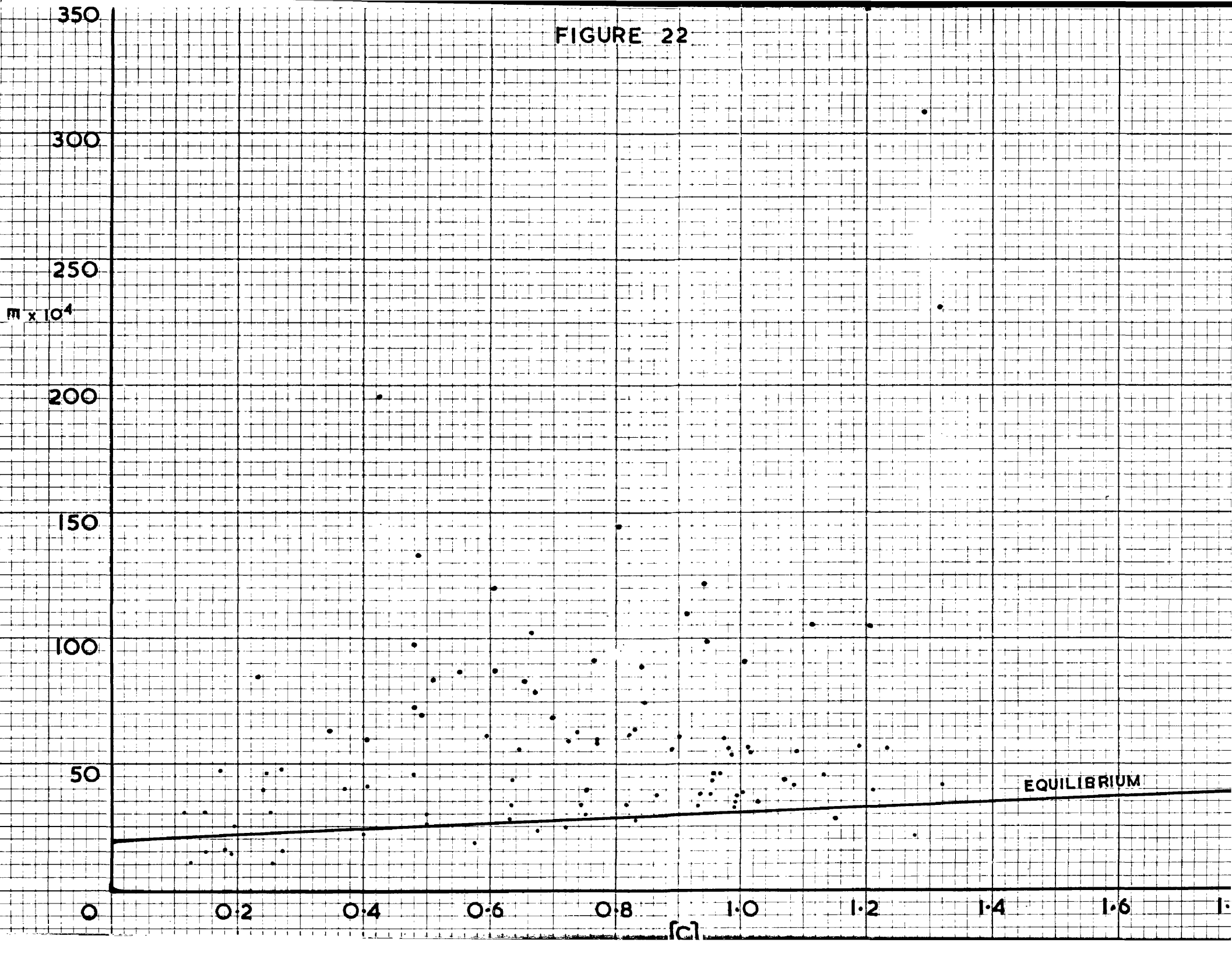
350
300
250
m x 10⁴
200
150
100
50
0
0·2
0·4
0·6
0·8
1·0
1·2
1·4
1·6
EQUILIBRIUM
[C]

pronounced as the run progressed. In most runs oxygen contents decreased after the last slag addition in spite of the fact that the carbon was decreasing. This latter effect is evident from the above data from runs 33 and 36 and earlier in the runs 25, and 33. . The extent of the supersaturation is shown in Figure 22 where m is plotted against carbon content and the equilibrium curve according to Chipman is also included. The calculated values of m are given in Table V and from these it will be seen that m always increased after a slag addition and then decreased if no further addition was made for some time. This is most clearly demonstrated by the samples drawn after the last slag addition to a heat, for example the last three samples from heat 36 gave the following figures.

Sample No.	Carbon %.	Oxygen %	m
36(4)	0.513	0.0165	0.0085
36(5)	0.491	0.0143	0.0070
36(6)	0.480	0.0096	0.0046

This closer approach to equilibrium after the last slag addition is of great interest. The additions involved were sufficient to cover the metal surface when first made but on reacting with the metal and changing in composition the slag, as has already been stated, became viscous. Sampling of the melt after the cessation of the initial reaction normally left the slag adhering to the crucible walls some distance above the metal, the surface of the latter being then exposed to the atmosphere of the furnace. Such was the case in heat 36 after sample (4) was drawn and this infers that the metal when exposed can come to equilibrium with respect to carbon and oxygen by means of the gas phase while being

prevented from doing so when under slag.

Effect of Additions to Crucible Bases.

Neither the addition of graded magnesia to the base of the crucible in heat 26 nor of graded magnesite to the crucible in heat 31 had any accelerating effect on the rate of carbon removal. Heat 22 was identical to heat 26 except for this magnesia addition and the carbon drop curves for these two heats plotted in Figure 13 are almost superimposable. Such an addition might be expected to increase the rate of decarburisation by reducing the difficulty in bubble formation. That there has been no noticeable alteration in the degree of supersaturation is clearly shown by the oxygen contents of 0.0081% and 0.0075% at 0.725% carbon and 0.771% carbon respectively in the two heats. Thus if supersaturation existed in heat 22 then it was almost certainly present in heat 26 as well.

Slag Decarburising Efficiency.

Table VII was drawn up to estimate the decarburising efficiency of the different slags employed in the laboratory slag-metal experiments. From the difference between the weight of carbon in the charge and that in the metal in the crucible at the end of each heat was subtracted the sum of the carbon physically removed in the metal samples, the carbon removed during melting down and the carbon removed by crucible reaction at 1550°C. The weight of carbon thus arrived at was, in the case of heats 18 to 24 inclusive and heat 26, taken to be that removed by the slag. The analyses of the metal samples drawn throughout all the heats

TABLE VII.

Laboratory Slag Metal Experiments.

Heat No.	Type of Crucible	Type of Slag.	Weight of slag additions (gms.)	Time at 1550°C (Mins.)	Total Carbon Removed (gms.)	Carbon removed by samples (gms.)	Carbon Removed in Melt Down (gms.)	Carbon removed by crucible action at 1550°C (gms.)	Carbon removed by slag (gms.)	Carbon Equivalent FeO (gms.)	Carbon Equivalent MnO (gms.)	Carbon Equivalent Total (gms.)	Carbon removed by slag Total carbon equivalent of FeO and MnO in slag. x 1
18	MgO	FeO	3.387	28	1.097	0.238	0.390	0.030	0.439	0.565	-	0.565	78
19	Al_2O_3	FeO	2.230	60	0.906	0.258	0.419	0.030	0.199	0.521	-	0.521	38
20	MgO	$2FeO.SiO_2$	4.971	180	1.479	0.648	0.236	0.167	0.428	0.586	-	0.586	73
21	Al_2O_3	$2FeO.SiO_2$	4.055	108	1.721	1.091	0.201	0.095	0.335	0.478	-	0.478	70
22	MgO	E230 A.O.H.	6.983	190	1.243	0.455	0.389	0.212	0.188	0.339	0.223	0.562	33
23	Al_2O_3	E230 A.O.H.	4.653	125	1.239	0.877	0.185	0.071	0.107	0.226	0.149	0.375	29
24	MgO	C161 A.O.H.	2.402	255	1.392	0.838	0.253	0.271	0.030	0.050	0.089	0.139	22
25	MgO	M251 (4) B.O.H.	6.380	110	1.041	0.700	0.017	+ C removed by P_2O_5 0.201	0.123	0.103	0.058	0.161	75
26	MgO + graded MgO	E230 A.O.H.	3.397	148	1.224	0.661	0.281	0.162	0.120	0.165	0.109	0.274	44

TABLE VII.(Cont'd).

Laboratory Slag Metal Experiments.

Heat No.	Type of Crucible.	Wt. of Slag addns.(gms.) M251(4)	FeO	Time at 1550°C (mins.)	Total carbon removed (gms)	Carbon removed by samples (gms.)	Carbon removed in melt down (gms.)	Carbon removed by crucible action at 1550(gms.)	Carbon removed by P_2O_5 in slag (gms.)	Carbon removed by slag excluding P_2O_5 (gms)	Carbon Equivalent. FeO gms.	MnO gms.	Total gms.	C removed by slag / C equ. of FeO and MnO in slag x 10
27	Magnesite	10.00	-	80	0.596	0.179	0.166	0.000	0.046	0.205	0.162	0.090	0.252	81
28	"	6.01	-	74	0.508	0.142	0.218	0.000	0.033	0.115	0.098	0.054	0.152	76
29	"	5.64	-	151	1.052	0.767	0.022	0.148	0.034	0.081	0.092	0.052	0.144	56
31	Magnesite + graded Magnesite	4.56	-	166	1.210	0.608	0.237	0.253	0.025	0.087	0.074	0.042	0.116	75
32	Magnesite	27.25	-	145	1.292	0.154	0.645	0.233	0.054	0.206	0.442	0.244	0.686	30
33	"	30.18	-	158	1.045	0.322	0.185	0.133	0.056	0.349	0.489	0.270	0.759	46
34	"	18.00	1.50	130	1.420	0.405	0.510	0.163	0.048	0.294	0.543	0.161	0.704	42
35	"	17.50	2.89	150	1.180	0.514	0.210	0.000	0.028	0.428	0.767	0.157	0.924	46
36	"	17.63	4.65	94	1.268	0.457	0.260	0.053	0.040	0.458	1.064	0.158	1.222	38

employing acid open-hearth slags showed considerable manganese pick up while those from the basic open-hearth slags showed both manganese and phosphorus pick up. The presence of these two elements indicates that the reactions

$$MnO + \underline{C} = \underline{Mn} + CO$$

and $$P_2O_5 + \underline{5C} = \underline{2P} + 5CO$$

have been responsible for the removal of carbon (probably by the intermediate formation of FeO) as well as the expected reaction with ferrous oxide,

$$FeO + \underline{C} = \underline{Fe} + CO$$

Consequently, from the figure obtained for the carbon removed by the slag as outlined above, that removed by phosphorus pentoxide, estimated from the phosphorus content of the metal, was subtracted for the basic slag runs. The decarburising power of the slag addition to each heat was then taken to be the weight of carbon involved in allowing the reactions

$$FeO + \underline{C} = \underline{Fe} + CO$$

$$MnO + \underline{C} = \underline{Mn} + CO$$

to go to completion; this figure in Table VII is called the total carbon equivalent of the slag additions. The weight of carbon removed by the slag divided by this carbon equivalent was then expressed as a percentage in the last column of Table VII.

Heats 18 and 19, in which the pure ferrous oxide additions were made, would be expected to show something like 100% for this quantity. From Table VII it will be seen that Heat 18 gave 78 while heat 19 only gave 38 percent. The large difference here can only be attributed to the loss of slag by virtue of the vigorous nature of the reaction since there was no obvious reaction with the Al_2O_3 crucible. For the purpose of the calculation

only the first three slag additions to heat 18 and the first two to heat 19 were considered, the carbon loss to these points being taken since in both cases the carbon had reached a very low figure before the last slag additions were made. The figures for the fayalite heats 20 and 21 are in very close agreement being 73% and 70% respectively in magnesia and alumina; that these again do not rise to nearer 100% is largely due to the loss of slag by the vigorous nature of the reaction, it being either expelled from the crucible altogether or moved up the walls where it is unable to react with the metal. Furthermore, this method of calculating the efficiency assumes the reactions to go to completion which is most unlikely. Certainly with the acid and basic open-hearth slags neither the ferrous oxide nor the manganous oxide would be expected to be completely reduced and consequently 100% efficiency would not be anticipated with additions of these.

The basic open hearth finishing slag M251(4) gave the highest figures with small slag additions. While this slag had a lower ferrous oxide activity than FeO or fayalite, the higher efficiency obtained is almost certainly due to the less vigorous nature of the reaction enabling all the slag to stay in the crucible and act upon the metal. The lower efficiencies obtained with the larger weights of basic slag were purely and simply a function of the bulk, the slag sticking to the sides of the crucibles when the metal samples were drawn and being lost as far as further reaction was concerned. The inclusion of ferrous oxide with the basic slag aggravated these effects and consequently produced low efficiency figures.

Where small slag bulks were employed the two acid open-hearth slags gave the lower carbon removal efficiencies. They were perhaps more

prone than any others to stick to the crucible walls when the metal was sampled and be lost for further reaction, their high viscosity probably increasing this effect.

CHAPTER 5.

OPEN HEARTH DATA.

OPEN HEARTH DATA.

Since attempted slag sampling had met with no success in the laboratory tests it was decided to investigate some works heats where slag samples could be readily obtained. Twelve heats of basic open-hearth and five heats of acid open-hearth steel were studied. During the working of these heats bomb samples were drawn for oxygen determination simultaneously with slag and metal spoon samples. The oxygen analyses were all determined by the vacuum fusion method and all the acid and some of the basic open-hearth samples were also analysed by a chemical method,(conversion to alumina followed by a nephelometric determination). The carbon drop curves and logs of these heats are given in an appendix.

By drawing tangents to the carbon drop curves at the times when samples were taken, the rates of carbon drop, expressed in percentage per minute, were calculated. These rates along with the carbon and oxygen contents of the samples and the products of carbon and oxygen are given in Table VIII.

The data of Herasymenko(7), obtained during the working of an acid open-hearth furnace, and basic open-hearth data obtained by Mackenzie(17) Fornander(24) and Kerlie(64) have also been used so that conclusions may be based on results which will not be biased by the mode of working the heats or the nature of any specific hearth.

TABLE VIII.

Sample Number.	[C]	[O] V.F.	[O] Chem.	[C][O] V.F.	Δ[O]	$\frac{-d[C]}{dt}$ %/min.
B.O.H. 2(7)	0.102	0.030_3	0.030	0.0030	0.008_8	0.002_1
B.O.H. 3(1)	0.213	0.017_1	0.016	0.0036	0.006_7	0.002_0
B.O.H. 3(2)	0.123	0.028_2	0.025	0.0035	0.010_2	0.001_7
B.O.H. 4(1)	0.337	0.009_6	0.013	0.0032	0.003_0	0.002_2
B.O.H. 4(2)	0.261	0.013_6	0.017	0.0036	0.005_1	0.002_2
B.O.H. 4(3)	0.228	0.018_7	0.017_5	0.0043	0.008_9	0.002_2
B.O.H. 4(4)	0.145	0.027_6	0.026	0.0040	0.012_3	0.002_2
B.O.H. 5(A)	0.614	0.007_6	0.011	0.0047	0.004_0	0.007_3
B.O.H. 5(B)	0.260	0.016_8	0.013	0.0044	0.008_3	0.003_9
B.O.H. 5(C)	0.160	0.020_8	0.019	0.0033	0.005_9	0.001_6
B.O.H. 6(1)	0.310	0.015_1	0.021	0.0047	0.007_9	0.003_2
B.O.H. 6(2)	0.257	0.018_2	0.021	0.0047	0.009_6	0.002_5
B.O.H. 6(3)	0.188	0.024_2	0.030	0.0045	0.012_4	0.002_5
B.O.H. 7(1)	0.605	0.006_8	0.011	0.0041	0.003_2	0.005_8
B.O.H. 8(1)	0.631	0.009_0	0.017	0.0057	0.005_5	0.007_2
B.O.H. 8(3)	0.172	0.017_2	0.018	0.0030	0.004_3	0.004_5
B.O.H. 8(4)	0.123	0.026_9	0.023	0.0033	0.008_9	0.002_3
B.O.H. 9(1)	0.505	0.011_1	0.010	0.0056	0.006_7	0.002_5
B.O.H. 9(2)	0.308	0.028_7	0.018	0.0088	0.021_5	0.006_3
B.O.H. 9(3)	0.128	0.030_2	0.030	0.0039	0.012_9	0.002_6
B.O.H.10(1)	0.702	0.009_4	0.012	0.0066	0.006_2	0.008_1
B.O.H.10(2)	0.405	0.013_9	0.012_5	0.0056	0.008_5	0.005_4
B.O.H.10(3)	0.175	0.025_7	0.019	0.0045	0.013_1	0.002_2
B.O.H.11(1)	0.576	0.009_3	-	0.0053	0.005_4	0.006_8
B.O.H.11(2)	0.237	0.016_9	0.017	0.0040	0.007_5	0.003_2
B.O.H.11(3)	0.075	0.033_7	0.026_5	0.0025	0.004_1	0.002_7
B.O.H.12(1)	0.720	0.010_5	-	0.0076	0.007_3	0.005_2
B.O.H.12(2)	0.300	0.022_9	-	0.0069	0.015_5	0.006_4
B.O.H.12(3)	0.196	0.020_7	-	0.0041	0.009_4	0.003_0
B.O.H.12(4)	0.117	0.044_3	-	0.0052	0.025_3	0.002_4
B.O.H.14(1)	0.406	0.013_8	-	0.0056	0.008_4	0.003_5
B,O.H.14(2)	0.273	0.016_9	-	0.0046	0.008_7	0.003_6
B.O.H.14(3)	0.177	0.022_7	-	0.0040	0.010_2	0.002_5
B.O.H.14(4)	0.115	0.031_2	-	0.0037	0.011_9	0.001_5
A.O.H. A(1)	0.740	0.007_0	0.007_2	0.0052	0.004_0	0.004_6
A.O.H. A(2)	0.330	0.011_7	0.008_9	0.0039	0.005_0	0.004_6
A.O.H. A(3)	0.224	0.012_9	0.016_3	0.0029	0.003_0	0.001_8
A.O.H. A(4)	0.170	0.020_6	0.023_3	0.0035	0.007_5	0.000_9
A.O.H. B(1)	0.960	0.004_8	0.004_6	0.0043	0.002_2	0.003_6
A.O.H. B(2)	0.405	0.012_9	0.008_4	0.0052	0.007_4	0.003_6
A.O.H. B(3)	0.250	0.018_7	0.020_0	0.0047	0.009_8	0.003_1
A.O.H. B(4)	0.123	0.026_1	0.032_0	0.0032	0.008_0	0.002_5
A.O.H. C(1)	0.669	0.006_9	0.008_4	0.0047	0.003_6	0.005_0

TABLE VIII. (Cont'd)

Sample Number	[C]	[O] V.F.	[O] Chem.	[C][O] V.F.	Δ[O]	$\frac{-d[C]}{dt}$ %/min.
A.O.H. C(2)	0.360	0.013_1	0.013_0	0.0047	0.007_0	0.005_2
A.O.H. C(3)	0.220	0.018_9	0.023_3	0.0042	0.008_8	0.002_4
				$[C][O]_{Chem.}$		
A.O.H. E(2)	0.515	-	0.007_4	0.0038	0.0031	0.003_5
				$[C][O]_{V.F.}$		
A.O.H. E(3)	0.393	0.008_1	0.011_6	0.0032	0.002_4	0.001_7
A.O.H. E(4)	0.220	0.018_7	0.021_0	0.0041	0.008_6	0.004_3
A.O.H. F(2)	0.620	0.011_6	0.009_3	0.0058	0.007_4	0.003_6
A.O.H. F(3)	0.390	0.011_8	0.013_0	0.0058	0.009_1	0.004_6
A.O.H. F(4)	0.360	0.010_2	0.016_0	0.0039	0.004_7	0.000_9
A.O.H. F(5)	0.350	0.012_0	0.020_0	0.0042	0.005_6	0.000_2

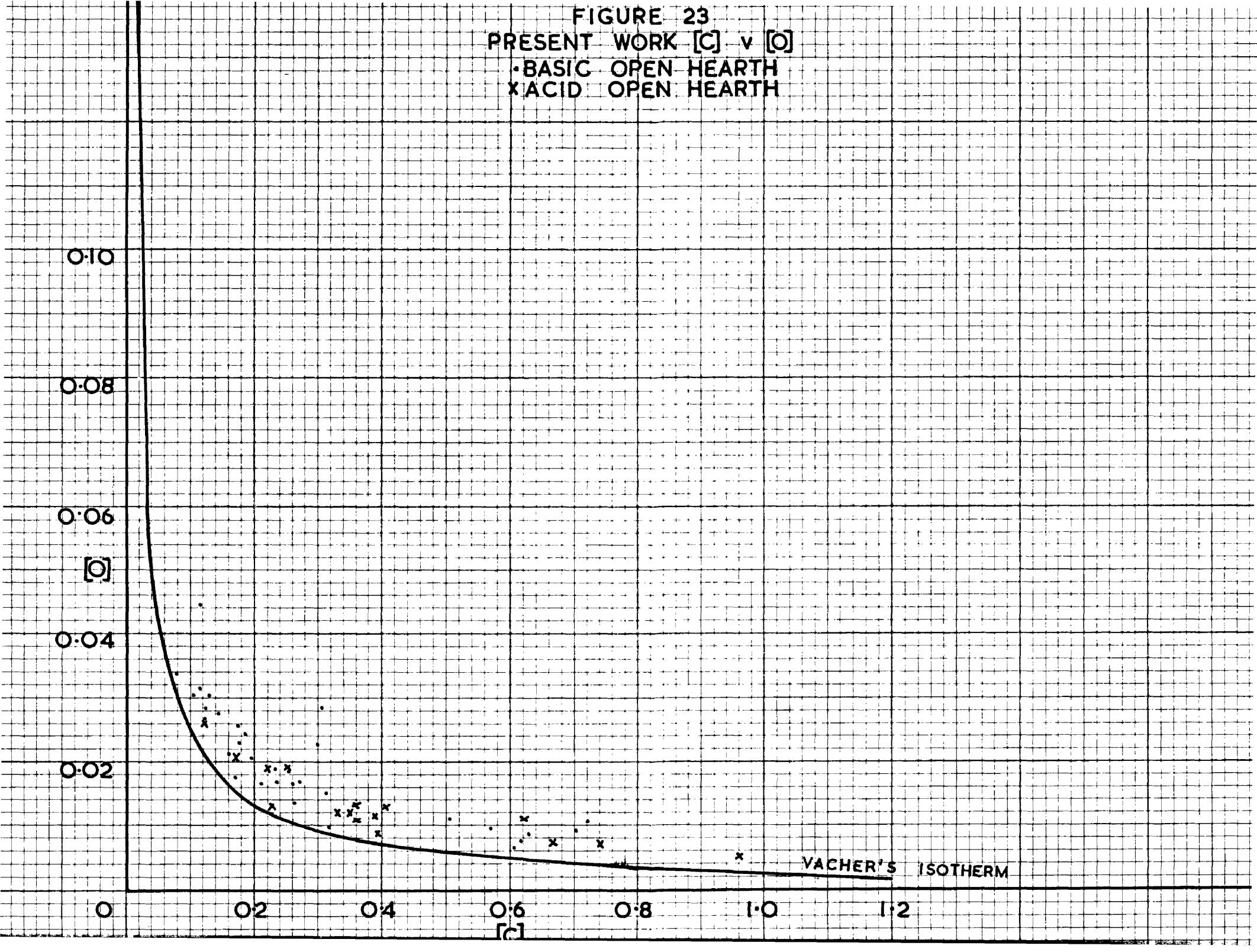
FIGURE 23
PRESENT WORK [C] v [O]
•BASIC OPEN HEARTH
xACID OPEN HEARTH
0·10
0·08
0·06
[O]
0·04
0·02
0
0·2
0·4
0·6
0·8
1·0
1·2
[C]
VACHER'S ISOTHERM

The Carbon-Oxygen Relationship in the Open-Hearth.

A plot of oxygen against carbon for both acid and basic open hearth heats in the present work was made in Figure 23 in which is reproduced the Vacher equilibrium isotherm. This verified the well known fact to which reference has been made in the introduction, that the oxygen in the open hearth is greater than that which would be in equilibrium with the carbon present.

This may be demonstrated otherwise by the plot of the carbon-oxygen product m against carbon content as shown in Figures 24A for the present work, 24B for the data of Herasymenko, Figure 24C for Mackenzie and Figure 24D for the data of Fornander and Kerlie. The best lines for these plots were also calculated and are included in the respective figures together with the equilibrium line of Chipman; Marshall and Chipman(3) attributed the increase in m with carbon content at equilibrium to the effect of carbon on the activity coefficient of oxygen, the latter decreasing rapidly with increasing carbon content. At the same time the activity coefficient of carbon was only slightly raised. This explanation has been generally accepted, only Herasymenko(7) preferring to believe that carbon increases the activity of oxygen. He attributed the variance between his results and those of Chipman to the manner in which the oxygen determinations of Chipman were made. The experiments of Chipman were carried out in magnesia crucibles in atmospheres of carbon monoxide and carbon dioxide and he added aluminium to the melts and estimated alumina in the solidified samples. Herasymenko believed that this method could lead to higher oxygen figures than were actually present in the liquid because of the possibility of reaction

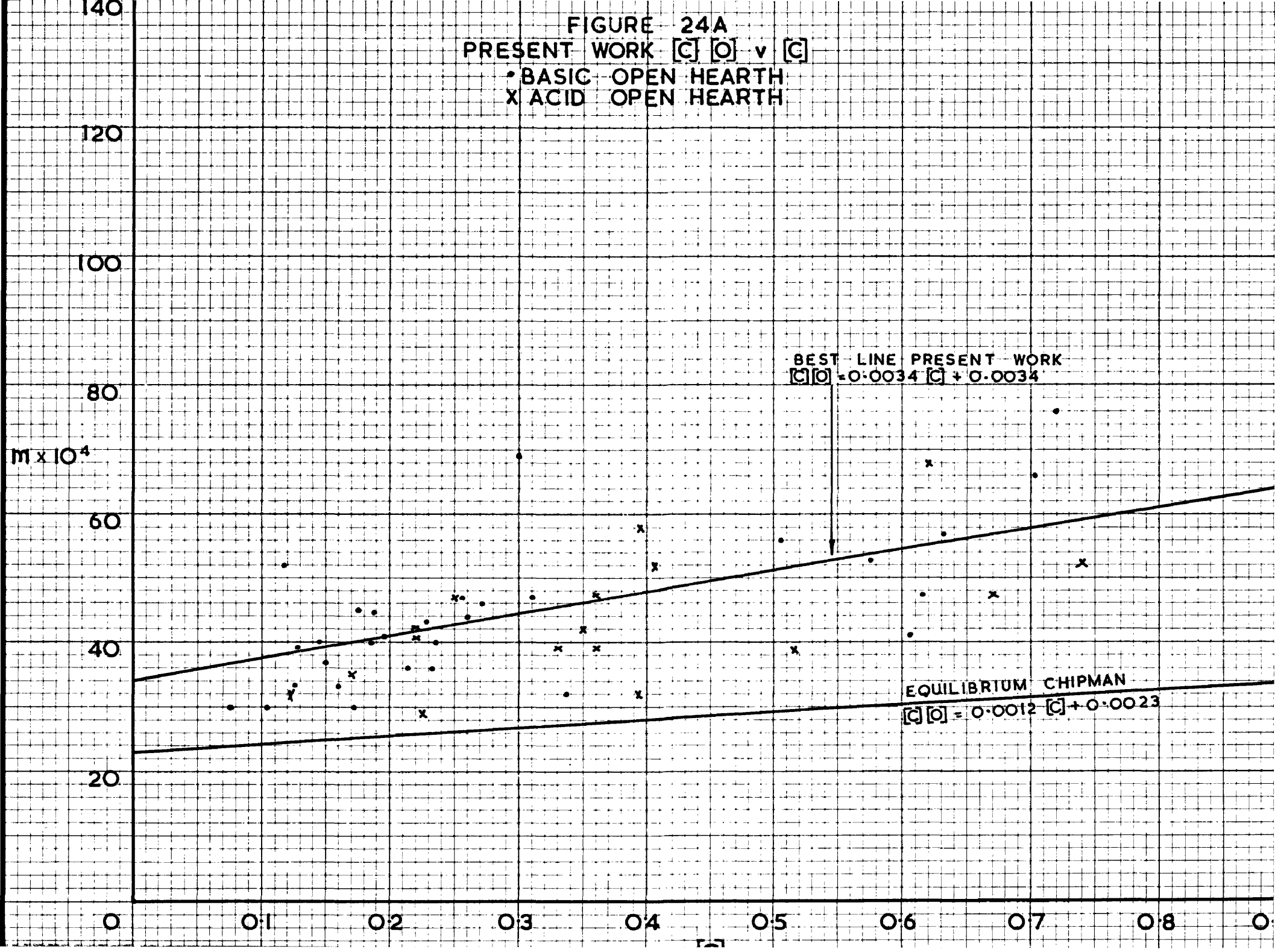
FIGURE 24A
PRESENT WORK [C] [O] v [C]
• BASIC OPEN HEARTH
X ACID OPEN HEARTH
BEST LINE PRESENT WORK
[C][O] = 0·0034 [C] + 0·0034
EQUILIBRIUM CHIPMAN
[C][O] = 0·0012 [C] + 0·0023
m x 10⁴
140
120
100
80
60
40
20
0
0·1
0·2
0·3
0·4
0·5
0·6
0·7
0·8
0
[C]

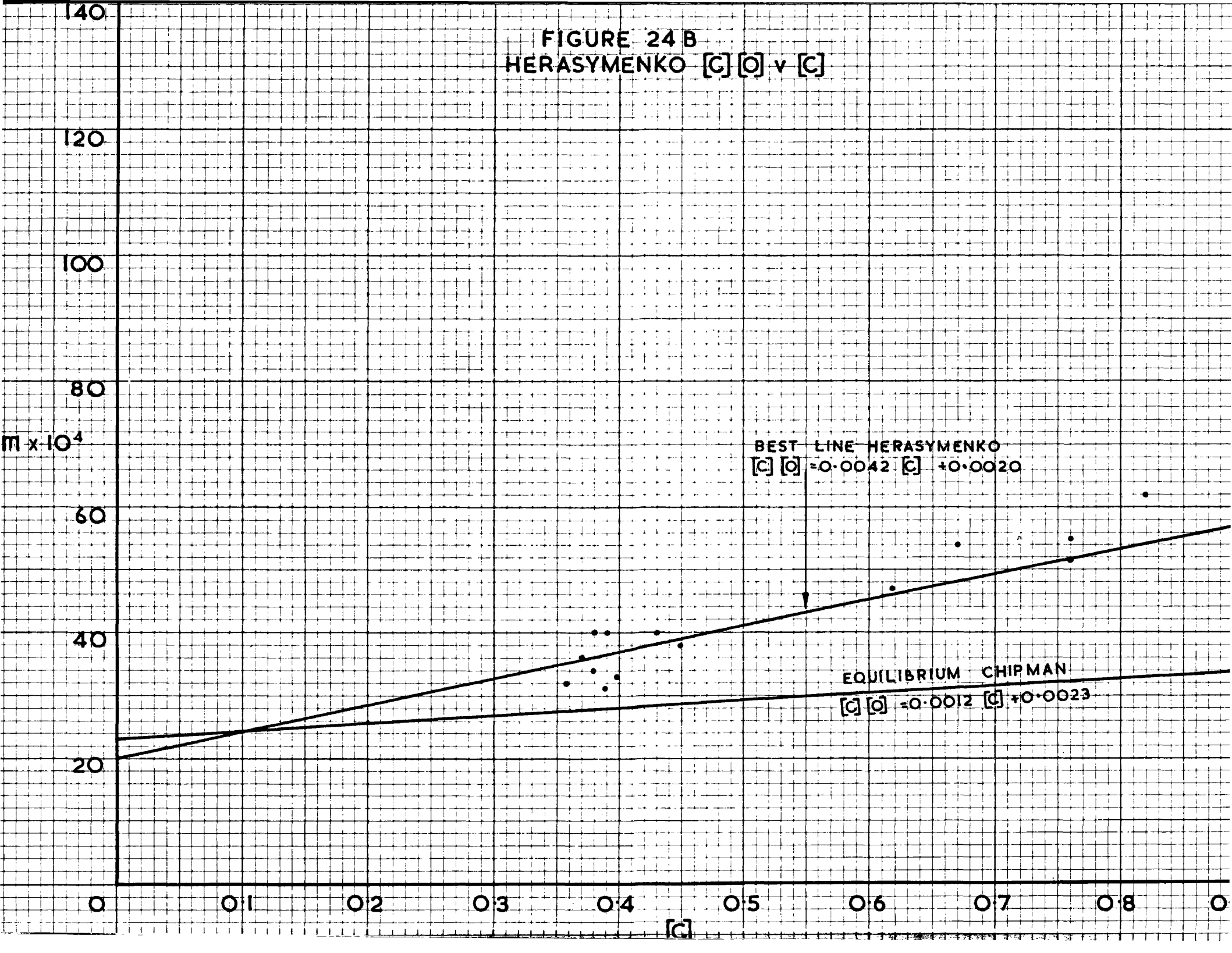
FIGURE 24 B
HERASYMENKO [C][O] v [C]
140
120
100
80
m x 10⁴
60
40
20
0
0·1
0·2
0·3
0·4
0·5
0·6
0·7
0·8
0
[C]
BEST LINE HERASYMENKO
[C][O] =0·0042 [C] +0·0020
EQUILIBRIUM CHIPMAN
[C][O] =0·0012 [C] +0·0023

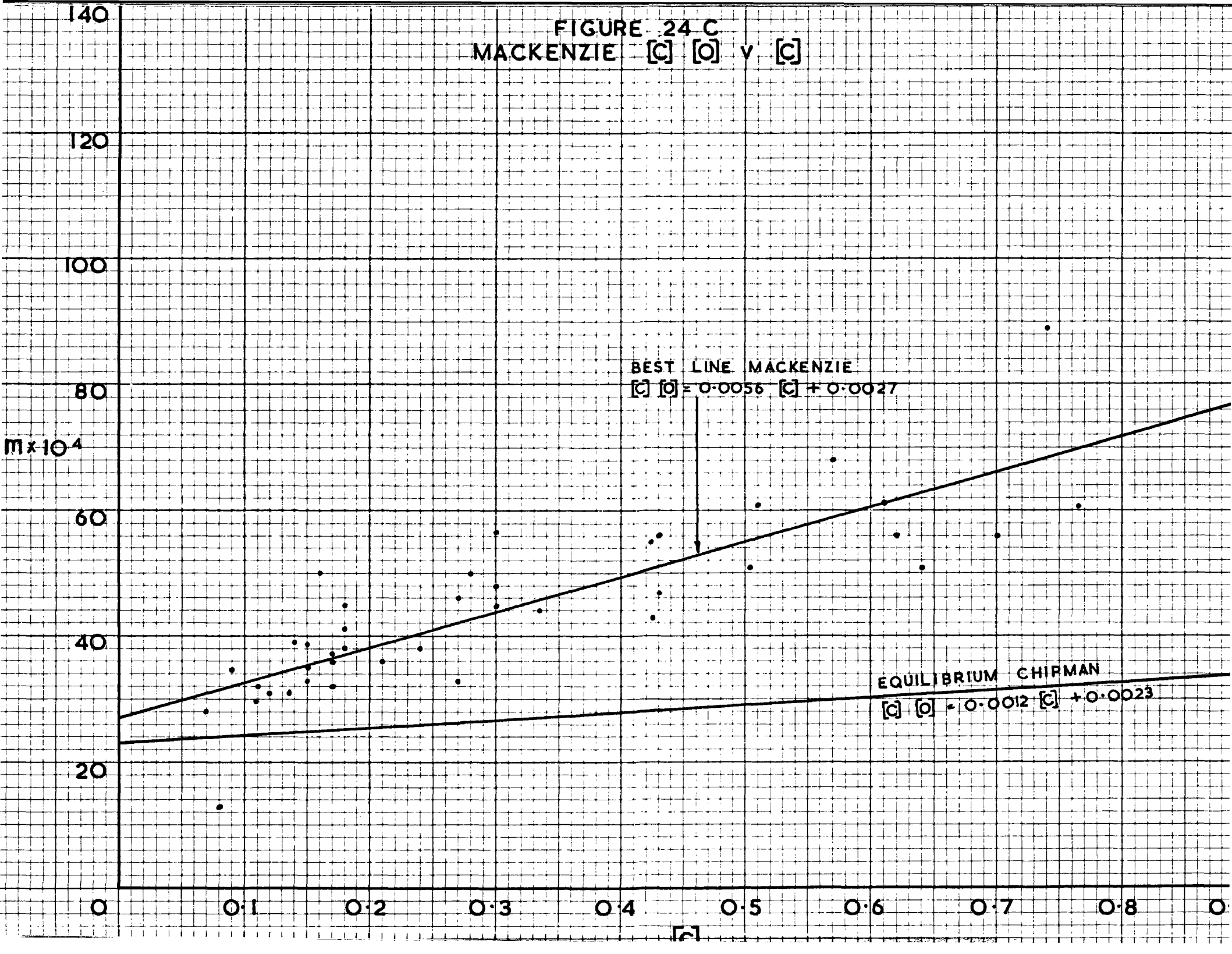
FIGURE 24 C
MACKENZIE [C] [O] v [C]
140
120
100
80
60
40
20
0
M x 10⁴
BEST LINE MACKENZIE
[C] [O] = 0·0056 [C] + 0·0027
EQUILIBRIUM CHIPMAN
[C] [O] = 0·0012 [C] + 0·0023
0·1
0·2
0·3
0·4
0·5
0·6
0·7
0·8
0
[C]

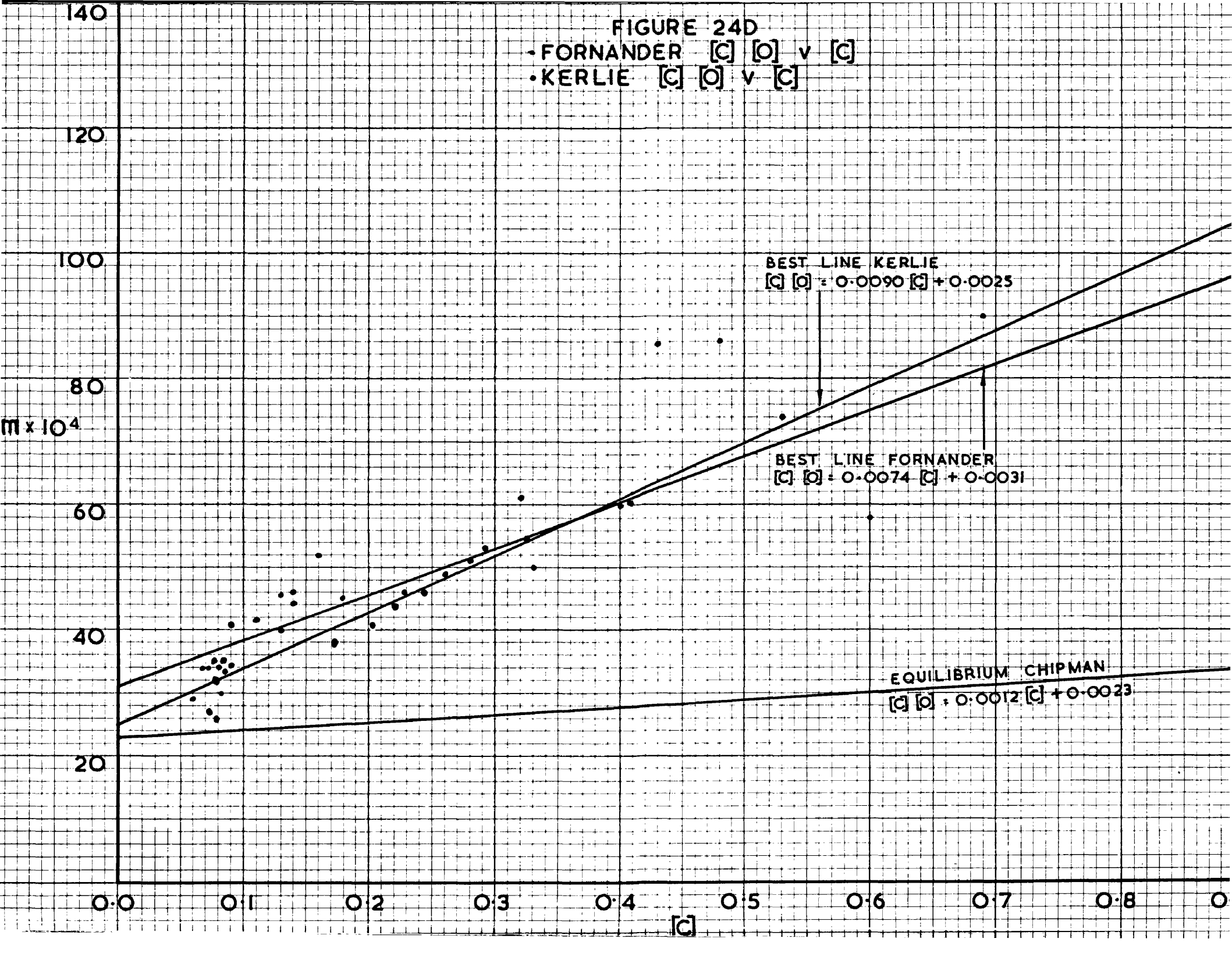
FIGURE 24D
• FORNANDER [C] [O] v [C]
• KERLIE [C] [O] v [C]
BEST LINE KERLIE
[C] [O] = 0·0090 [C] + 0·0025
BEST LINE FORNANDER
[C] [O] = 0·0074 [C] + 0·0031
EQUILIBRIUM CHIPMAN
[C] [O] = 0·0012 [C] + 0·0023
m x 10⁴
140
120
100
80
60
40
20
0·0
0·1
0·2
0·3
0·4
0·5
0·6
0·7
0·8
[C]

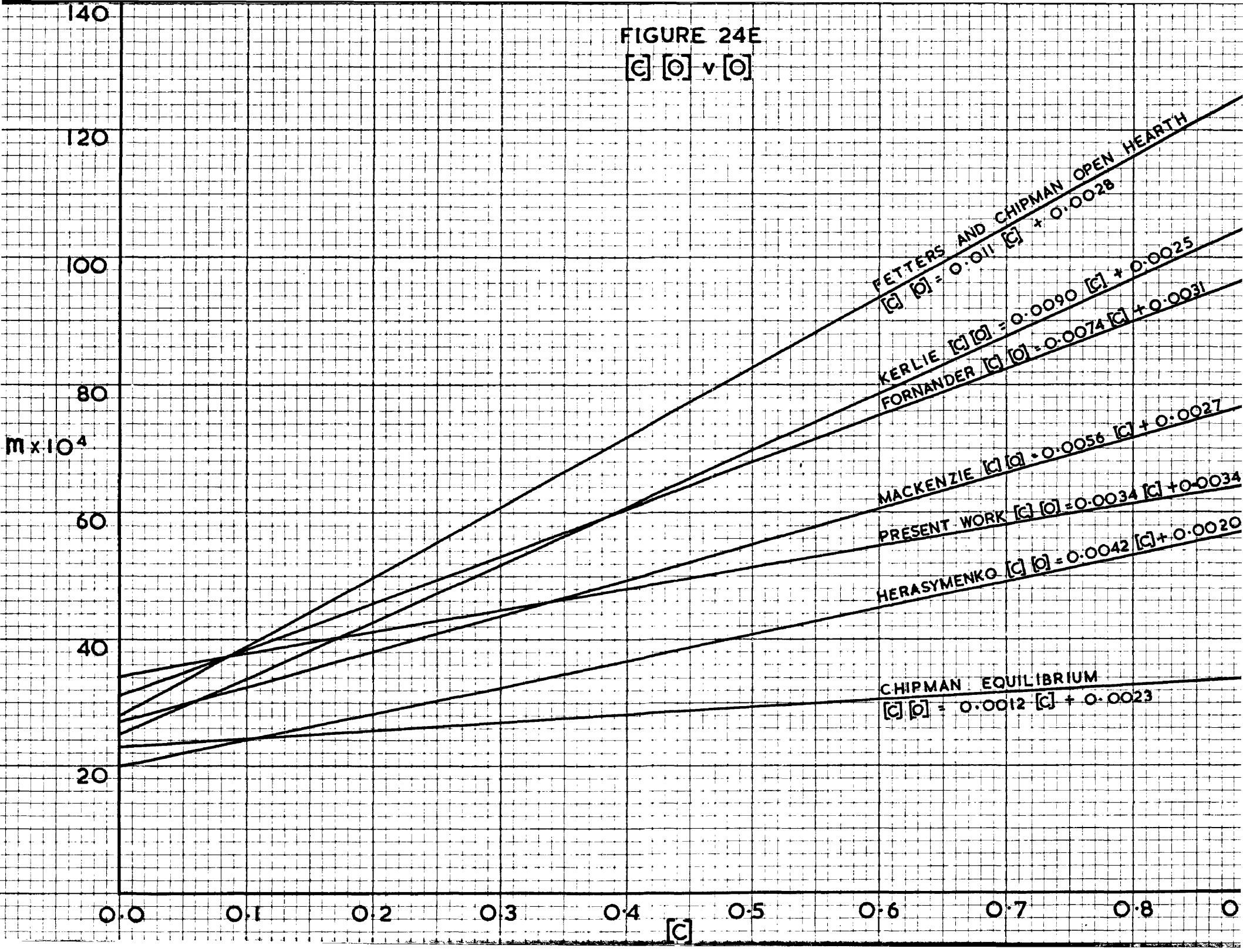
FIGURE 24E
[C] [O] v [O]
140
120
100
80
m x 10⁴
60
40
20
0·0
0·1
0·2
0·3
0·4
0·5
0·6
0·7
0·8
0
[C]
PETTERS AND CHIPMAN OPEN HEARTH
[C] [O] = 0·011 [C] + 0·0028
KERLIE [C] [O] = 0·0090 [C] + 0·0025
FORNANDER [C] [O] = 0·0074 [C] + 0·0031
MACKENZIE [C] [O] = 0·0056 [C] + 0·0027
PRESENT WORK [C] [O] = 0·0034 [C] + 0·0034
HERASYMENKO [C] [O] = 0·0042 [C] + 0·0020
CHIPMAN EQUILIBRIUM
[C] [O] = 0·0012 [C] + 0·0023

between aluminium dissolved in the melt and iron oxide dissolved or absorbed in the walls of the magnesia crucible and with the gas phase. Further laboratory work would require to be undertaken before this point could be finally settled. For the purpose of discussion the results of Chipman will be accepted as correct.

The best lines drawn in Figures 24A to D, are brought together in Figure 24E, which also includes the equilibrium line of Chipman and a line determined by Fetters and Chipman(19) from an investigation of open-hearth heats. All of the lines for the open-hearth data show two common features.

(a) They all indicate that, in the open hearth, $\underline{m}$ increases with carbon content, and

(b) The values of $\underline{m}$ are always in excess of equilibrium.

For a given carbon content the vertical displacement between any of these lines from the equilibrium line is given by :

$$[C][O] - [C][O]_{equ.} = [C]\,\Delta[O]$$

where $\Delta[O]$ is the excess oxygen over equilibrium as described by Larsen(20). From a vast quantity of open-hearth data Larsen concluded that the excess oxygen was independent of the carbon content although its average value was related to the bath condition being greatest following an ore addition (0.023-0.035%), least during a lime boil or bottom boil (0.009-0.015%) and intermediate (0.015-0.025%) during what he referred to as "steady state" conditions, i.e., during the refining period when no recent addition has been made to metal or slag.

FIGURE 25

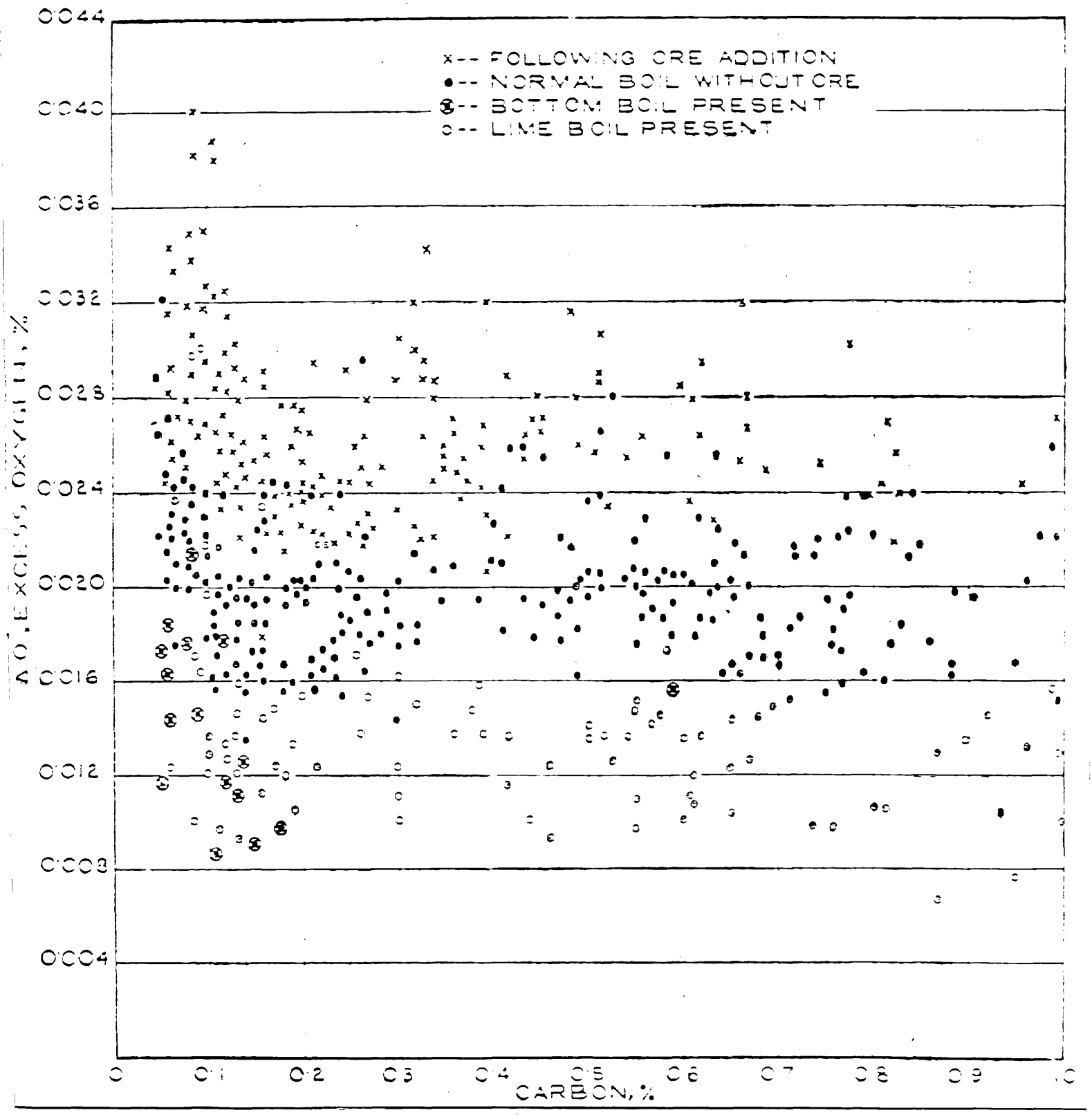
x-- FOLLOWING ORE ADDITION
•-- NORMAL BOIL WITHOUT ORE
⊗-- BOTTOM BOIL PRESENT
○-- LIME BOIL PRESENT
0.044
0.040
0.036
0.032
0.028
0.024
0.020
0.016
0.012
0.008
0.004
0
0.1
0.2
0.3
0.4
0.5
0.6
0.7
0.8
0.9
1.0
CARBON, %

It may at once be concluded from Figure 24E that whatever the value of $\Delta[O]$ may be it is neither constant during the refining period of one heat nor is it constant from furnace to furnace. Larsen's plot of $\Delta[O]$ against carbon content is given in Figure 25 from which the points representing the normal boil seem to support his contention that $\Delta[O]$ is independent of carbon content.

Larsen considered the formation of carbon monoxide bubbles to take place at crevices in the hearth and Richardson(37) has shown that the minimum carbon-oxygen product in the bath for crevices in the hearth to act as continuous sources of bubbles is that in equilibrium with a carbon monoxide pressure given by

$$P_{CO} = \left(1 + P_{Fe} + \frac{2T}{r}\right)$$ where P_{Fe} = ferrostatic pressure.

T = surface tension of the steel.

r = radius of the crevice in question.

from which it is possible to derive a relationship between r and $\Delta[O]$. The surface tension of steel at open hearth operating temperatures may be taken as 1550 dynes/sq.cm.(65) while for a bath depth of 28 inches P_{Fe} has the value 0.5 atmosphere. The above expression then reduces to:

$$P_{CO} = \left(1.5 + \frac{3100}{r} \times 9.87 \times 10^{-7}\right)$$

According to Richardson the carbon-oxygen product in the bath has to be such that it is in equilibrium with a carbon monoxide pressure given by this expression.

This carbon monoxide pressure is given by:

$$P_{CO} = K[C][O]$$

or $$P_{CO} = \frac{[C][O]}{m}$$

where m may be given the value 0.0023 at fairly low carbon contents. Then the condition for the hearth crevices to act as continuous sources of bubbles is that.

$$\frac{[C][O]}{0.0023} = 1.5 + \frac{3100}{r} \times 9.87 \times 10^{-7}$$

The oxygen term, [O], may be written as $([O]_{equ.} + \Delta[O])$ where the first term represents the oxygen in equilibrium with the carbon and $\Delta[O]$ the difference between that figure and the value determined by analysis.

Thus we now have.

$$\frac{[C]\,([O]_{equ.} + \Delta[O])}{0.0023} = 1.5 + \frac{3100}{r} \times 9.87 \times 10^{-7}$$

$$\text{or} \quad \frac{0.0023 + [C]\Delta[O]}{0.0023} = 1.5 + \frac{3100}{r} \times 9.87 \times 10^{-7}$$

$$\frac{[C]\,\Delta[O]}{0.0023} = 0.5 + \frac{3100}{r} \times 9.87 \times 10^{-7}$$

$$[C]\,\Delta[O] = 0.0023\,(0.5 + \frac{3100}{r} \times 9.87 \times 10^{-7})$$

$$\therefore \quad \Delta[O] = \frac{0.0023}{[C]}\,(0.5 + \frac{3100}{r} \times 9.87 \times 10^{-7})$$

From this expression the variation of excess oxygen with carbon may be calculated for different values of bubble radius. This has been done

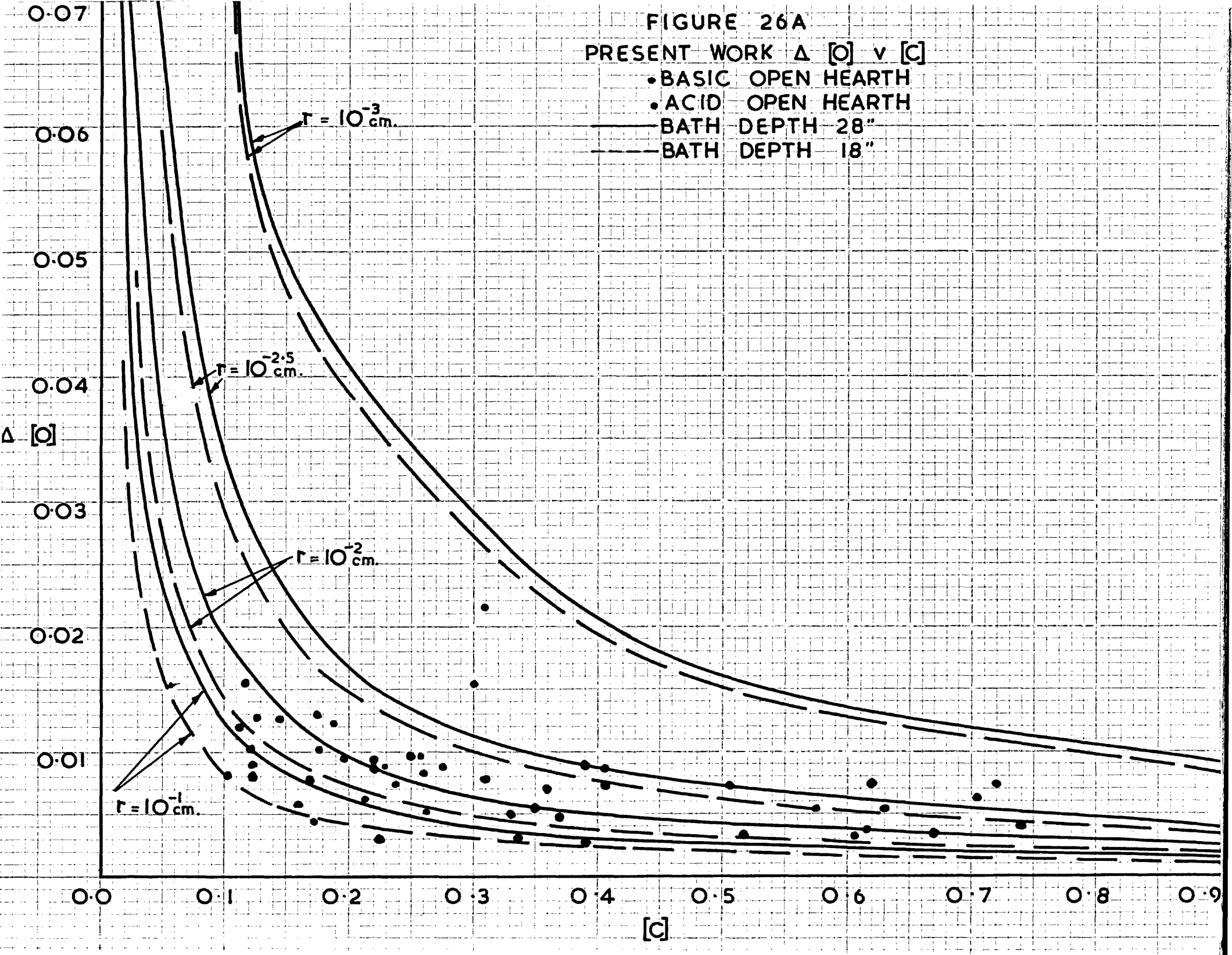
FIGURE 26A
PRESENT WORK Δ [O] v [C]
• BASIC OPEN HEARTH
• ACID OPEN HEARTH
——— BATH DEPTH 28"
– – – – BATH DEPTH 18"
r = 10⁻³ cm.
r = 10⁻²·⁵ cm.
r = 10⁻² cm.
r = 10⁻¹ cm.
0·07
0·06
0·05
0·04
0·03
0·02
0·01
Δ [O]
0·0
0·1
0·2
0·3
0·4
0·5
0·6
0·7
0·8
0·9
[C]

for bubble radii of 10^{-1} cm., 10^{-2} cm., $10^{-2.5}$ cm., and 10^{-3} cm. and the results graphed in Figure 26A for bath depths of 28and 18 inches,the latter being the bath depth in the basic open hearth and one of the acid open hearth heats. The bath depth for the remainder of the acid open hearth heats was 24 inches. The effect of a reduction in bath depth is most noticeable at low carbon contents and large crevice radii but even that is not great for a difference of 10 inches. The family of curves in Figure 26A shows that, contrary to the findings of Larsen, the excess oxygen would be expected to decrease as the carbon content increased for a fixed bubble radius. There must also be a fairly narrow range of crevice radii in which nucleation can occur. The upper limit will be fixed by the maximum size of crevice which will prevent the entry of molten steel, the maximum being related to the surface tension of steel. There is little data available from which this maximum may be calculated. Several combinations of circumstances are possible depending upon whether the pores are open or closed and on whether the steel wets the material of the hearth. It is known that iron-carbon alloys form contact angles of 120-140° with magnesia(66) this angle being decreased by the addition of iron oxide to the magnesia. It is reasonable to assume that similar angles will be obtained with dolomite hearths and that the hearth is not wetted by molten steel.

Considering firstly the case of a pore open to the atmosphere. This opening need not be vertically down through the hearth but possibly through the furnace banks. If the pore radius is such that $P_{Fe} < \frac{2T}{r}$ the molten steel will not penetrate and the crevice may act as a nucleating centre. This restriction limits the useful crevices with

with bath depths of 28" and 18" to those having radii less than 0.006 and 0.01 cm. respectively. The range of hearth crevices found in this study and given below could therefore contain some of the open variety. The further assumption would require to be made that the CO pressure inside the crevice builds up so quickly that bubbles are released to the bath before the pressure is decreased by the carbon monoxide escaping at the other end of the pore.

No such relationship can be derived for closed pores for which it may only be saidthat there is no tendency for gas, trapped by liquid metal, to escape unless agitation or vibration causes drops of liquid to fall into the cavity and displace gas.

The lower limit is controlled by the permissible values of excess oxygen since the latter increases rapidly as the radius decreases. Thus, the excess oxygen values at 0.10, 0.20 and 0.30% carbon for a hearth radius of 10^{-4} cm. to promote bubble formation are 0.72, 0.36 and 0.24% respectively. These are, of course, impossibly high values being in excess of the saturation limit for normal steelmaking temperatures.

The values of Δ [O] for the samples drawn in the present study were calculated, tabulated in Table VIII and plotted in Figure 26A. These points support the view that Δ [O] is in fact dependent upon the carbon content and decreases as the latter increases. No allowance was made in these calculations for the variation of $\underline{m}$ with carbon content but this will not be great at the carbon contents involved and will have the effect of reducing the Δ [O] values even further at higher carbon contents. The disposition of the points when the excess

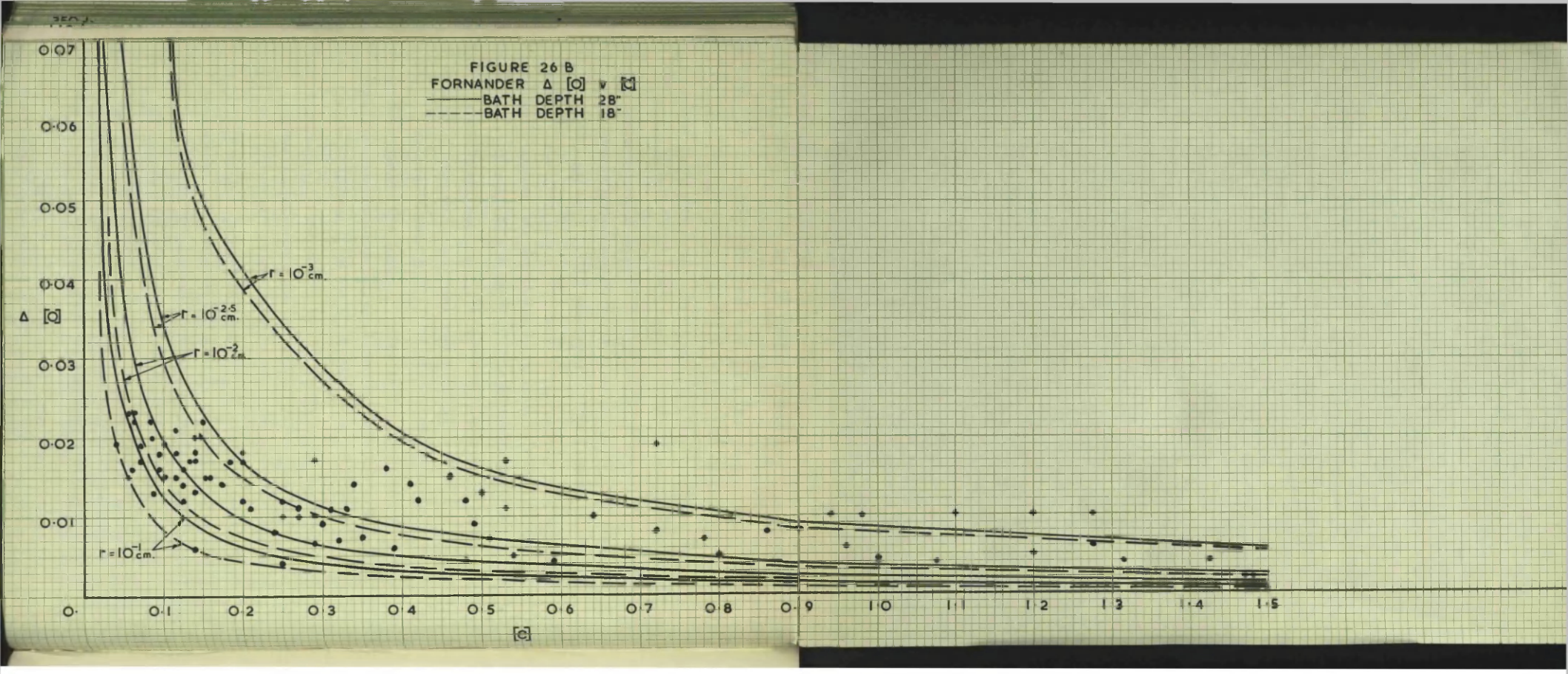
FIGURE 26 B
FORNANDER Δ [Q] v [c]
BATH DEPTH 28"
BATH DEPTH 18"
0·07
0·06
0·05
0·04
0·03
0·02
0·01
0·
Δ [Q]
r = 10⁻³ cm.
r = 10⁻²·⁵ cm.
r = 10⁻² cm.
r = 10⁻¹ cm.
0·1
0·2
0·3
0·4
0·5
0·6
0·7
0·8
0·9
1·0
1·1
1·2
1·3
1·4
1·5
[c]

FIGURE 26 C
MACKENZIE Δ [O] v [C]
———BATH DEPTH 28"
— — —BATH DEPTH 18"

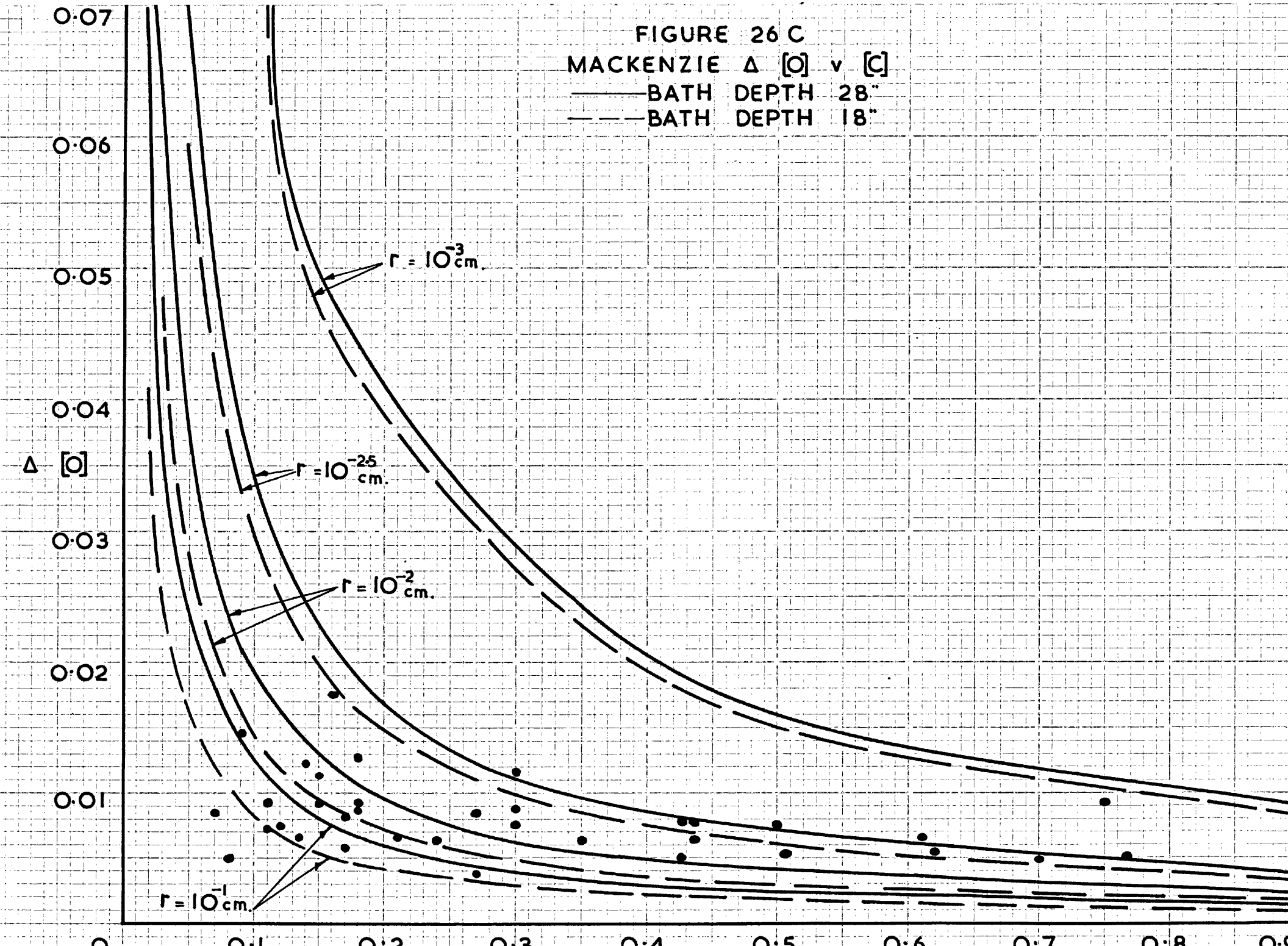

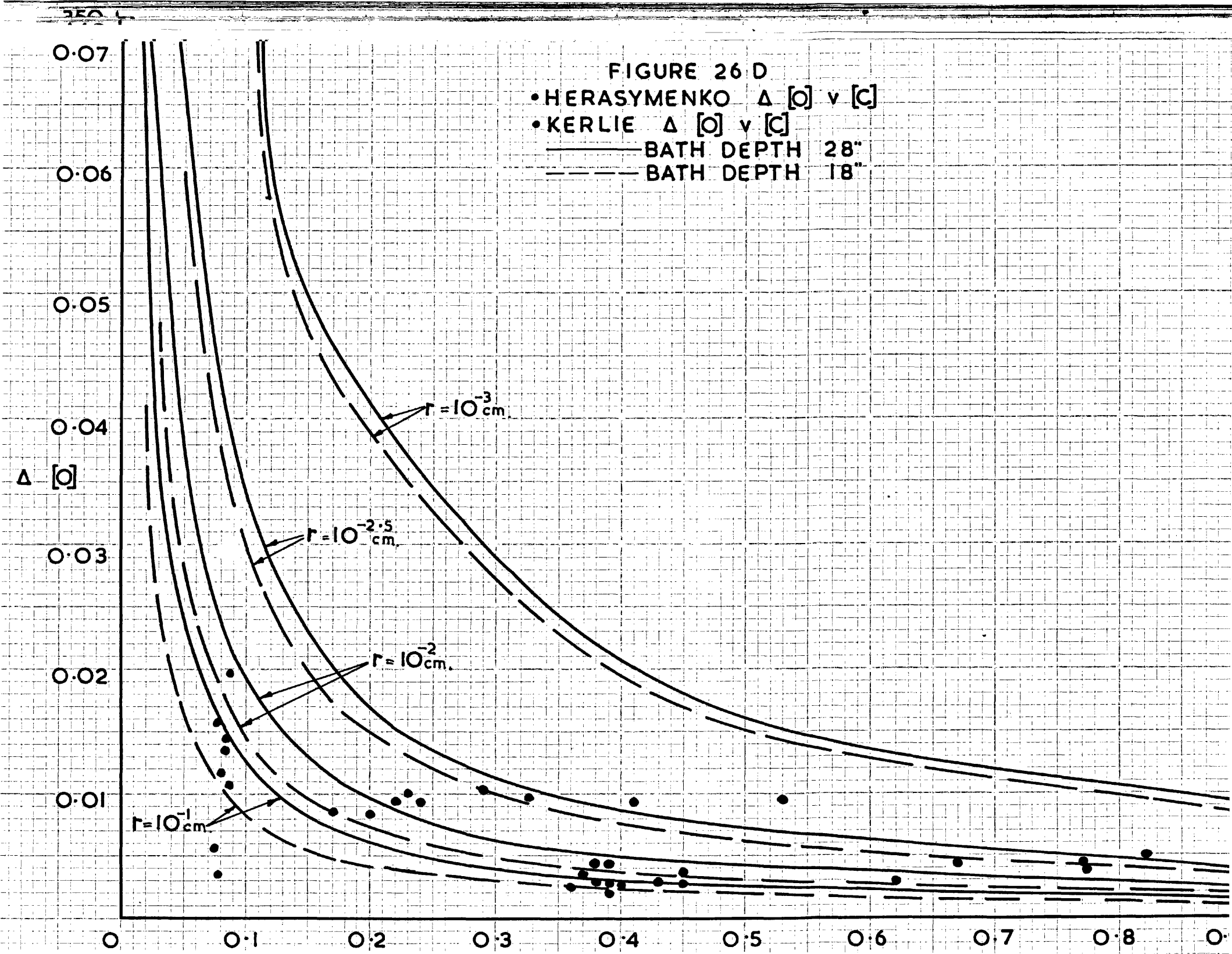
FIGURE 26 D
• HERASYMENKO Δ [O] v [C]
• KERLIE Δ [O] v [C]
BATH DEPTH 28"
BATH DEPTH 18"
r = 10^-3 cm.
r = 10^-2·5 cm.
r = 10^-2 cm.
r = 10^-1 cm.
Δ [O]
0·07
0·06
0·05
0·04
0·03
0·02
0·01
0
0·1
0·2
0·3
0·4
0·5
0·6
0·7
0·8

oxygen is plotted against carbon content is in agreement with the hypothesis that nucleation takes place at the hearth and indicates that the productive hearth crevices have radii within the range 10^{-1} - $10^{-2.5}$ cm.

The value of excess oxygen was also calculated from the results of Fornander, Mackenzie, Herasymenko and Kerlie and is plotted against carbon content in Figures 26B, 26C, and 26D respectively. The graphs of Fornander and Mackenzie clearly substantiate the findings of the present work while the results of Kerlie show a similar if less emphatic agreement. The results of Herasymenko suggest rather the constancy of Δ [O] which may be due to the fact that Herasymenko reports no carbon contents below 0.35 per cent and it is only really below this figure that the increase in Δ [O] becomes noticeable in the other graphs.

The indicated size range of crevices in all cases shows good agreement but it may also be inferred that while the excess oxygen increases as the carbon drops the actual increase is not sufficient to maintain the smaller crevices as nucleating centres towards the end of the process. Other things being equal this should show itself as a decrease in the rate of carbon removal; this will be discussed more fully later.

Finally, with the exception possibly of the data of Fornander, the excess oxygen of all the workers referred to above is considerably lower than the figure Larsen quoted for the steady state boil and the data of Fornander only approach this value at very low carbon contents.

FIGURE 27

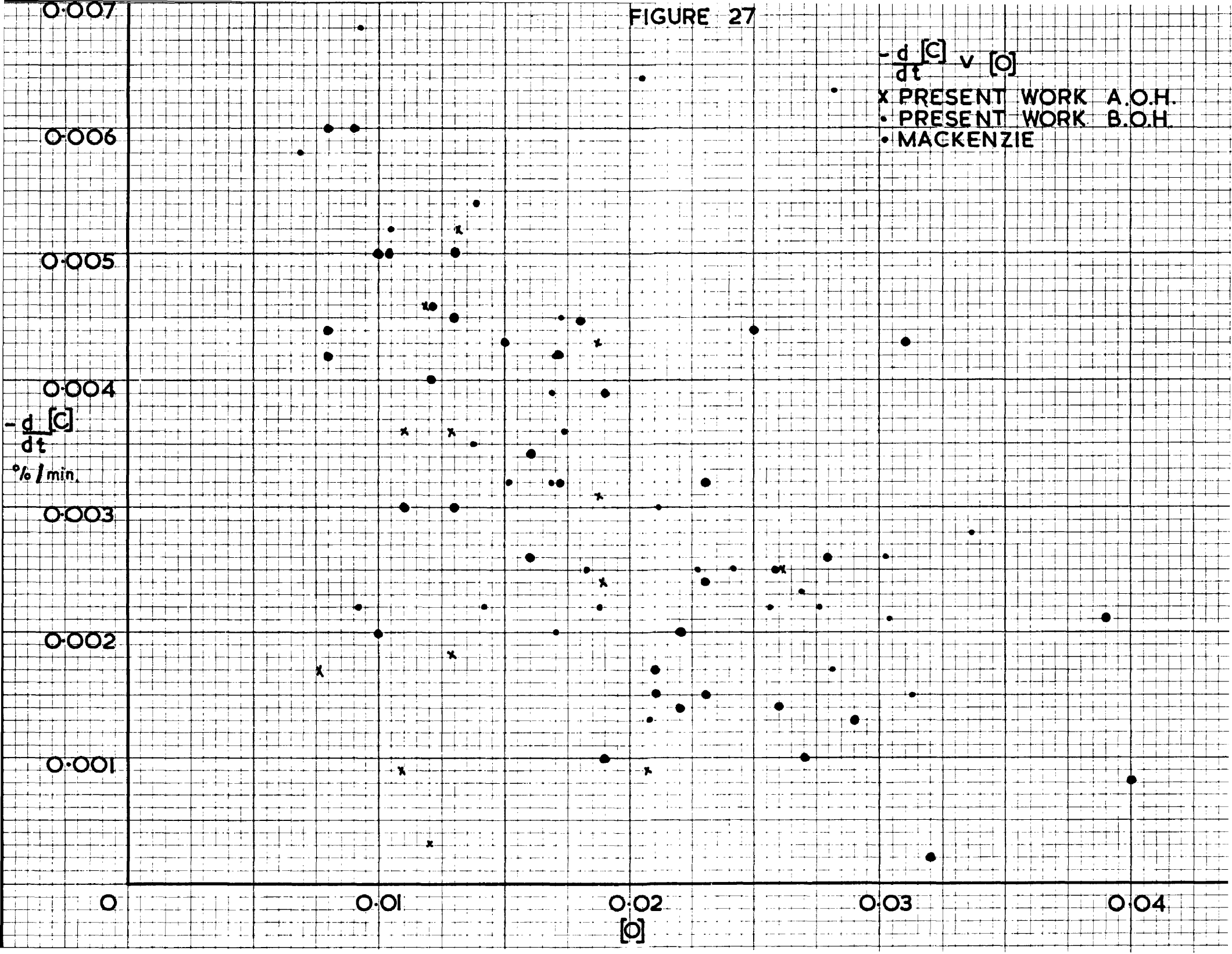
$-\frac{d[C]}{dt}$ v [O]
x PRESENT WORK A.O.H.
• PRESENT WORK B.O.H.
• MACKENZIE
0·007
0·006
0·005
0·004
$-\frac{d[C]}{dt}$
% / min.
0·003
0·002
0·001
0
0·01
0·02
0·03
0·04
[O]

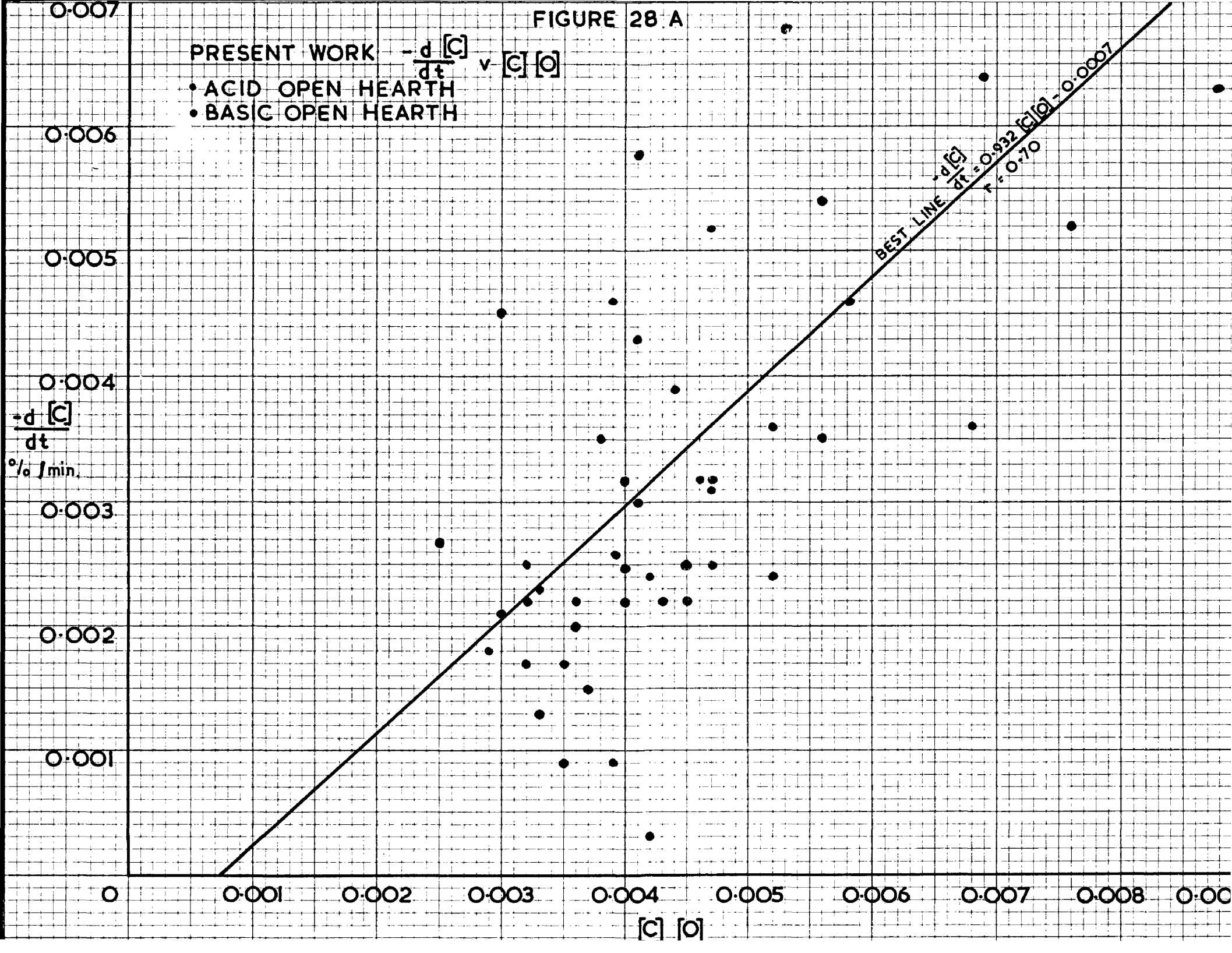
FIGURE 28 A
PRESENT WORK $-\frac{d[C]}{dt}$ v [C] [O]
• ACID OPEN HEARTH
• BASIC OPEN HEARTH
BEST LINE $-\frac{d[C]}{dt} = 0.932\,[C][O] - 0.0007$
r = 0.70
0·007
0·006
0·005
0·004
0·003
0·002
0·001
0
$-\frac{d[C]}{dt}$
% / min.
0·001
0·002
0·003
0·004
0·005
0·006
0·007
0·008
[C] [O]

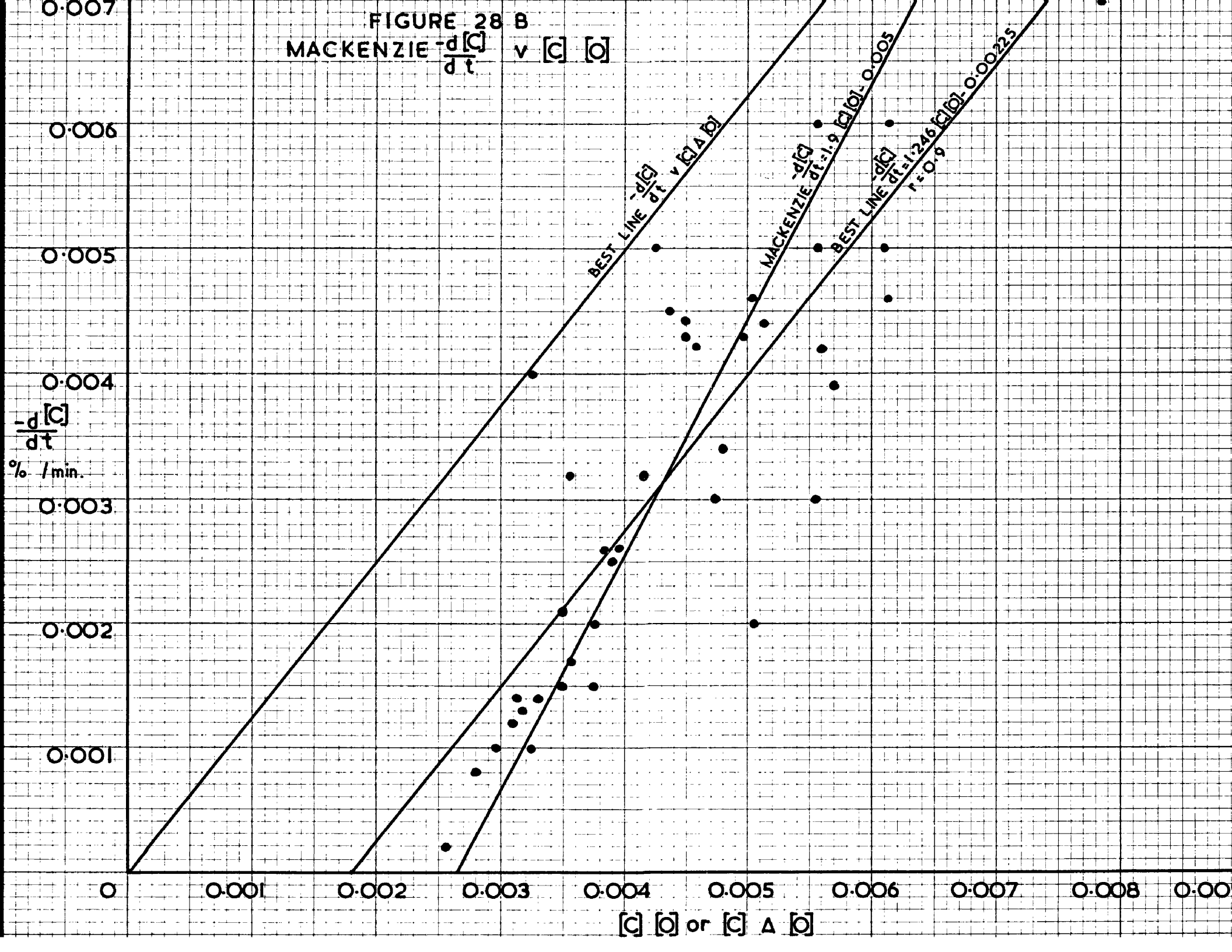
FIGURE 28 B
MACKENZIE $\frac{-d[C]}{dt}$ v [C] [O]
BEST LINE $\frac{-d[C]}{dt}$ v [C] Δ [O]
MACKENZIE $\frac{-d[C]}{dt}$ = 1·9 [C] [O] - 0·005
BEST LINE $\frac{-d[C]}{dt}$ = 1·246 [C] [O] - 0·00225
r = 0·9
$\frac{-d[C]}{dt}$ % / min.
0·007
0·006
0·005
0·004
0·003
0·002
0·001
0
0·001
0·002
0·003
0·004
0·005
0·006
0·007
0·008
0·00
[C] [O] or [C] Δ [O]

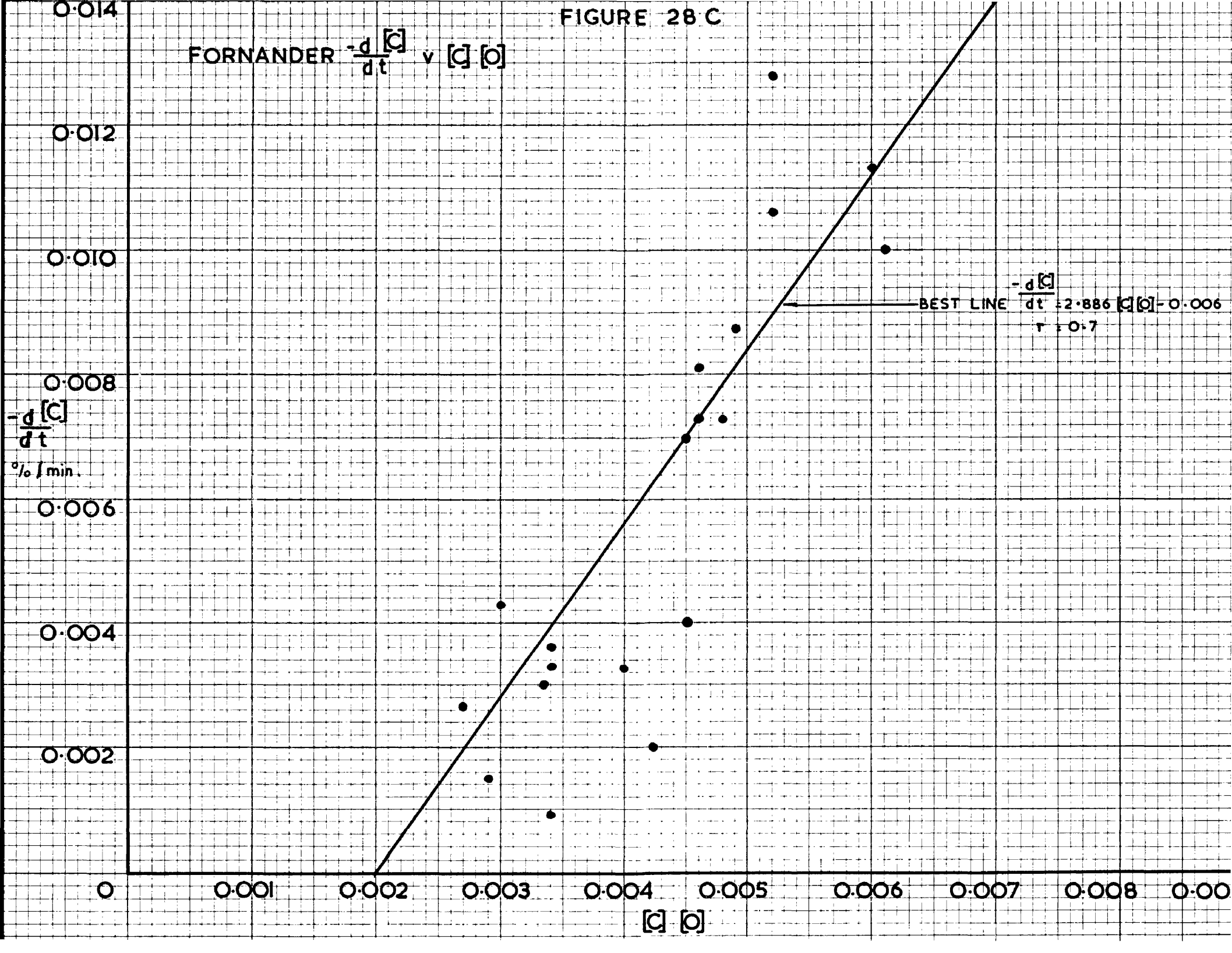
FIGURE 28 C
FORNANDER $\frac{-d[C]}{dt}$ v [C] [O]
BEST LINE $\frac{-d[C]}{dt} = 2 \cdot 886\,[C][O] - 0 \cdot 006$
r = 0·7
$\frac{-d[C]}{dt}$
% / min.
0·014
0·012
0·010
0·008
0·006
0·004
0·002
0
0·001
0·002
0·003
0·004
0·005
0·006
0·007
0·008
0·00
[C] [O]

FIGURE 28 D

HERASYMENKO $-\frac{d[C]}{dt}$ v [C] [O]

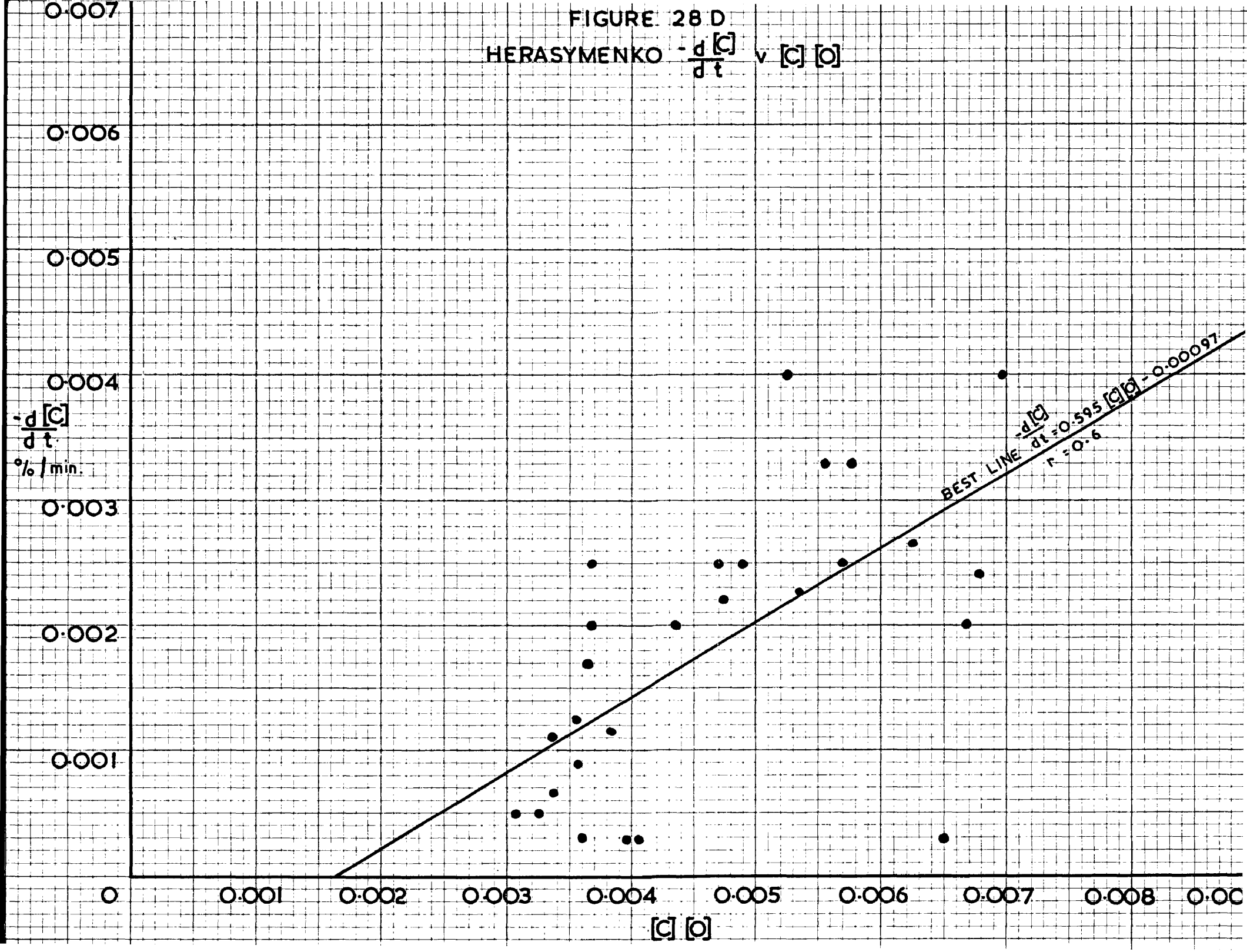

FIGURE 28 E

KERLIE $\frac{-d\,[C]}{dt}$ v [C] [O]

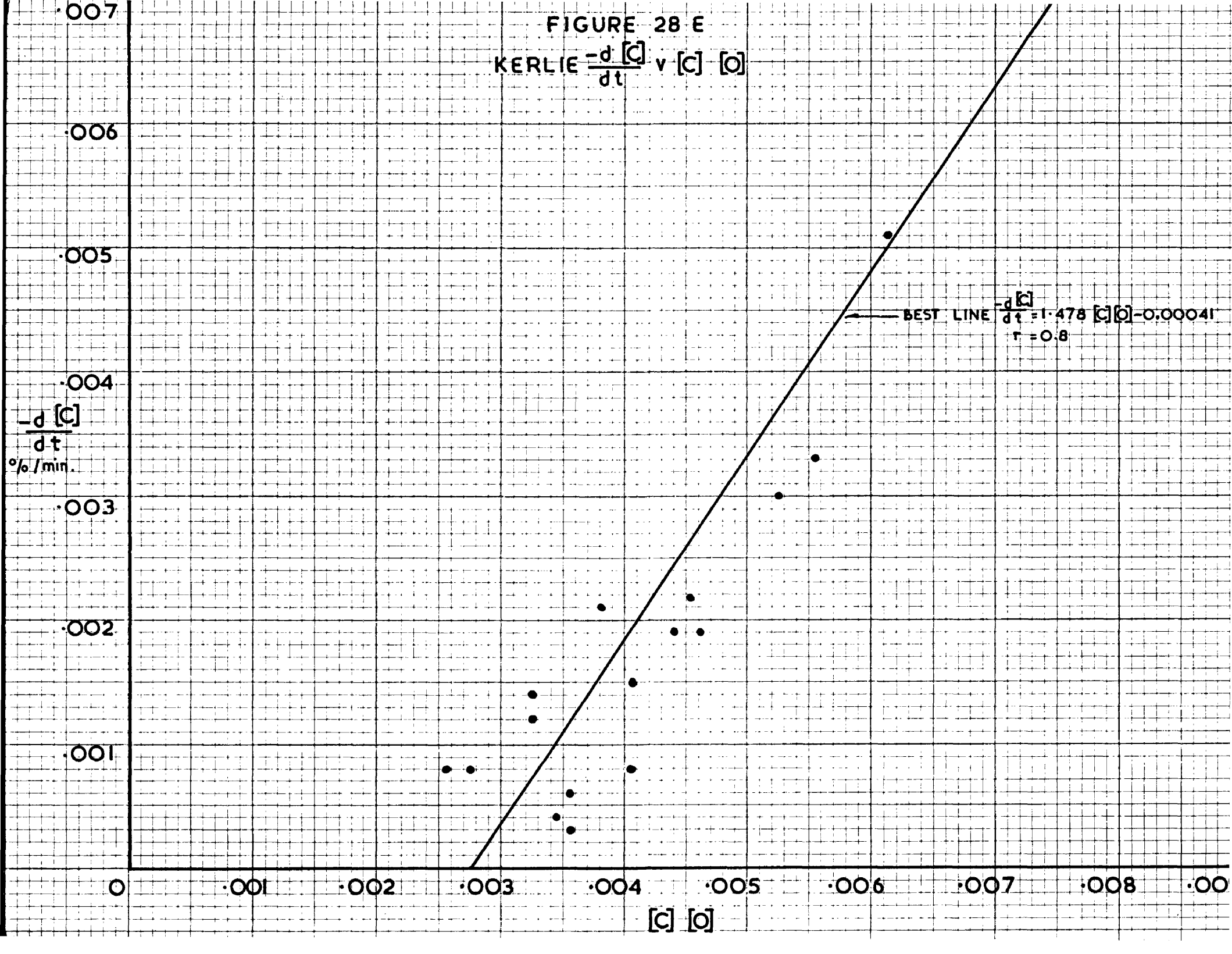

Larsen reported that the boil appeared to stop when Δ [O] was less than 0.014%. This would indicate a lack of larger crevices in his hearths. It is possible that these differences in Δ [O] may be attributed to differing techniques of sampling and analyses although all the workers mentioned used the bomb method of sampling and all used the vacuum fusion method of analysis except Kerlie who used a chemical method.

Rate of Carbon Removal and the Mechanism of the Carbon-Oxygen Reaction.

From the data given in Table VIII for the present work and from the results of Mackenzie a graph of rate of carbon removal against oxygen content was plotted as shown in Figure 27. A series of graphs, 28A, B, C, D and E, of rate of carbon removal against carbon-oxygen product was plotted for the present work and for the results of Mackenzie, Fornander, Herasymenko and Kerlie respectively, the results of Herasymenko below 1550°C being omitted. The quantity $2[C]^2[O]$ was also calculated for the present work and from the results of Mackenzie and rate of carbon removal plotted against this in Figure 29A, a similar plot in 29B covering the data of Herasymenko and Fornander.

Jay(67), using data from an acid open-hearth heat estimated the degree of oxidation from the silicon and manganese contents of the bath and concluded, from a comparison of the rates of carbon removal at the end of the ore boil and during the lime boil, that the rate of carbon removal was proportional to the degree of oxidation of the bath. He assumed that the reaction was initiated by the formation of molecular bubbles of carbon monoxide in the bath as the result of a homogeneous reaction. This latter state of affairs has been shown by Sims(32),

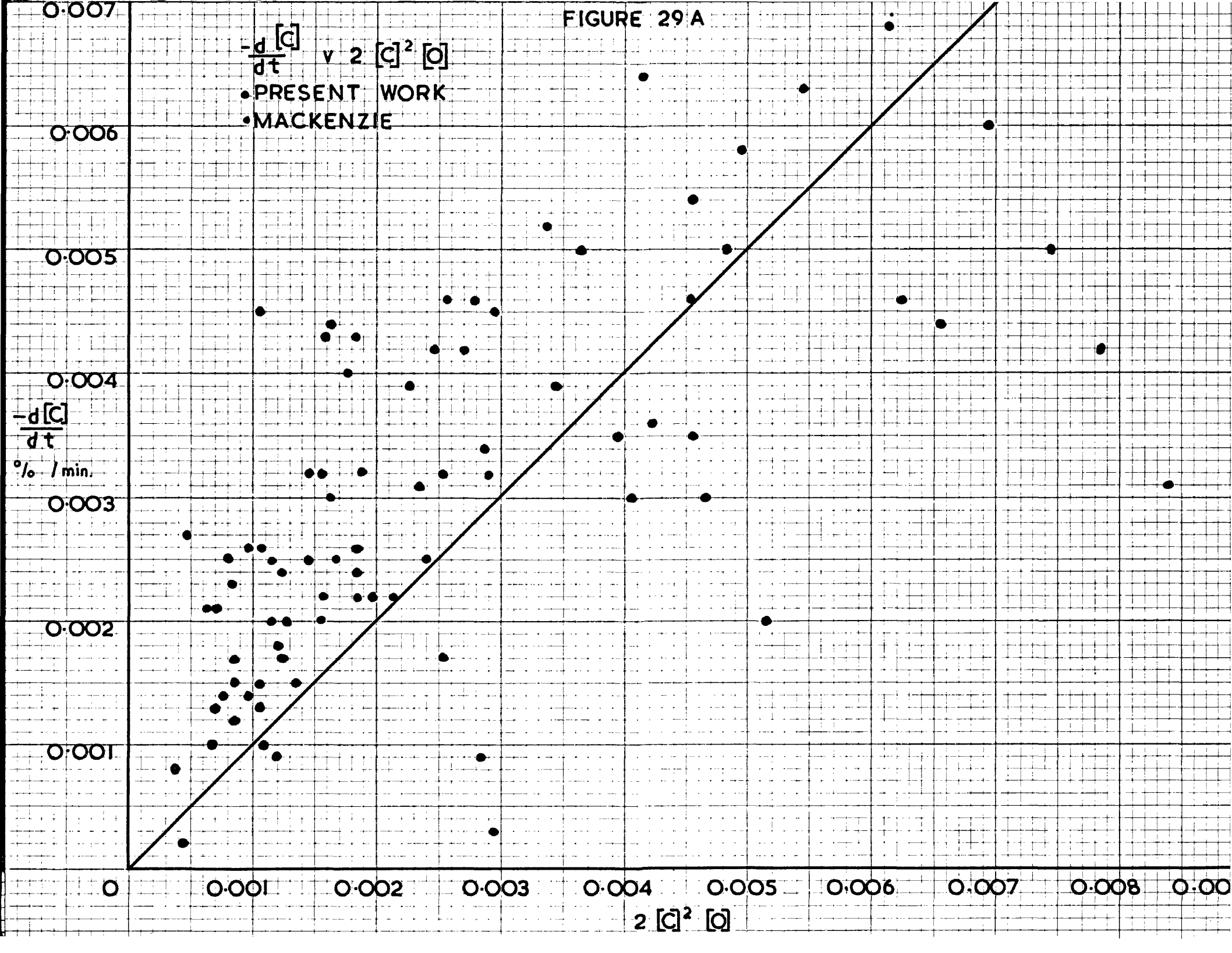
FIGURE 29 A
$-\frac{d[C]}{dt}$ v $2[C]^2[O]$
• PRESENT WORK
• MACKENZIE
0·007
0·006
0·005
0·004
$-\frac{d[C]}{dt}$
% / min.
0·003
0·002
0·001
0
0·001
0·002
0·003
0·004
0·005
0·006
0·007
0·008
0·00
$2[C]^2[O]$

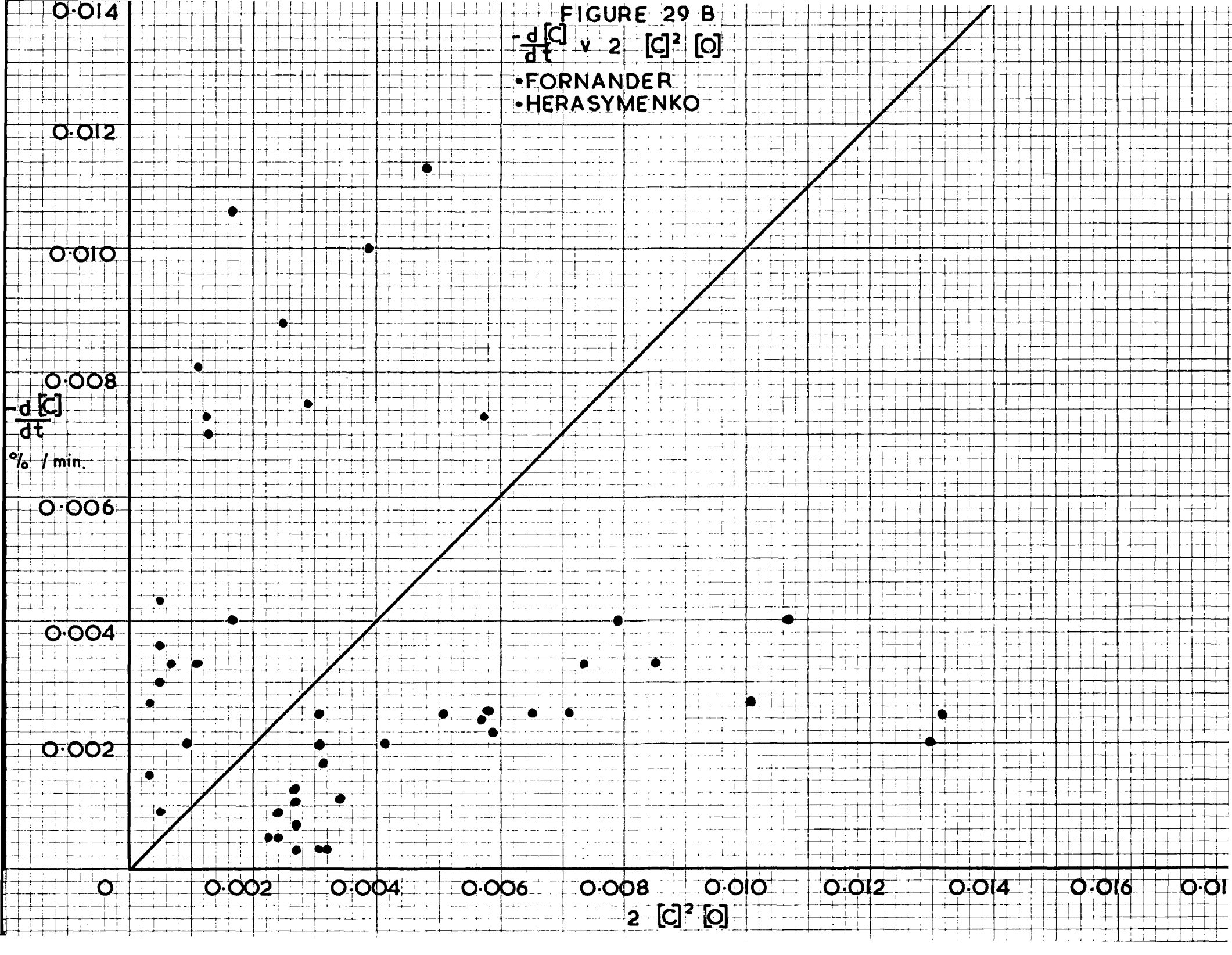
FIGURE 29 B
$-\frac{d[C]}{dt}$ v 2 $[C]^2$ [O]
•FORNANDER
•HERASYMENKO
0·014
0·012
0·010
0·008
0·006
0·004
0·002
0
$-\frac{d[C]}{dt}$
% / min.
0·002
0·004
0·006
0·008
0·010
0·012
0·014
0·016
0·01
2 $[C]^2$ [O]

Ranque(33) and Richardson(34) to be improbable. Furthermore the graph of rate of carbon removal against oxygen content in Figure 27 indicates, if anything, that the former is inversely proportional to the latter.

In a recent paper Kerlie(64) found that the rate of carbon removal could be represented by the equation:

$$\frac{-d[C]}{dt} = 2[C]^2 [O]$$

although he did not attempt to explain the derivation of this equation and commented that the results might be somewhat fortuituous. The rates of carbon removal calculated from this equation for the present work and from the data of Mackenzie show a relatively poor agreement with measured rates. Below about 0.004%/minute the measured rates are higher but beyond this point the calculated values exceed the actual values; the latter are largely at the beginning of refining when the carbon is high. The poor agreement in Figure 29B for the results of Fornander and Herasymenko indicates that there is indeed little sound basis for the equation derived by Kerlie.

The graphs of $\frac{-d[C]}{dt}$ against [C][O] show that a fairly close relationship exists between carbon-oxygen product and rate of carbon removal. The correlation coefficients calculated from the results are 0.7, 0.9, 0.7, 0.6 and 0.8 for the data of the present study, Mackenzie, Fornander, Herasymenko and Kerlie respectively. The form of the equations of the derived best lines $\frac{-d[C]}{dt} = k_1 [C][O] - k_2$ is similar to the equation of Schenck(13) who considered that the reaction between carbon and oxygen was rate determining. While Schenck was able to predict rates of carbon removal which agreed well

with observed values his proposed mechanism may be criticised for at least three reasons.

(a) Homogeneous reactions at steelmaking temperatures should be extremely rapid unless the activation energy is particularly high, viz., in excess of 100 Kg. cal./gm.mol.; such values are not common in ordinary chemical reactions at high temperatures.

(b) A homogeneous reaction between carbon and oxygen would necessitate a carbon monoxide pressure of the order of 55 atmospheres before gas evolution could start within liquid steel. This possibility has already been shown to be improbable in connection with the theory put forward by Jay.

(c) If the reaction between carbon and oxygen is to be considered as rate determining then it must be assumed that the slag and metal are in equilibrium with respect to oxygen. This has never been accepted as the case, the oxygen content of the metal falling far short of that which would be in equilibrium with the ferrous oxide activity of the slag.

Herasymenko(7)(63) also regarded the primary reaction between carbon and oxygen as the slowest step in carbon removal but in his theory of the mechanism he overcame the objections to the ideas put forward by Schenck, by assuming that although the reaction between carbon and oxygen had a high activation energy, it could be reduced by the adsorption of the reactants on crystalline surfaces such as those of the hearth. He also attempted to show that the slag and

metal in both the acid and basic open-hearth furnaces were indeed in equilibrium with respect to oxygen. His evidence for the existence of this equilibrium lay in the comparison of the oxygen distribution in steelmaking with that obtained in the pure Fe-Mn-Si-O system under equilibrium conditions. He attributed the deviation of the results of the practical melts from those of the laboratory melts to the effect of carbon on the activity coefficient of oxygen which he believed to be raised by the presence of carbon. The doubt attached to his derivation of these coefficients has been discussed in the introduction to this study and in the absence of further evidence in support of Herasymenko, the conclusion of Marshall and Chipman that carbon lowers the activity coefficient of oxygen will be accepted.

From what has already been said the presence of and necessity for excess oxygen in the bath is amply clear; coupled with this fact is the evidence which shows bubble radii at the hearth to be of the order of $10^{-2.5}$ - 10^{-1} cm. while bubbles bursting at the surface of the bath have been observed to be of the order of as much as 10 cms. in diameter. This rapid growth can hardly be indicative of an inherently slow rate of reaction between carbon and oxygen although it should be borne in mind that part of this growth may be due to coalescence of bubbles.

In view of these facts it is proposed to accept as postulated by Larsen, that carbon removal commences with the formation of carbon monoxide gas in the hearth crevices which act as nuclei. The open-hearth process possesses the factors demanded by such a precipitation - controlled process, namely:

(1) the chemical substance to be precipitated from the solution must be present in a concentration appreciably greater than equilibrium -

excess oxygen giving a carbon-oxygen product greater than equilibrium. (2) nuclei or centres of precipitation must be present, these are the small carbon monoxide pockets in the hearth crevices.

By this means carbon monoxide may diffuse from the metal into the hearth crevices at much lower carbon monoxide pressures than demanded by the formation of carbon monoxide bubbles within the liquid metal.

Carbon monoxide may enter the nuclei by either of two methods. The first of these is by the formation of an activated complex. In the main body of the bath there will be little attraction between carbon and oxygen atoms since they are present in relatively small proportions, but presented with an interface it is possible for this attraction to increase if carbon and oxygen are surface active, and for the strength of the bond between atoms of carbon and oxygen in close proximity to each other to approach that of the carbon monoxide molecule, the latter being eventually formed and passing into the already present nucleus. The mutual lowering of the activities of carbon and oxygen in solution together lends some support to this theory, although the effect is small, but, as the quantities of the two elements in the bath are so small, it is suggested that this is not the mode of growth of the nuclei. Instead the nuclei may grow as a result of the two-stage reaction represented by the equations:

$$CO + \underline{O} = CO_2 \quad \ldots\ldots\ldots\ldots\ldots\ldots (1)$$

$$CO_2 + \underline{C} = 2CO \quad \ldots\ldots\ldots\ldots\ldots\ldots (2)$$

The rate of the first reaction for unit surface area is given by

$$k_1 P_{CO} [O] - k_2 P_{CO_2} \quad \ldots\ldots\ldots\ldots\ldots\ldots (3)$$

and that of the second by

$$k_3 P_{CO_2} [C] - k_4 P_{CO}^2 \quad \ldots\ldots\ldots\ldots\ldots\ldots (4)$$

FIGURE 30

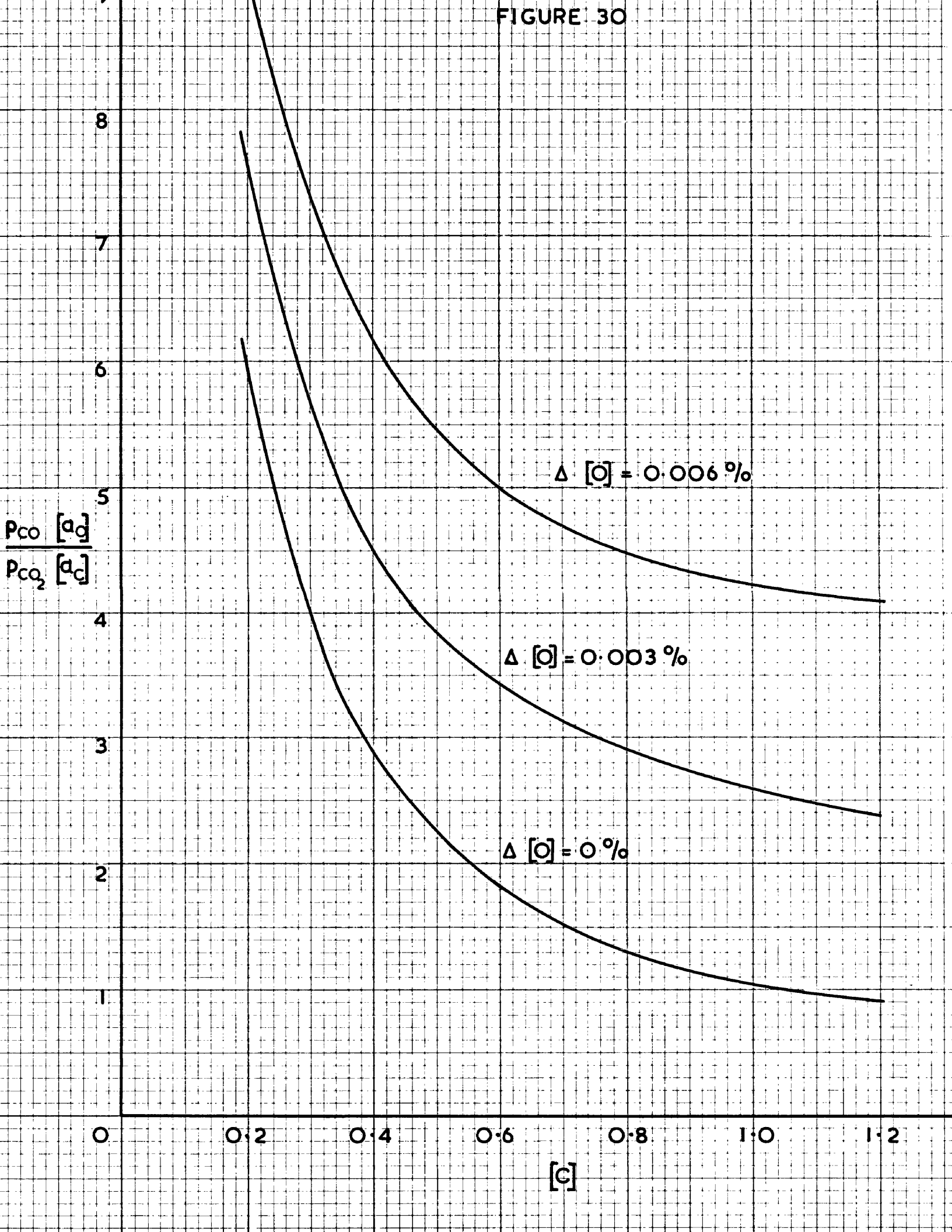
8
7
6
5
4
3
2
1
0
0·2
0·4
0·6
0·8
1·0
1·2
[C]
$\frac{P_{CO}\ [a_g]}{P_{CO_2}\ [a_C]}$
Δ [O] = 0·006 %
Δ [O] = 0·003 %
Δ [O] = 0 %

Now the ratio of the frequency of collisions for the first reaction to the frequency of collisions for the second reaction is given by :

$$\frac{P_{CO}\,[a_O]}{P_{CO_2}[a_C]}$$

The value of this expression has been determined from the results of Marshall and Chipman(3) at 1600°C and is plotted against carbon content for equilibrium and for an excess oxygen of 0.003% and 0.006% in Figure 30, from which it will be seen that the ratio is greater than unity except at high carbon contents. This means that if the activation energies of the two reactions represented by equations (1) and (2) are similar, which is most likely, then the second reaction will be slower than the first. Under these circumstances the carbon dioxide will tend to build up to its equilibrium value given by:

$$p_{CO_2} = \frac{k_1}{k_2}\, p_{CO}\,[O]$$

Substituting this for p_{CO_2} in equation (4) we got the overall rate of the reaction, viz.,

$$k_3\,\frac{k_1}{k_2}\, p_{CO}\,[C][O] - k_4\, p_{CO_2}^2$$

which simplifies to

$$p_{CO}\,(k^1\,[C][O] - k_4\, p_{CO})$$

If A is the total surface area of the bubbles in the bath at any instant then the rate of carbon removal will be :

$$\frac{-d[C]}{dt} = A\, p_{CO}\,(k^1[C][O] - k_4\, p_{CO}) \quad \ldots\ldots\ldots\ldots\ldots (5)$$

Now a very short time after breaking away from the hearth the CO pressure in the bubbles will become equal to or just greater than one atmosphere. If then p_{CO} is put equal to unity equation (5) becomes

$$\frac{-d[C]}{dt} = A\,(k^1\,[C][O] - k_4) \qquad \ldots\ldots\ldots\ldots(6)$$

The correlation coefficients obtained from the graphs of $\frac{-d[C]}{dt}$ against [C][O] in Figures 28A to 28E inclusive, justify the acceptance of the proposed theory.

Mackenzie(17) employed the equation

$$\frac{-d[C]}{dt} = 1.9\,[C][O] - 0.005 \qquad \ldots\ldots\ldots\ldots(7)$$

which, it will be seen from Figure 28B, is not the best line through his points but the one, the selected constants for which gave the best agreement between the calculated and nephelometrically determined oxygen contents.

Equation(7) may be modified by substituting $([O]_{C.E.} + \Delta[O])$ for [O] where $[O]_{C.E.}$ is the oxygen in equilibrium with the particular carbon and $\Delta[O]$ is the excess oxygen of Larsen. If this is done and m = [C][O] is given the value 0.0026 used by Mackenzie, equation (7) reduces to:

$$\frac{-d[C]}{dt} = 1.9\,[C]\Delta[O] \qquad \ldots\ldots\ldots\ldots\ldots(8)$$

This is similar to the equation derived by Vallet (30)

$$\frac{-d[C]}{dt} = K.S.[C]\Delta[O]$$ where K is a rate constant and S is surface area of all the rising bubbles. In the derivation of this Vallet assumed that the rate of carbon drop was controlled by the rate at which carbon monoxide was formed at the gas-metal interfaces of the CO bubbles which rose through the metal after nucleation at the hearth.

Included in Figure 28B is the best line for the graph of $\frac{-d[C]}{dt}$ against $[C]\Delta[O]$ the slope of which is the same as that obtained by plotting rate of carbon removal against the carbon-oxygen product but the intercept is now zero.

From equation(6), by expressing the surface area A in terms of the volume of the bubbles, an expression may be derived from which the ultimate size of the bubble arising from any specific hearth crevice may be calculated.

Thus equation (6) is

$$\frac{-d[C]}{dt} = A\,(k_1\,[C][O] - k_4)$$

$$= A\,M \text{ where } M = k_1\,[C][O] - k_4$$

Now for any bubble of radius r the surface area is

$$A = 4\pi r^2$$

and the volume is $V = \frac{4\pi}{3} r^3$

$$\therefore \quad r = \left(\frac{3V}{4\pi}\right)^{\frac{1}{3}}$$

$$\text{and} \quad A = 4\pi \left(\frac{3V}{4\pi}\right)^{\frac{2}{3}}$$

Then the rate of carbon removal $= \frac{-d[C]}{dt} = AM$

$$= 4\pi \left(\frac{3V}{4\pi}\right)^{\frac{2}{3}} M$$

The rate of increase in volume of any bubble is then given by

$$\frac{dV}{dt} = \frac{22.4 \times 10^3\, M}{12}\, 4\pi \left(\frac{3}{4\pi}\right)^{\frac{2}{3}} V^{\frac{2}{3}}$$

$$= NV^{\frac{2}{3}} \quad \text{where } N = \frac{22.4 \times 10^3\, M}{12} 4\pi \left(\frac{3}{4\pi}\right)^{\frac{2}{3}}$$

$$\text{Hence} \quad N\,dt = \frac{dV}{V^{\frac{2}{3}}}$$

$$\text{Now} \quad V = \frac{4}{3}\pi r^3$$

$$\therefore \quad \frac{dV}{dr} = 4\pi r^2 \text{ and } dV = 4\pi r^2\,dr$$

$$\therefore \quad N\,dt = 4\pi r^2\,dr.\left(\frac{1}{\frac{4}{3}\pi r^3}\right)^{\frac{2}{3}}$$

$$= \left(\frac{3}{4\pi}\right)^{\frac{2}{3}} 4\pi\,dr.$$

$$= 0.8945\,dr.$$

It has already been determined that hearth crevice radii are within the range $10^{-2.5}$ - 10^{-1} cm. If it is assumed that nucleation is taking place at crevices of these radii and that the time for the bubbles to rise through the bath is the same in each case, then for the crevice of radius 10^{-1} cm.

$$\int_0^t N\,dt = \int_{r=10^{-1}}^{r=r_1} 0.8945\,dr.$$

and for the crevice of radius $10^{-2.5}$ cm.

$$\int_0^t N.dt = \int_{r=10^{-2.5}}^{r=r_2} 0.8945\,dr.$$

$$\text{Hence} \quad 0.8945r_1 - 0.8945.10^{-1} = 0.8945r_2 - 0.8945.10^{-2.5}$$

$$\therefore\ r_1 - r_2 = 10^{-1} - 10^{-2.5} = 0.097 \text{ cm.}$$

Thus, assuming that $p_{CO} = 1$ and that both bubbles take the same time to rise, the difference between the ultimate radii of the bubbles nucleated from the largest and smallest hearth crevices is less than 10^{-1} cm.

According to Stokes' Law the smallest bubbles take longer to rise so the difference in ultimate radii will be even less. There will be, therefore, very little difference in the contribution of the bubbles from these two hearth crevices to carbon removal, the overall rate of carbon removal being controlled by the total number of bubbles being nucleated.

True steady state conditions do not exist in the open hearth. If this were the case the oxygen diffusing from the slag to the metal would be exactly equal to the oxygen passing from the metal to the gas phase as carbon monoxide and the metal composition would remain constant with respect to oxygen. While this is not completely true of the open hearth process it may be assumed to be closely approached over a short period of time during which the oxygen content of the metal does not vary appreciably. An expression may then be derived for the oxygen content of the bath as follows.

The rate of supply of oxygen to the metal is controlled by the concentration gradient existing between slag and metal and is given by.

$$k_1 ([O]_{S.E.} - [O])$$

where $[O]_{S.E.}$ and $[O]$ are the oxygen content of the bath in equilibrium with the slag and the actual bath oxygen content respectively. The rate of passage of oxygen from the metal to the gas phase is proportional to the rate of formation of carbon monoxide and is given by $A(k_2[C][O] - k_3)$, if P_{CO} is taken as approximately unity. Now if steady state conditions exist these two expressions may be equated .

Thus

$$k_1 ([O]_{S.E.} - [O]) = A(k_2[C][O] - k_3)$$

$$k_1 [O]_{S.E.} - k_1[O] = Ak_2 [C][O] - A k_3$$

$$k_1 [O] + Ak_2 [C][O] = k_1 [O]_{S.E.} + A k_3$$

$$\therefore [O] = \frac{k_1 [O]_{S.E.} + Ak_3}{k_1 + Ak_2 [C]}.$$

$$[O] = \frac{k_1 [O]_{S.E.} + Ak_3}{k_1 + Ak_2 [C]} \qquad \text{.....(9)}$$

It may be deduced from this expression that the oxygen content of the bath will increase with the value of the oxygen which would be in equilibrium with the slag, i.e., the oxygen content of the metal will increase with increasing ferrous oxide activity in the slag. At the same time the oxygen content of the metal will increase with decreasing carbon content. The effect of an increase or decrease in A, the total surface area of the bubbles in the bath at any instant is not easy to assess since it appears in both numerator and denominator multiplied in each case by different constants.

If equation (9) is rearranged the following expression is derived for k_1

$$k_1 = \frac{Ak_2 [C][O] - Ak_3}{[O]_{S.E.} - [O]}$$

The constant k_1 was evaluated from the results of the present work in the basic open-hearth furnace and from the data of Fornander and the values obtained are given with the mean values in Table IX. Considering that steady state conditions have been assumed to calculate this constant, the deviation from the mean is remarkably small.

Knowing k_1 it is now possible to assess the effect of a variation in A, the total surface area of the bubbles in the bath at any instant. Equation (9) gives the oxygen content of the metal as

TABLE IX.

Evaluation of k_1.

Present Data.			Data of Fornander.		
Heat No.	k_1 using own constants for Alk_2, Alk_3	k_1 using MacKenzie's constants for Alk_2, Alk_3.	Heat No.	k_1 using constants for Alk_2, Alk_3 derived from plot of $\frac{C_1 - C_{oly}}{dt}$	k_1 using Mackenzie's constants for Alk_2, Alk_3.
2(7)	0.03860	0.01842	2	0.08704	0.05094
3(2)	0.04541	0.03546	2	0.11610	0.06968
4(4)	0.06034	0.06276	2	0.10540	1.06034
5(B)	0.03756	0.04195	2	0.08537	0.04742
(C)	0.03153	0.02127	5	0.13970	0.08642
6(2)	0.05356	0.06404	5	0.10910	0.06425
(3)	0.04572	0.05236	5	0.12890	0.07446
8(4)	0.04472	0.03013	5	0.06462	0.02972
9(2)	0.10120	0.17000	6	0.17080	0.10410
(3)	0.05939	0.05147	6	0.12310	0.07377
10(3)	0.04531	0.05188	6	0.06418	0.03031
11(2)	0.03827	0.03792	7	0.03829	0.01441
(3)	0.01914		7	0.03989	0.01347
12(2)	0.06781	0.10410	8	0.08463	0.04889
(4)	0.07086	0.09230	8	0.05883	0.02777
			8	0.06270	0.02961
			9	0.11290	0.06463
			9	0.09910	0.05367
			9	0.04140	0.00862
Mean k_1	0.050	0.050	Mean k_1	0.091	0.050

$$[O] = \frac{k_1 [O]_{S.E.} + Ak_3}{k_1 + Ak_2 [C]}$$

Substituting the mean value of 0.05 obtained for k_1 as above and 0.09 for $[O]_{S.E.}$ which is a fair average for the basic open-hearth results of the present work, equation (9) becomes :

$$[O] = \frac{(0.05 \times 0.09) + Ak_3}{0.05 + Ak_2 [C]}$$

$$= \frac{0.0045 + Ak_3}{0.05 + Ak_2[C]}$$

If now the values derived by Mackenzie for Ak_3 and Ak_2, 0.005 and 1.9 respectively, are inserted the expression for [O] reduces to

$$[O] = \frac{0.0045 + 0.005}{0.05 + 1.9 [C]}$$

Suppose [C] = 1%

Then $[O] = \frac{0.0095}{1.95} = 0.0049\%$

If A is doubled $[O] = \frac{0.0145}{3.85} = 0.0038\%$

Suppose [C] = 0.1% $[O] = \frac{0.0095}{0.24} = 0.0396\%$

If A is doubled $[O] = \frac{0.0145}{0.43} = 0.0337\%$.

Thus it would appear that an increase in A leads to a decrease in [O], the effect being relatively small.

If steady state conditions are approached then the rate of supply of oxygen to the metal should give a similar picture of the rate of carbon removal as did the rate of transfer of oxygen to the gas phase. As stated above the rate of supply of oxygen to the metal is equal

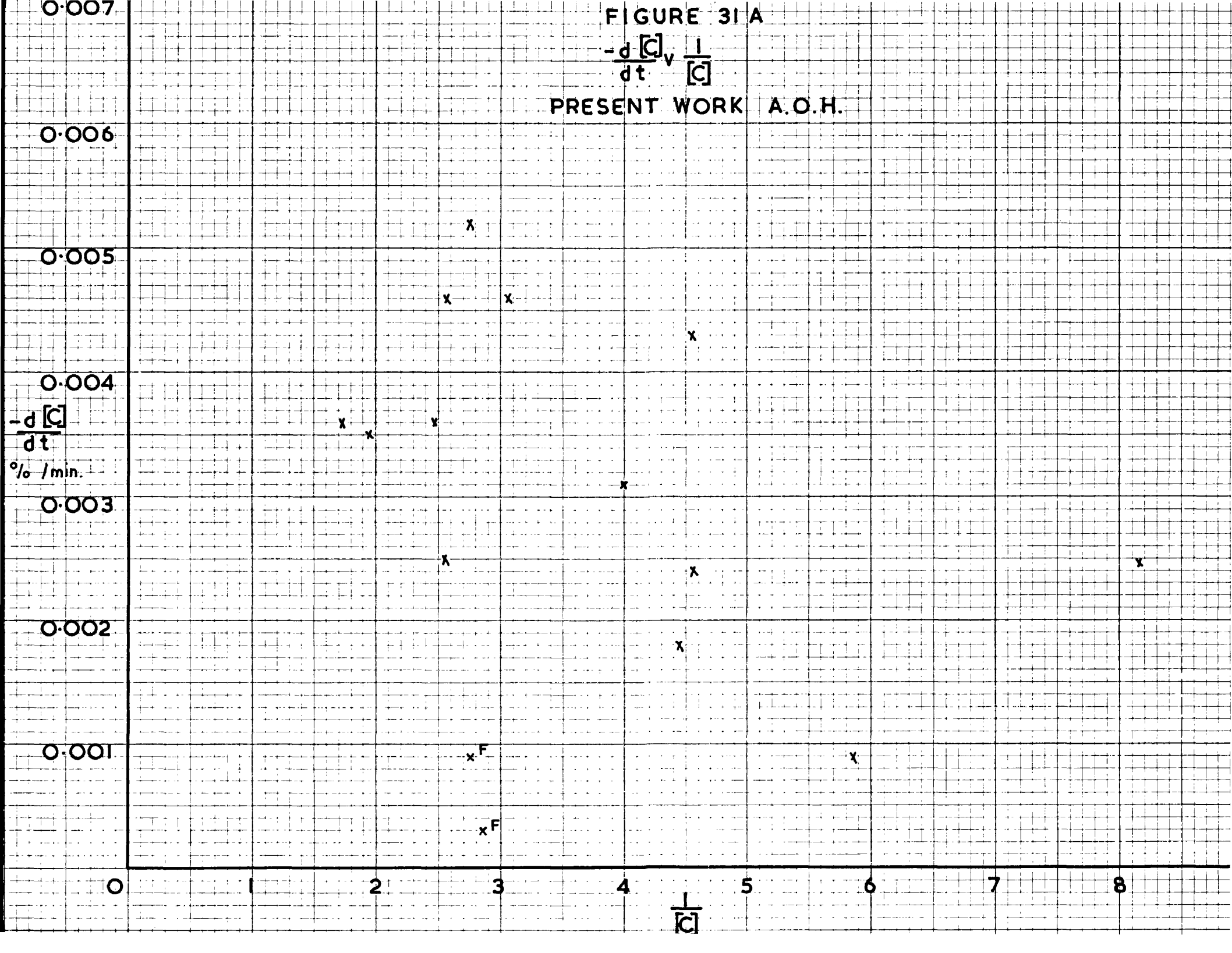
FIGURE 31 A
$-\frac{d[C]}{dt} \frac{1}{[C]}$
PRESENT WORK A.O.H.
0·007
0·006
0·005
0·004
$-\frac{d[C]}{dt}$
% /min.
0·003
0·002
0·001
F
F
0
1
2
3
4
5
6
7
8
$\frac{1}{[C]}$

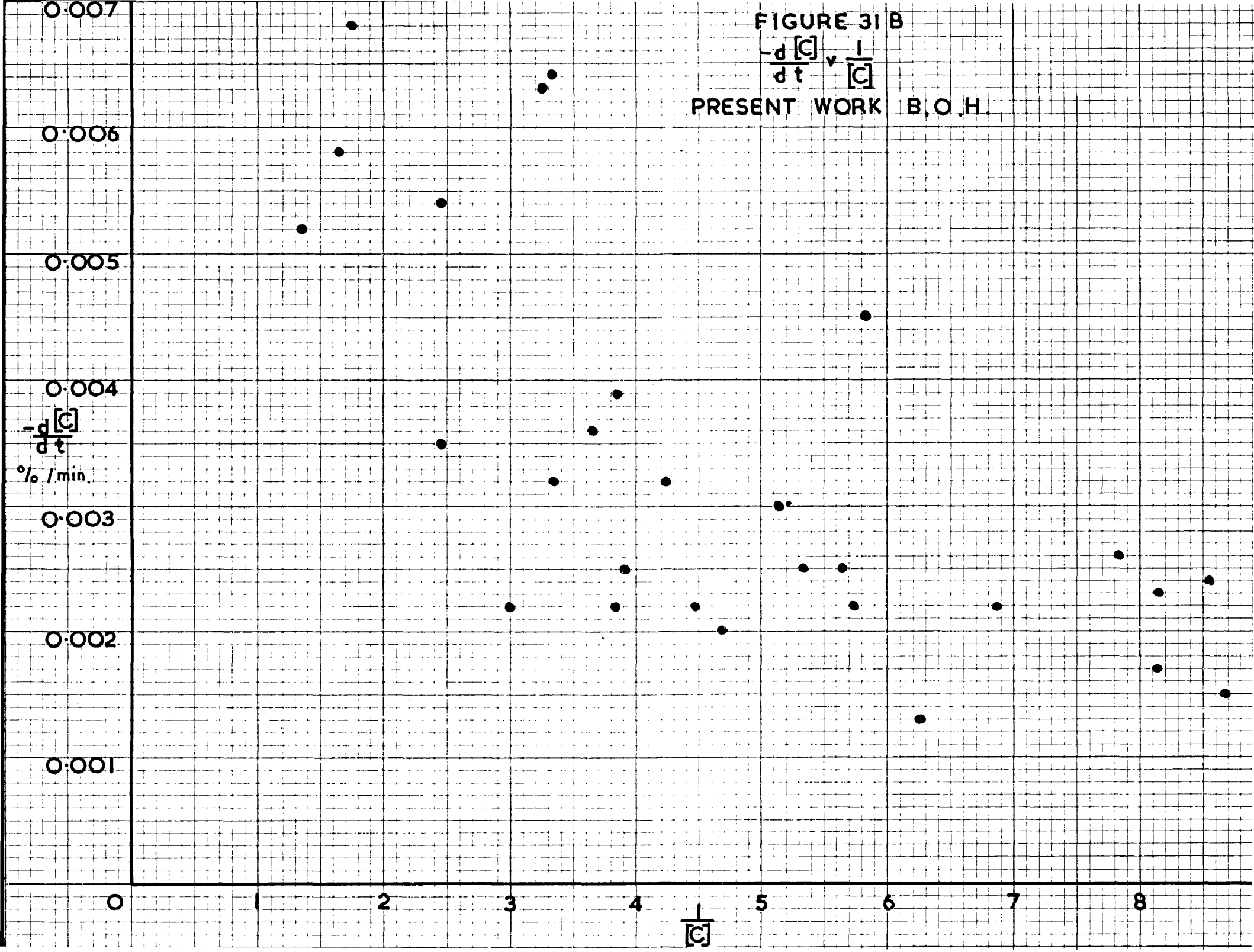
FIGURE 31 B
$\frac{-d[C]}{dt}$ v $\frac{1}{[C]}$
PRESENT WORK B.O.H.
0·007
0·006
0·005
0·004
$\frac{-d[C]}{dt}$
% / min.
0·003
0·002
0·001
0
1
2
3
4
5
6
7
8
$\frac{1}{[C]}$

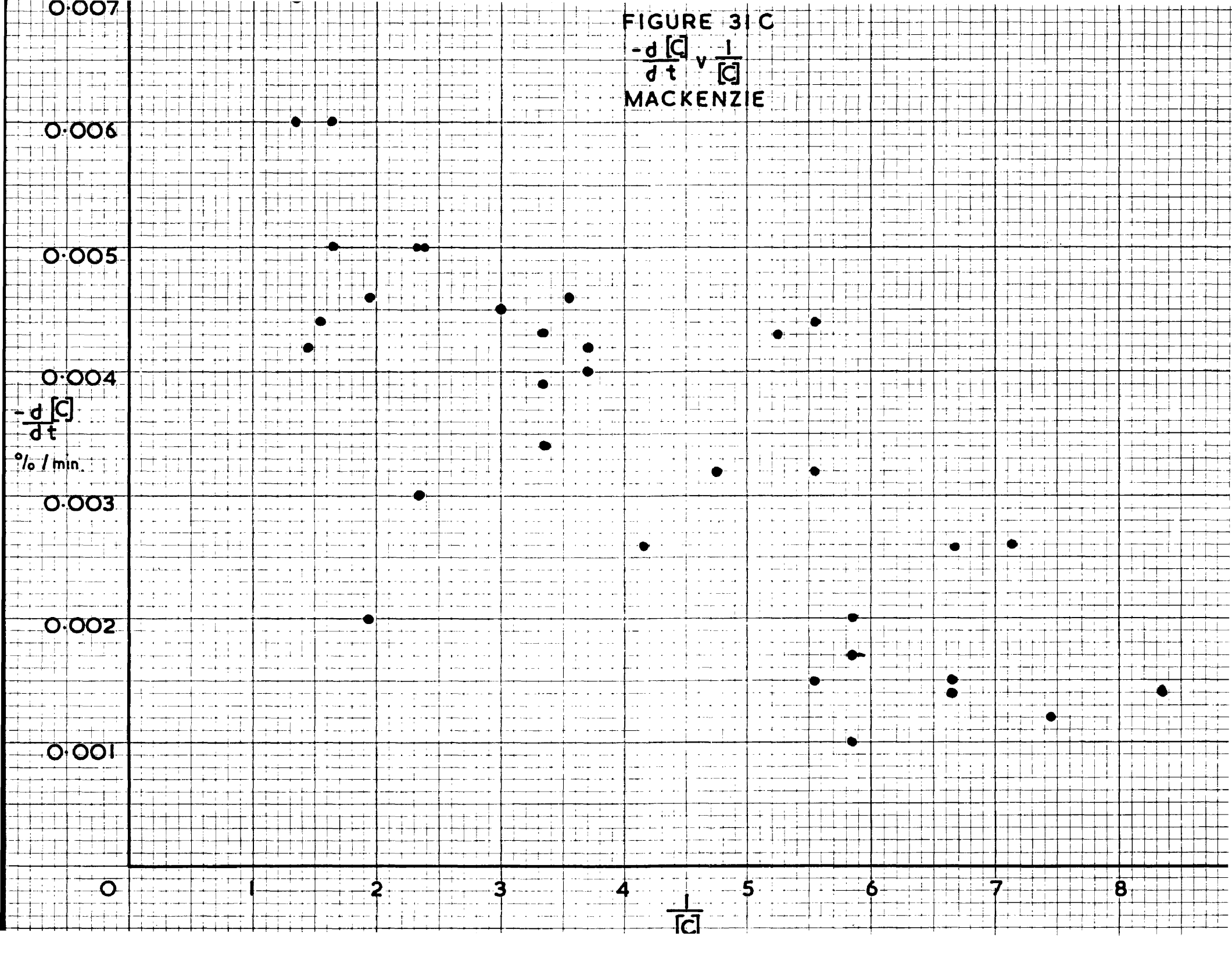
FIGURE 31 C
$-\frac{d[C]}{dt}$ v $\frac{1}{[C]}$
MACKENZIE
0·007
0·006
0·005
0·004
$-\frac{d[C]}{dt}$
% / min.
0·003
0·002
0·001
0
1
2
3
4
5
6
7
8
$\frac{1}{[C]}$

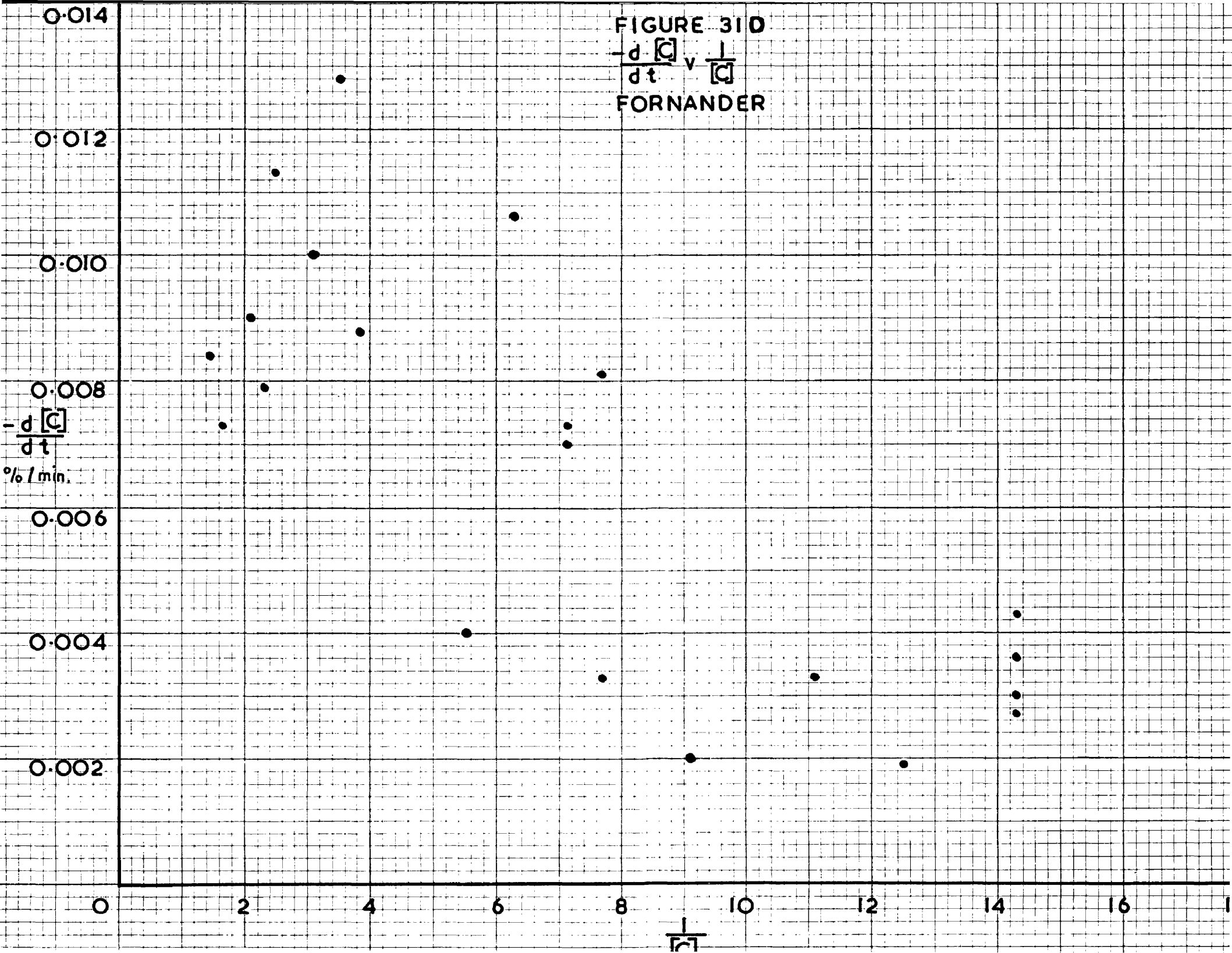
FIGURE 31D
$-\frac{d[C]}{dt}$ v $\frac{1}{[C]}$
FORNANDER
0·014
0·012
0·010
0·008
$-\frac{d[C]}{dt}$
% / min.
0·006
0·004
0·002
0
2
4
6
8
10
12
14
16
$\frac{1}{[C]}$

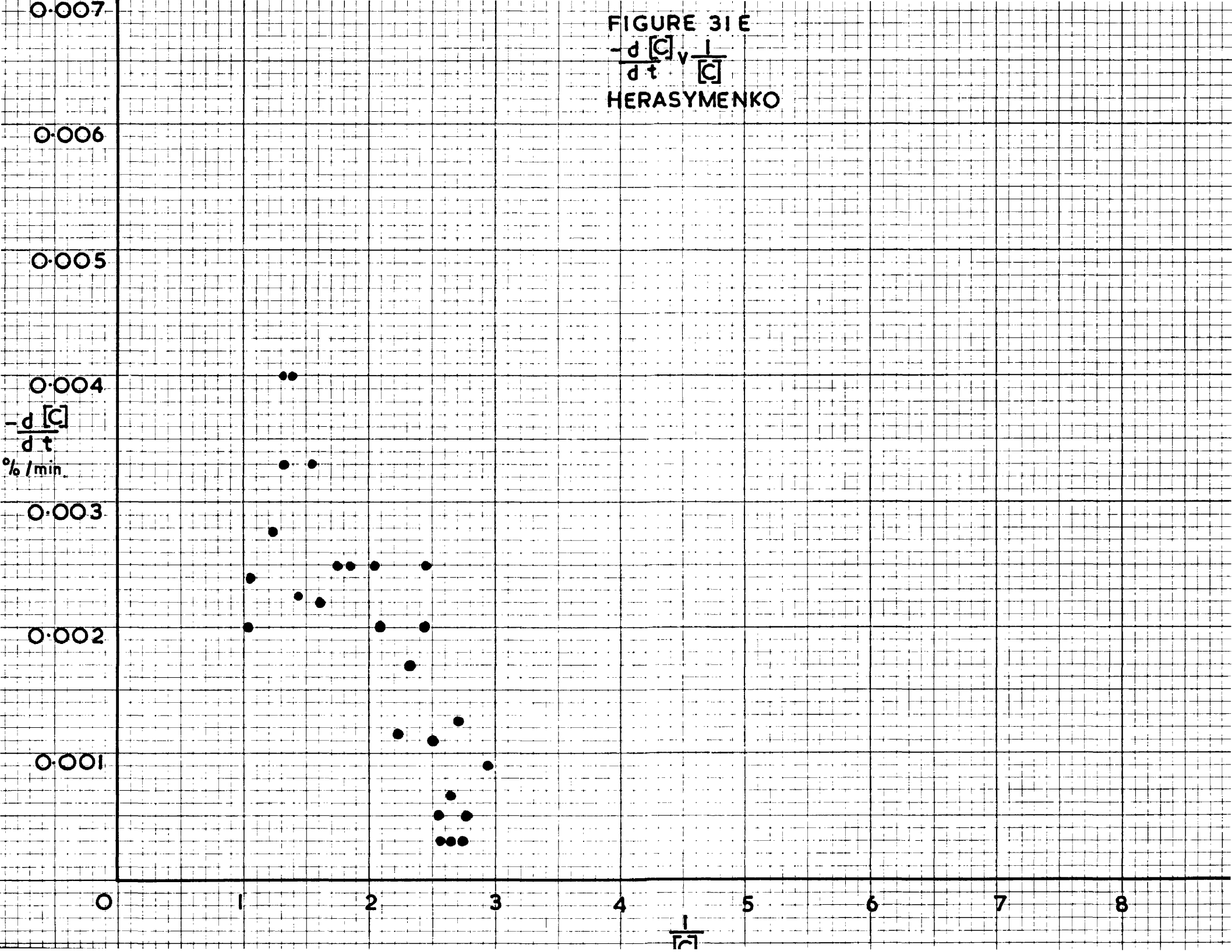
FIGURE 31 E
$-\frac{d[C]}{dt}$ v $\frac{1}{[C]}$
HERASYMENKO
0·007
0·006
0·005
0·004
$-\frac{d[C]}{dt}$
% / min.
0·003
0·002
0·001
0
1
2
3
4
5
6
7
8
$\frac{1}{[C]}$

FIGURE 31 F

$-\frac{d[C]}{dt}$ v $\frac{1}{[C]}$

KERLIE

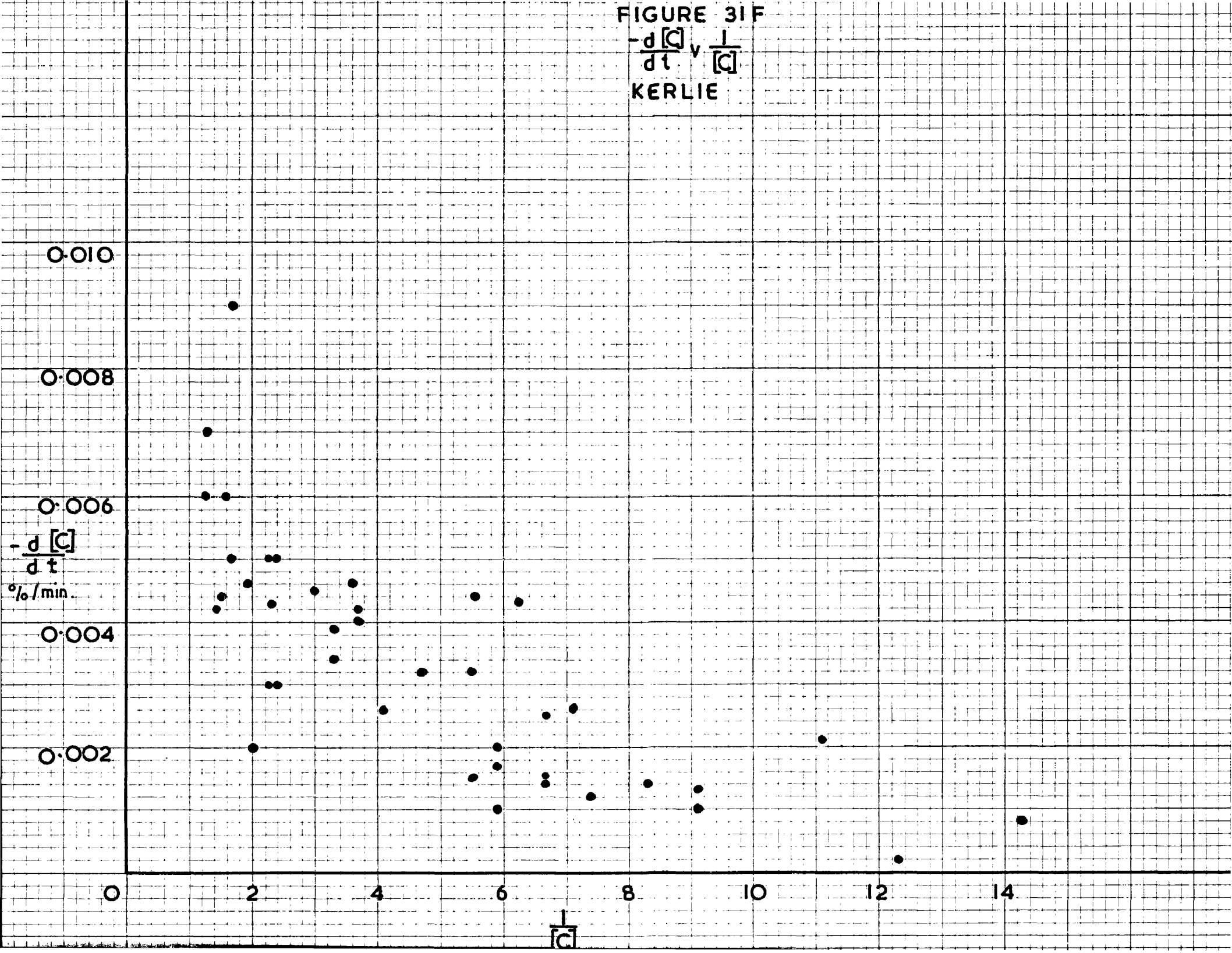

to k_1 $([O]_{S.E.} - [O])$. Now [O] may be written as $(\Delta[O] + [O]_{C.E.})$ where $\Delta[O]$ is the excess oxygen over that in equilibrium with the carbon and $[O]_{C.E.}$ is the oxygen in equilibrium with the carbon.

Then the rate of supply of oxygen to the metal =

$$= k_1 \left([O]_{S.E.} - \left\{\Delta[O] + [O]_{C.E.}\right\}\right)$$

$$= k_1 \left([O]_{S.E.} - \Delta[O] - \frac{m}{[C]}\right)$$

But $\Delta[O] = \frac{m}{[C]} \left(p_{Fe} + \frac{2T}{r}\right)$

∴ Rate of supply of oxygen to the metal =

$$= k_1 \left([O]_{S.E.} - \left\{\frac{m}{[C]} \left(p_{Fe} + \frac{2T}{r}\right) + \frac{m}{[C]}\right\}\right)$$

Then rate of carbon removal =

$$= \frac{-d[C]}{dt} = \frac{12}{16} k_1 \left([O]_{S.E.} - \left\{\frac{m}{[C]} \left(1 + p_{Fe} + \frac{2T}{r}\right\}\right)\right) \quad \ldots\ldots(10)$$

Rate of carbon removal has been plotted against $\frac{1}{[C]}$ in Figures 31A and B for the acid and basic open-hearth furnaces in the present work and in Figures 31 C, D, E and F for the data of Mackenzie, Fornander, Herasymenko and Kerlie respectively.

This plot would only be expected to yield a straight line if the slag iron oxide activity and metal temperature remained constant throughout the refining period. As far as the basic open-hearth results are concerned the temperature did remain reasonably constant but the iron oxide activity of the slag increased as lower carbon contents were approached. Thus the basic open hearth plots in Figures 31 B, C, D and F tend to change their slope at the lower carbon contents.

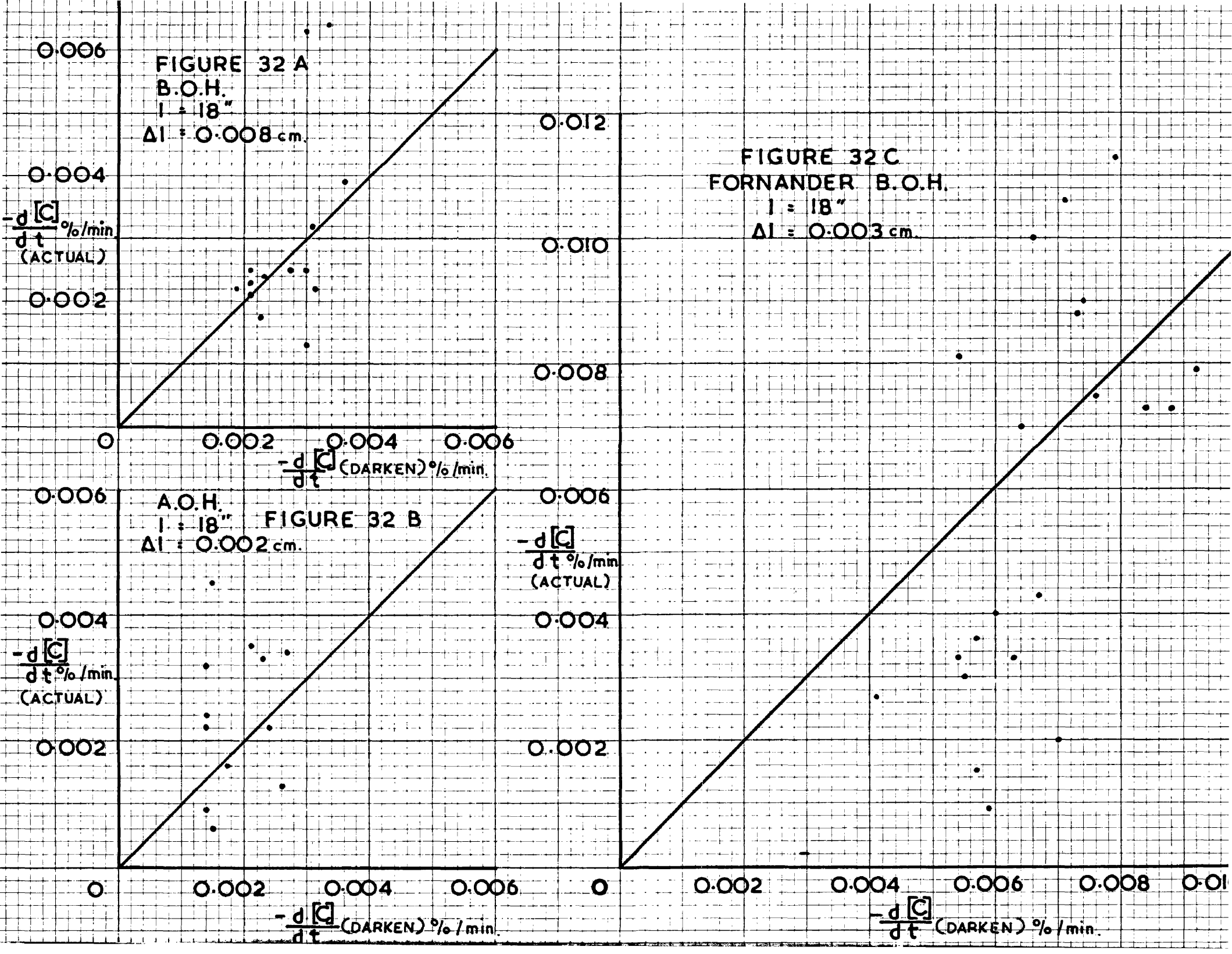
FIGURE 32 A
B.O.H.
l = 18"
Δl = 0·008 cm.
0·006
0·004
0·002
0
0·002
0·004
0·006
$-\frac{d[C]}{dt}$ %/min (ACTUAL)
$-\frac{d[C]}{dt}$ (DARKEN) %/min.
FIGURE 32 B
A.O.H.
l = 18"
Δl = 0·002 cm.
FIGURE 32 C
FORNANDER B.O.H.
l = 18"
Δl = 0·003 cm.
0·012
0·010
0·008
0·006
0·004
0·002
0
0·002
0·004
0·006
0·008
0·01

On the other hand the acid open hearth results of Herasymenko in Figure 31E are reasonably well represented by a straight line as are those for the present acid open hearth data in Figure 31A with the exception of the last two points in Heat F where the temperature fell considerably. These points are marked in Figure 31A. Slag ferrous oxide activity in both sets of acid open-hearth data remained substantially constant throughout.

The expression for the rate of carbon removal given in equation (10) is similar to that of Darken(40)

$$\frac{-d[C]}{dt} = \frac{D.([O]_{S.E.} - [O])\ \frac{60.12}{16}}{\ell\ \Delta\ell}$$

which was discussed in the introduction. Values of rate of carbon removal calculated from this formula were obtained from the data in the present study and of Fornander. The best agreement in the basic open-hearth results was obtained, as shown in Figure 32, with a film thickness of 0.003 cm. which lies between the values of 0.01 cm. and 0.003 cm. proposed respectively by Samarin and Shvartzman(69) and by Darken. The results of Fornander fall reasonably well on the line when 0.003 cm. is used for the film thickness while the acid open-hearth results suggest a film thickness of 0.002 cm. It would appear therefore that the film thickness varied from furnace to furnace. Moreover it would appear that diffusion through a dead film of metal adjacent to the slag is the controlling factor in the transfer of oxygen to the bulk of the metal despite the differing slag viscosities in the acid and basic open-hearth processes, which might be expected to slow down the diffusion of oxygen

through the acid slag. The lower value of film thickness obtained in the present work for the acid furnace compared with the basic might reasonably be due largely to the average temperature in the former being 30-40°C in excess of the average in the latter.

In conclusion, it may be said that previous investigators of carbon removal assumed particular stages of the process as rate controlling, and with these assumptions derived equations to predict the rate of removal. In the present study carbon removal has been viewed as a whole and it has been shown that the earlier hypotheses are not as unrelated as would appear at first sight. Thus, equally good predictions may be made by considering the rate of removal in relation to the rate of passage of oxygen from the metal to the gas bubbles (the rate controlling step of Vallet) and the rate of supply of oxygen to the metal from the slag (a governing factor in the rate of removal of carbon in the hypothesis of Darken). The results obtained in the present work indicate that no single step is rate controlling. Thus, if no suitable nuclei were present at the hearth, or if the slag were unsuitable for transferring oxygen from the gas phase to the metal, carbon removal would cease. Carbon removal will clearly be related to the number of nuclei present, but for a given number of nuclei, the rate of removal will increase with the rate of supply of oxygen from the gas phase via the slag to the metal/gas interfaces arising from these nuclei.

REFERENCES.

1. H.C.Vacher and E.H.Hamilton: Trans. A.I.M.E., 1931, 95, 80.
   H.C.Vacher: Bureau of Standards, Journal of Research, 1933,11,541.

2. G.Phragmén and B.Kallings: Jernkonterets Annaler, 1939, 123, No.5 199.

3. S. Marshall and J. Chipman: Trans. A.S.M., 1942, 30, 695.

4. M.G.Fontana and J.Chipman: Trans. A.S.M., 1936, 24, 313.

5. L.S.Darken: Trans. A.I.M.E., 1940, 140, 204.

6. E.T.Turkdogan, L.S.Davis, L.E.Leake and G.G.Stevens: J.Iron and S.Inst., 1955, 181, 123.

7. P.Herasymenko: J.Iron and S. Inst., 1947, 157, 515.

8. P.Bardenheur and G.Thanheiser: Mitt.Kaiser-Wilhelm Inst. für Eisenforschung, 1934, 16, 189.

9. F.Körber and W.Oelsen: Mitt Kaiser-Wilhelm Inst.für Eisenforschung, 1936, 56, 207.

10. F.D.Richardson: Faraday Soc. Discussion, 1948, 4, 114.

11. S.Matoba and S.Banya: Tech.Reps., Tohuku Univ., 1955, 20, 131.

12. C.H.Herty, Jr., C.F.Christopher, H.Freeman and J.F.Sanderson: Carnegie Inst. of Technology, Mining and Metallurgy Investigation, Bulletin No.68, 1934.

13. H.Schenck, W.Riess and E.O.Brüggemann: Zeitt. für Elektrochemie, 1932, 38, 562. Stahl und Eisen, 1932, 52, 831.

14. K.C.McCutcheon and J.Chipman: Trans. A.I.M.E., 1938, 131, 206.

15. R.J.Sarjant: J.Iron and S. Inst., 1946, 154, 265.

16. A.McCance: Symposium on Steelmaking (Iron and Steel Inst.,1938) 331.

17. I.M.Mackenzie: J.Iron and S.Inst., 1946, 154, 55.

18. K.C.McCutcheon: Trans. A.I.M.E., 1940, 140, 133.

19. K.L.Fetters and J.Chipman: Trans. A.I.M.E., 1940, 140, 170.

20. B.M.Larsen: Trans. A.I.M.E., 1941, 145, 67.

21. H.Schenck: "Physical Chemistry of Steelmaking" (British Iron and Steel Research Association, 1945).

22. C.R.Taylor and J.Chipman: Trans. A.I.M.E., 1943, 154, 228.

23. E.T.Turkdogan and J.Pearson: J.Iron and S.Inst., 1953, 173, 217.

24. S. Formander: Faraday Soc. Discussion, 1948, 4, 296.

25. A.L.Feild: Trans. A.I.M.E., 1928, 80, 114.

26. E.R.Jette: Trans. A.I.M.E., 1931, 95, 80.

27. H.Schenck: "Physical Chemistry of Steelmaking" (British Iron and Steel Research Association 1945).

28. F.Körber and W.Oelsen: Mitt.Kaiser-Wilhelm Inst. für Eisenforschung, 1932, 14, 181.

29. C.F.Goodeve: Faraday Soc. Discussion, 1948, 4, 9.

30. P. Vallet: Rev. Metall., 1954, 51, 709.

31. F. Körber and W.Oelsen: Mitt.Kaiser-Wilhelm Inst.für Eisenforschung, 1935, 17, 39.

32. C.E. Sims: Trans. A.I.M.E., 1947, 172, 176.

33. G. Ranque: Rev. Metall., 1942, 39, 331.

34. F.D. Richardson: J.Iron and S.Inst., 1948, 158, 455.

35. T.E.Brower and B.M.Larsen: Trans. A.I.M.E., 1947, 172, 137.

36. T.E.Brower and B.M.Larsen: Trans. A.I.M.E., 1947, 172, 164.

37. F.D.Richardson: Faraday Soc.,Discussion, 1948, 4, 335.

38. P.T.Carter: Steelmaking Reactions, "Metallurgical Progress" 1953, 43.

39. L.S.Darken: Trans. A.I.M.E., 1947, 172, 190.

40. L.S.Darken: "Basic Open-Hearth Steelmaking" (A.I.M.E. 1951) 592.

41. J.Chipman: "Basic Open-Hearth Steelmaking" (A.I.M.E. 1951) 621.

42. J.R.Rait, Q.C. McMillan and R.Hay: J.Royal Technical College, Glasgow, 1939, 4, 449.

43. A. McCance: J.West of Scotland Iron and S.Inst., 1933-34, 41, 1.

44. R.Hay, J.M.Ferguson and J.White: Symposium on Steelmaking (Iron and Steel Inst., 1938), 52.

45. J.H. Whiteley and A.F.Hallimond: J.Iron and S.Inst., 1919, 99, 199.

46. G.R. Fitterer: Trans. A.S.M., 1945, 34, 41.

47. A.L.Bradley, J.H.Chesters, J.M.Ferguson and R.J.Sarjant: Iron and Steel Inst., Special Report No.33, 1946, 117.

48. R. Kennedy: B.Sc., Thesis, Glasgow University, 1951.

49. D.W. Morgan and J.A.Kitchener: Trans. Faraday Soc., 1954, 50, 51.

50. W.O.Philbrook, K.M.Goldmann and M.M.Helzel: Trans. A.I.M.E., 1950, 188, 361.

51. N.A.Gokcen and J.Chipman: Journal of Metals, 1953, 197, 173.

52. H.Wentrup and G.Hieber: Tech.Mitt.Krupp, A.Forschungs-Berichte, (1939) 1, No.2, 47.

53. D.C. Hilty and W.Crafts: Trans. A.I.M.E., 1950, 188, 414.

54. M.S.Beletski and M.B.Rapoport: Doklady Akad Nauk U.S.S.R. 1951, 80, 751.

55. M. Hoch and H.L.Johnston: J.Amer.Chem. Soc., 1954, 76, 2560.

56. L. Brower and A.W.Searcy: J.Amer.Chem. Soc., 1951, 73, 5308.

57. W.Geller: Archiv.für das Eisenhüttenwesen, 1942, 15, 479.

58. T.E.Dancy: J.Iron and S.Institit., 1951, 169, 17.

59. T.B.Winkler and J.Chipman: Trans. A.I.M.E., 1946, 167, 111.

60. N.J. Grant and J.Chipman: Trans. A.I.M.E., 1946, 167, 134.

61. W.A.Fischer and H. vom Ende: Archiv für das Eisenhütt., 1952, 23, 21.

62. K.Balajiva, A.G.Quarrel and P.Vajragupta: J.Iron and S.Inst., 1946, 153, 115.

63. R.Schuhmann and P.J.Ensio: J.Iron and S.Inst., 1951, 189, 401.

64. W.L.Kerlie: J.Iron and S.Instit., 1951, 167, 9.

65. P.Kozakevitch, S.Chatel and M.Sage: Compt. rendus Acad.Sci., Paris, 1953, 236, 2064.

66. R. Bruce: Private communication.

67. A.H.Jay: J.Iron and S.Inst., 1947, 157, 167.

68. P.Herasymenko and G.E.Speight: J.Iron and S.Inst., 1950, 166, 289.

69. A.M.Samarin and L.A.Shvartzman: J.Phys.Chem. U.S.S.R., 1948, 22,565.

A C K N O W L E D G E M E N T S.

The author wishes to express his thanks to Professor R. Hay for his encouragement and interest, to Dr. P.T. Carter, who directed the work, for his enthusiastic help and guidance and to the Directors of R.B. Tennent Ltd., for sponsoring the investigation.

The work was carried out in the Metallurgy Department of the Royal College of Science and Technology, Glasgow.

Appendix.

FIGURE A
CARBON DROP CURVES

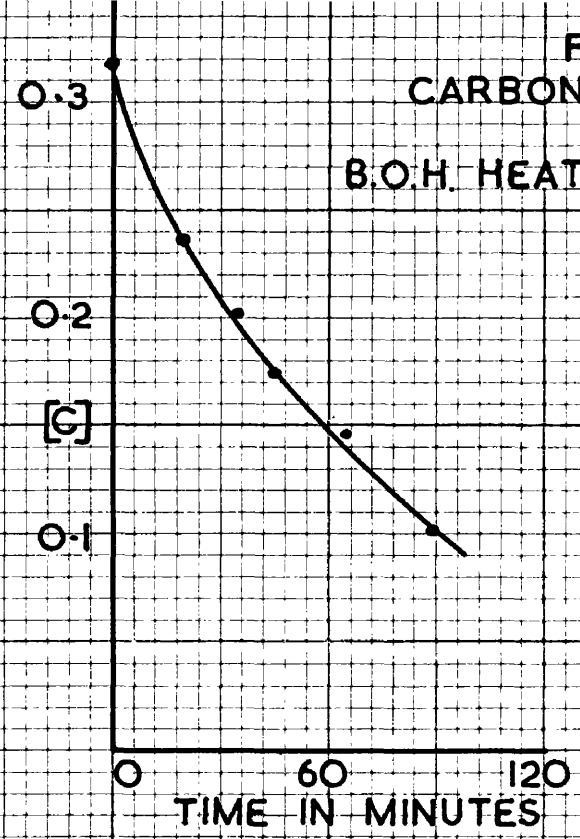

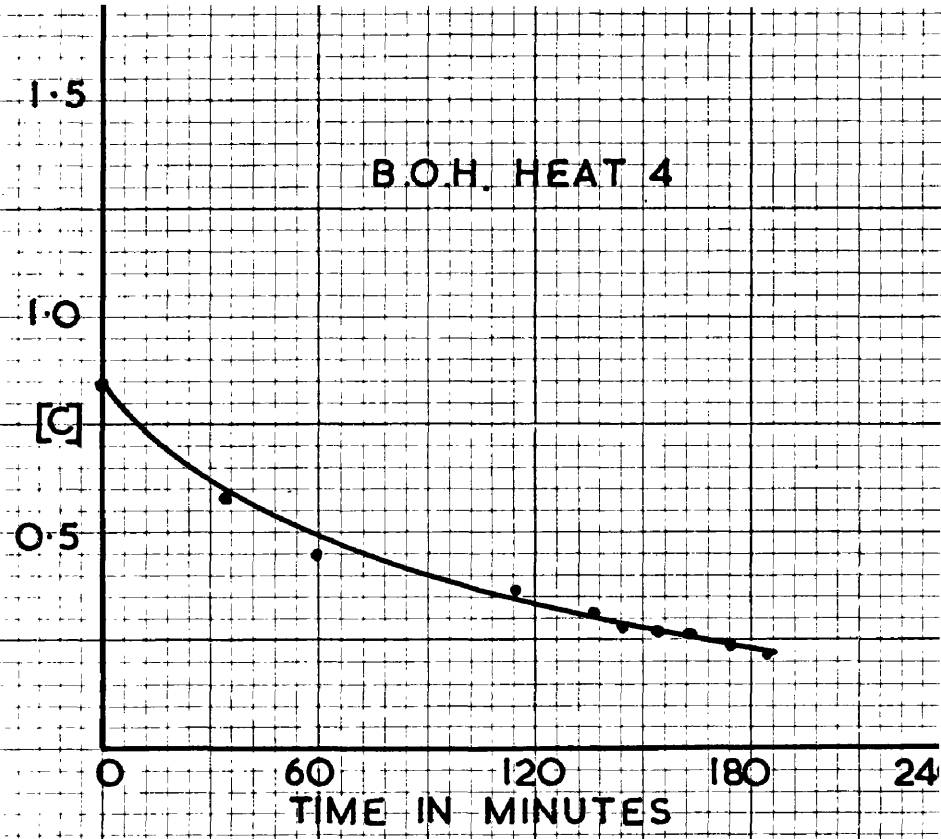

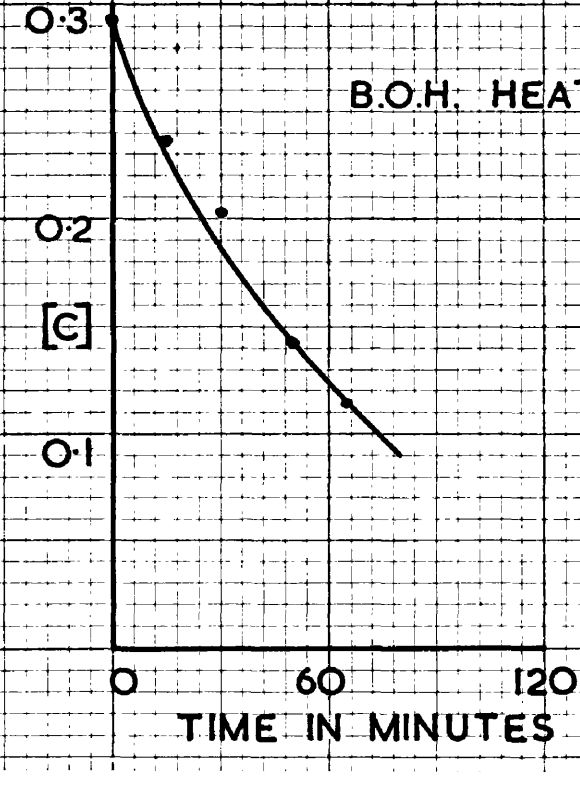

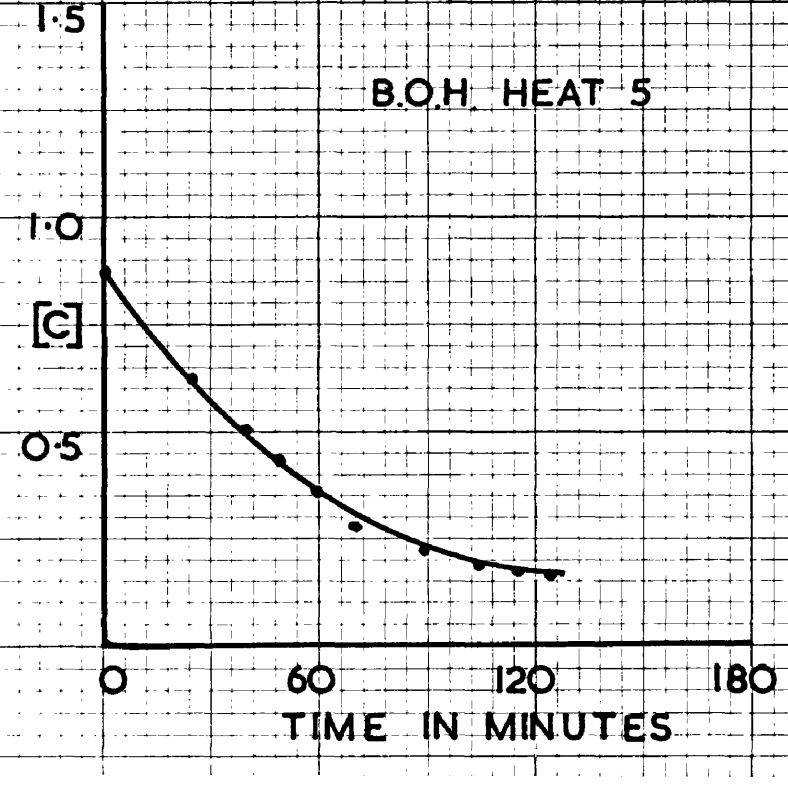

FIGURE 8
CARBON DROP CURVES

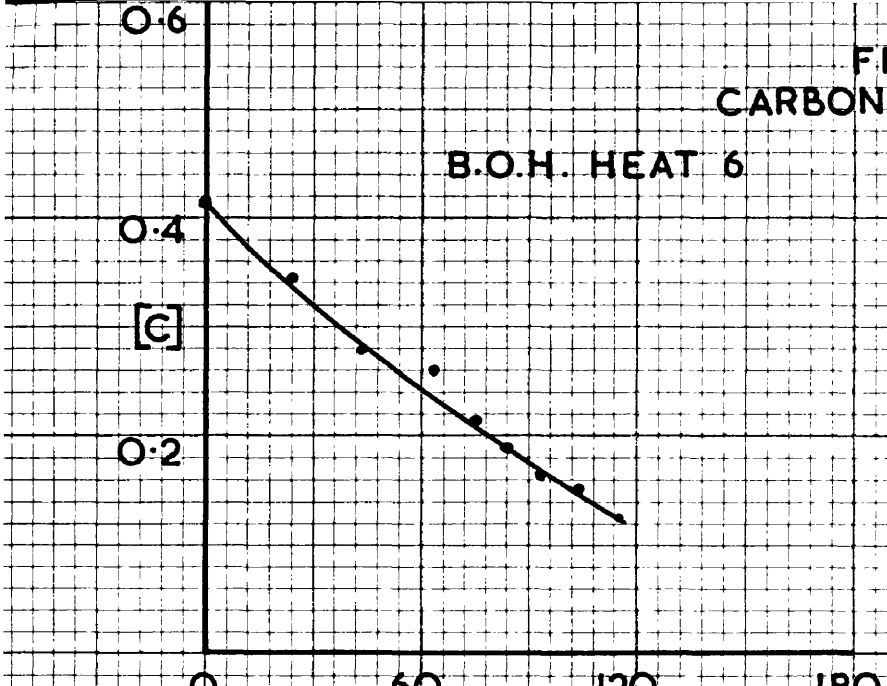

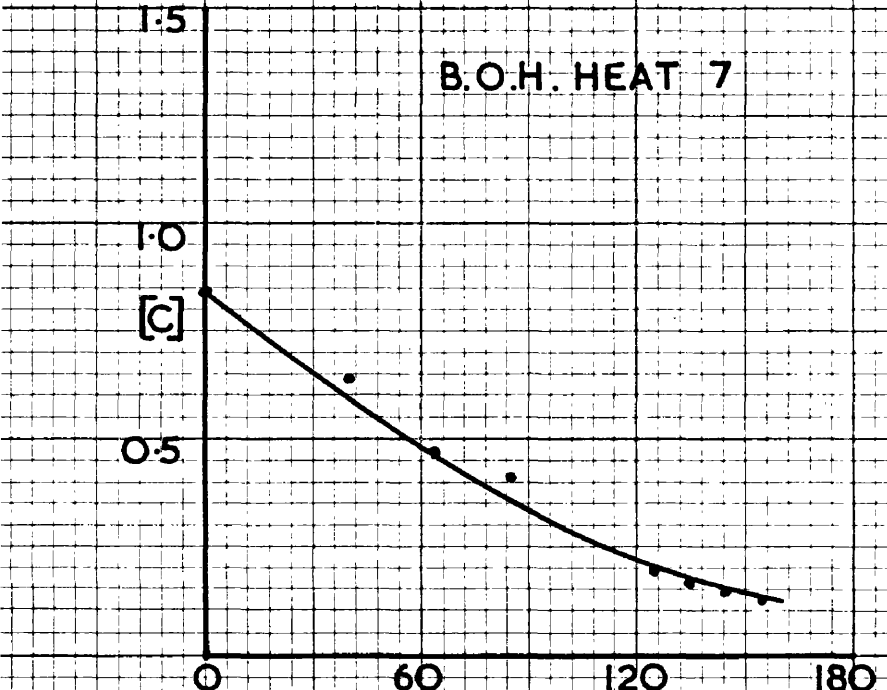

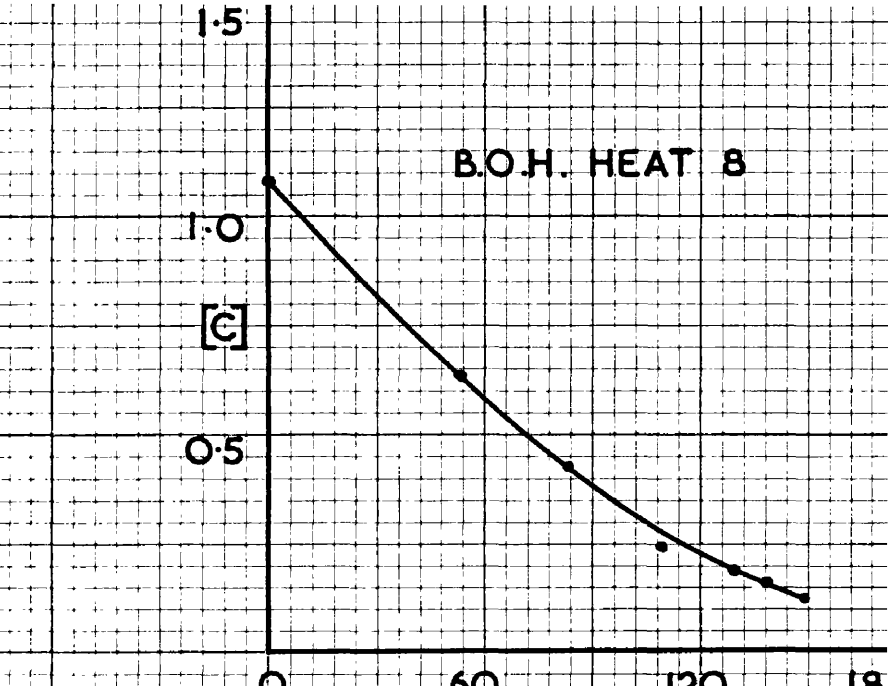

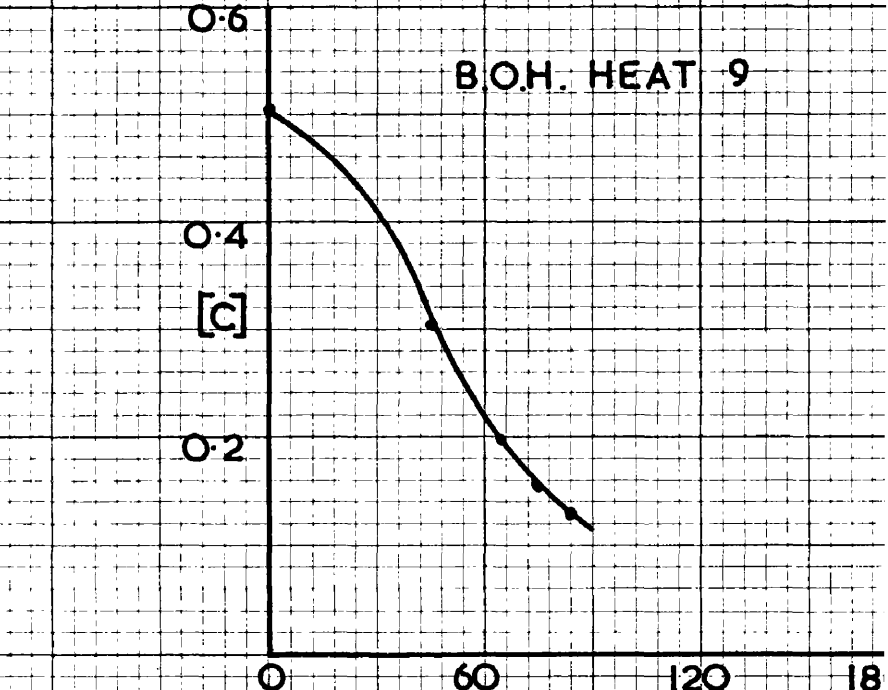

FIGURE C
CARBON DROP CURVES

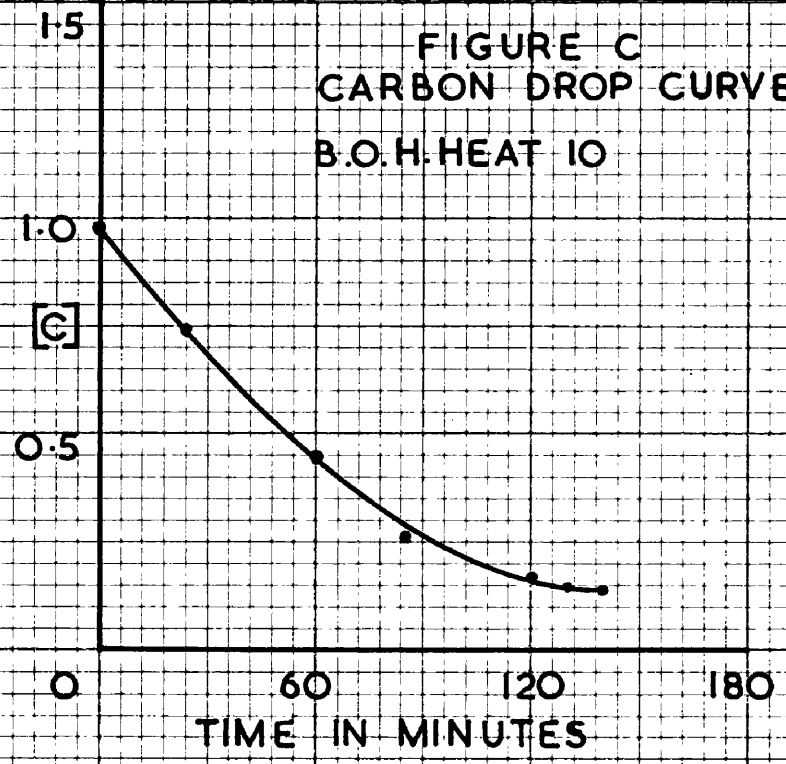

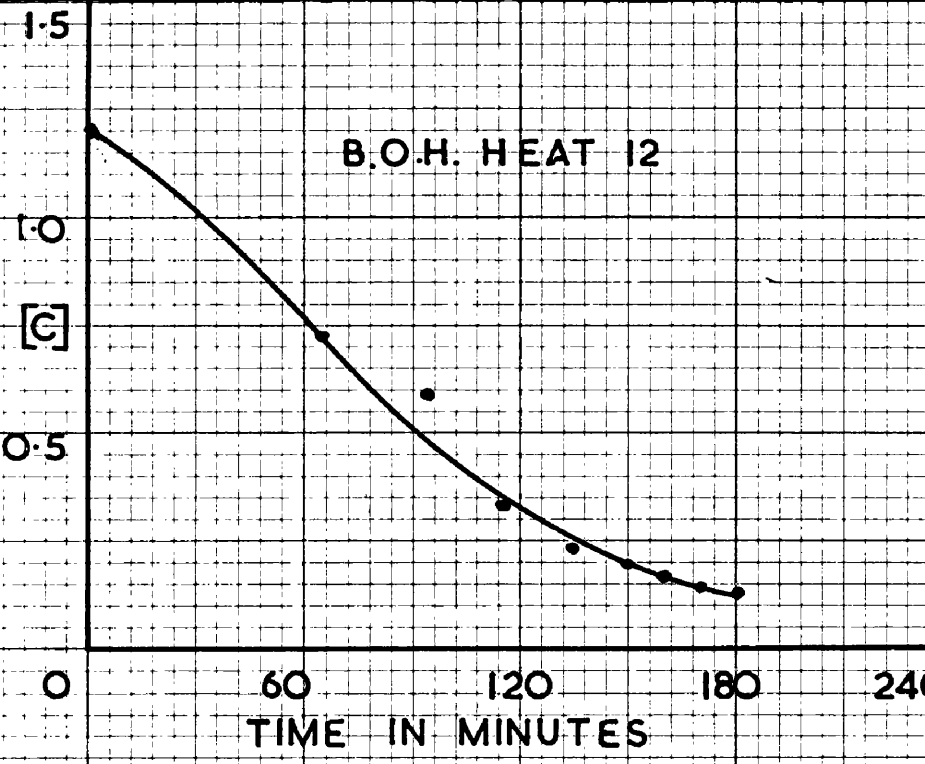

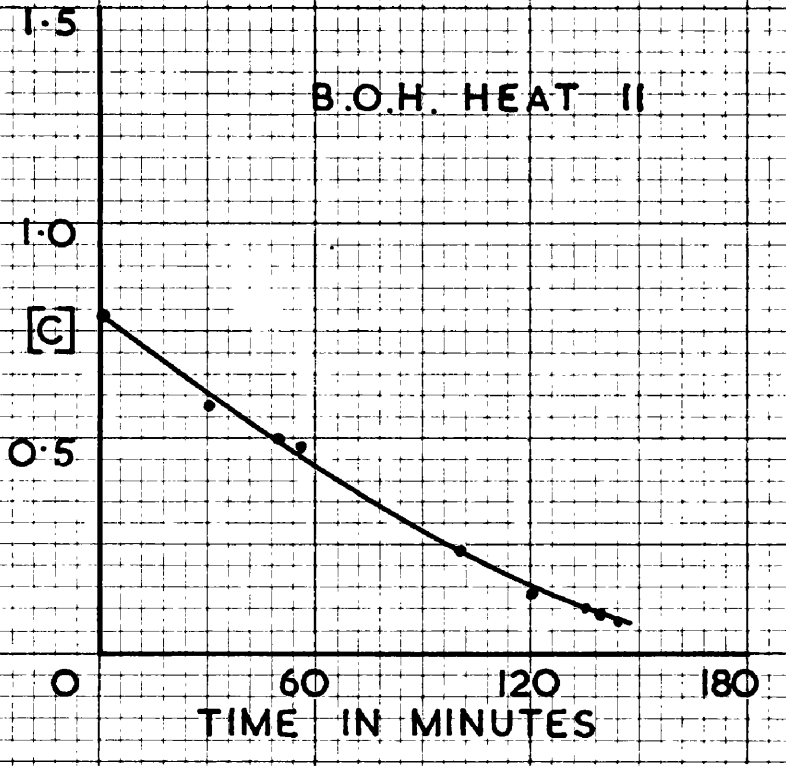

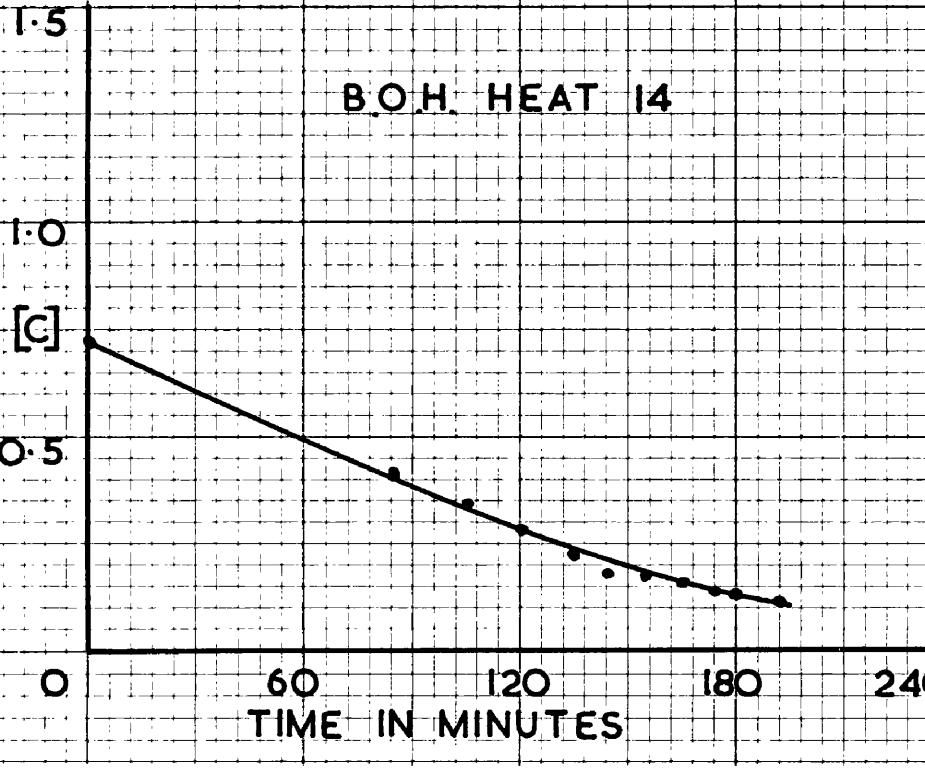

FIGURE D
CARBON DROP CURVES

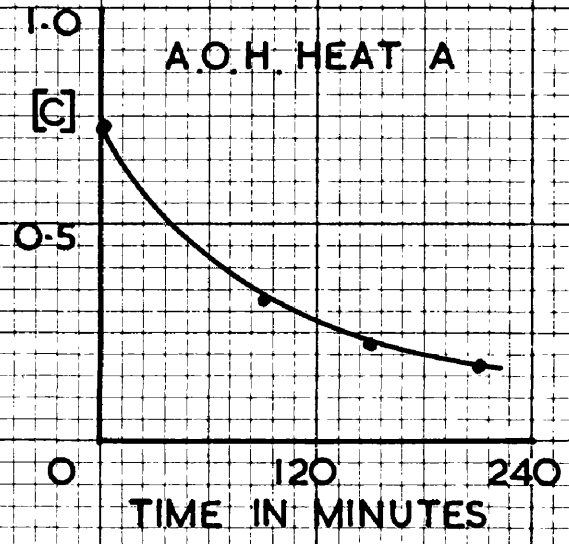

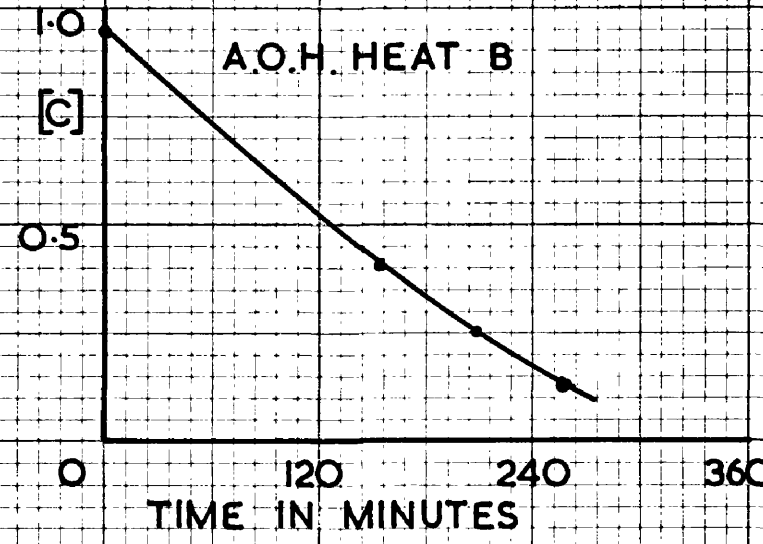

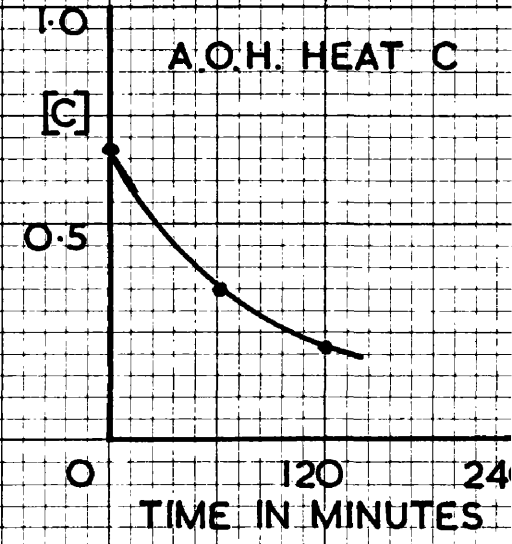

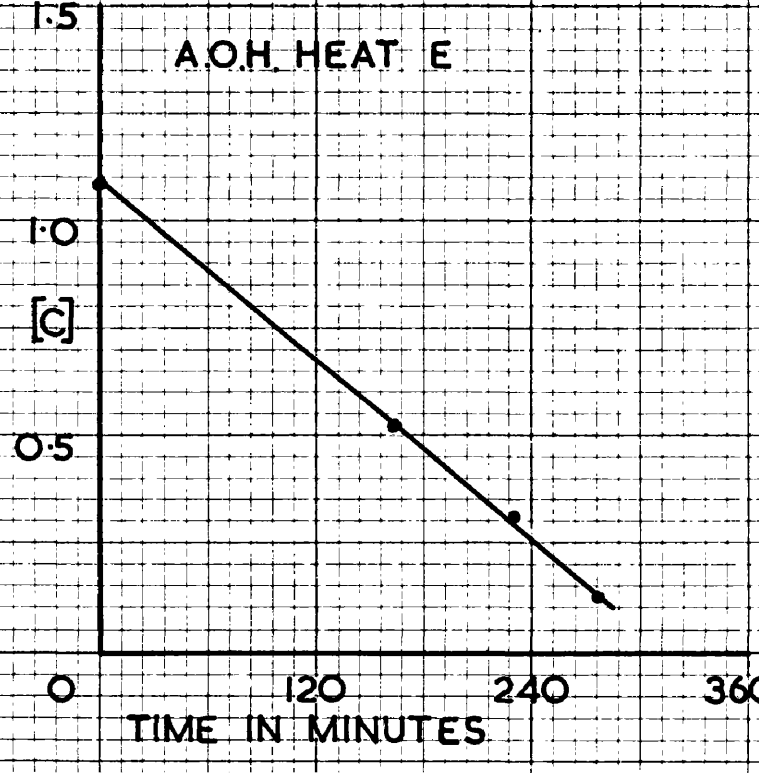

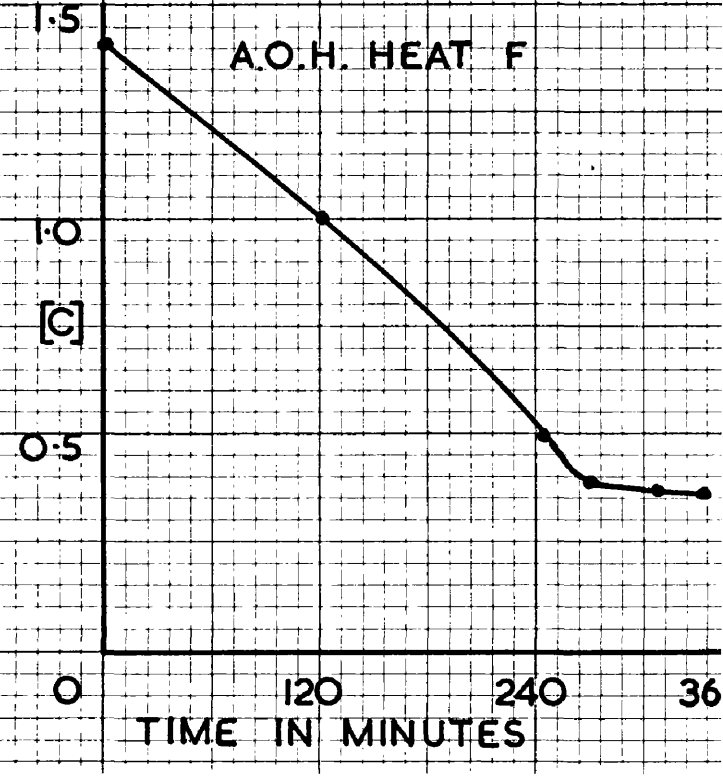

HEAT LOG B.O.H. HEAT 2.

Charge Composition	Tons.	Cwts.	Time	Sample	Temperature °C.	[C]	Remarks.
Scrap	51	0					
Pig	26	15					
Soft Billet C473			7.50 p.m.	Test Sample		0.234	
			8.05-9.10				Pigged back with 3 tons of Bilston.
			8.25	Melt-out Sample		0.240	
			8.27				5 cwt. Silico manganese. 5 cwt. ferro silicon. 10 cwt. burnt lime.
			8.50				4 cwt. fluorspar.
			8.55	Bath Sample and Slag Sample.	1515	0.278	
			9.25	Bath Sample Slag Sample	1562	0.319	
			9.45	" "		0.237	10 cwt. burnt lime.
			10.00	" "		0.202	
			10.10	" "		0.173	
			10.20	" "	1600	0.154	
			10.30	" "		0.147	
			10.40	" "	1608	0.117	
			10.43	Bomb sample 2(7) Slag Sample	1610	0.102	
			10.50	Bath Sample Slag Sample		0.095	
			10.53				TAPPED.

HEAT LOG B.O.H. HEAT 3.

Charge Composition	Tons.	Cwts.	Time	Sample	Temperature. °C.	[C]	Remarks.
Scrap	51	8					
Pig	25	12					
Soft Billet C476.			6.30 a.m.	Test Sample		0.254	
			7.00				Pigged back 3T 15 Cwt. Bilston Pig.
			7.20				Melt out.
			7.35	Bath Sample Slag Sample	1544	0.234	10 cwt. Burnt Lime, 4 cwt. spar.
			7.50				1 T. 15 cwt. Bilston Pig Iron.
			8.05	Bath Sample Slag Sample		0.292	9 cwt. of burnt lime.
			8.20	Bath Sample Slag Sample		0.237	10 cwt. of burnt lime.
			8.30	Bomb Sample 3(1) Slag Sample		0.213	
			8.35	Bath Sample Slag Sample	1582	0.202	
			8.45	"		0.177	10 cwtslime, 2 cwt. Fluorspar
			9.05	"		0.147	
			9.15	Bath Sample Slag Sample	1594	0.131	
			9.20	Bomb Sample 3(2) Slag Sample		0.123	
			9.25	Bath Sample Slag Sample		0.115	
			9.35		1596		1 cwt. Fe Mn 2 cwt. Fe.Si.
			9.40				TAPPED.

HEAT LOG B.O.H. HEAT 4.

Charge Composition.	Tons.	Cwt.	Time	Sample	Temperature °C.	[C]	Remarks.
Scrap	49	5					
Pig	29	6					
Soft Billet C479.			6.10 a.m.	Premelt Sample Slag Sample		0.844	
			6.45	" "		0.570	Unmelted scrap still present.
			6.55				10 cwt.lime charged as slag very acid.
			7.10	Bath Sample Slag Sample		0.449	Melt still not complete.
			7.29				10 cwt. Burnt Lime added.
			7.30				4 cwt. Fluorspar.
			7.40				30 cwt. Pig charged.
			8.05	Bath Sample Slag Sample	1520	0.36	
			8.15	Bomb Sample 4(1) Slag Sample		0.337	
			8.21				Fluorspar and scale charged.
			8.27	Bath Sample Slag Sample	1550	0.311	
			8.35	" "		0.277	10 cwt. lime 3 cwt. scale fed.
			8.44	Bomb Sample 4(2) Slag Sample		0.261	
			8.45	Bath Sample Slag Sample		0.261	
			8.55	" "		0.254	
			8.58			0.	5 cwt. lime and 2 cwt. scale fed.
			9.06	Bath Sample Slag Sample		0.228	
			9.08	Bomb Sample 4(3) Slag Sample	1585	0.228	
			9.15	Bath Sample Slag Sample		0.206	1/2 cwt. Fluorspar fed.
			9.22				2 cwt. Scale charged.
			9.25	Bath Sample Slag Sample		0.180	
			9.35	" "		0.158	
			9.40	Bomb Sample 4(4) Slag Sample	1605	0.145	
			9.48				

III.

HEAT LOG B.O.H. HEAT 5.

Charge Composition.	Tons.	Cwts.	Time	Sample	Temperature °C.	[C]	Remarks.
Scrap	49	7					
Pig	28	9					
Soft Billet C482.			5.35 a.m.	Premelt Sample Slag Sample.		0.862	
			6.10	Clear Melt Sample		0.614	
			6.10	Bomb Sample 5(A) Slag Sample	1509	0.614	
			6.16				10 cwt. Lime and 10 cwt.Scale fed.
			6.35	Bath Sample Slag Sample		0.432	
			6.38				10 cwt.Lime and 10 cwt.Scale charged.
			6.55	Bath Sample Slag Sample	1548	0.267	
			6.58	Bomb Sample 5(B) Slag Sample		0.260	
			7.00				10 cwt. Lime fed.
			7.05				2 cwt. Fluorspar Fed.
			7.15	Bath Sample Slag Sample		0.218	
			7.23				12 cwt. Lime charged.
			7.30	Bath Sample Slag Sample		0.180	
			7.40	Bomb Sample 5(C) Slag Sample	1563	0.160	
			7.46				5 cwt. Lime fed.
			7.50	Bath Sample Slag Sample		0.150	
			8.00	" "		0.142	
			8.11	" "		0.110	
			8.25	" "	1594	0.100	1 cwt.Fe Mn. 2 cwt. Fe Si fed.
			8.35				TAPPED.

IV.

HEAT LOG B.O.H. HEAT 6.

Charge Composition.	Tons.	Cwts.	Time	Sample	Temperature °C.	[C]	Remarks.
Scrap	49	11					
Pig	28	5					
Soft Billet C485.			6.30 p.m.	Premelt Sample		0.087	
				Slag Sample			
			6.45				25cwt. pig charged.
			7.10				20cwt. pig and 6cwt FeSi charge
			7.15				7cwt. Burnt Lime fed. d
			7.30				1cwt. Fluorspar fed.
			7.35	Bath Sample		0.41	
				Slag Sample			
			7.45				10cwt. pig, 7cwt.Burnt lime fed
			8.00	Bath Sample		0.412	
				Slag Sample			
			8.05				10cwt.Burnt Lime, 1cwt Fluor-
			8.25	Full melt	1522	0.341	12cwt. Lime fed. spar.
			8.35	Bomb Sample 6(1)		0.310	
				Slag Sample			
			8.40				1cwt. Fluorspar.
			8.45	Bath Sample		0.280	
				Slag Sample			
			8.50	Bomb Sample 6(2)	1550	0.257	
				Slag Sample			
			8.55				10cwt.Burnt Lime, Furnace door removed for repair.
			8.58				New door fitted.
			9.05	Bath Sample		0.26	
				Slag Sample			
			9.12				10cwt.Lime, 4cwt.Scale charged.
			9.15	Bath Sample		0.21	
				Slag Sample			
			9.25	Bomb Sample 6(3)	1583	0.188	
				Bath Sample		0.188	
				Slag Sample			
			9.34	Bath Sample		0.161	3cwt.lime, & 2cwt Scale fed.
				Slag Sample			
			9.55	Bath Sample		0.091	1cwt. FeMn, 2 cwt. FeSi.
			10.00				TAPPED.

HEAT LOG B.O.H. HEAT 7.

Charge Composition	Tons.	Cwts.	Time	Sample	Temperature °C.	[C]	Remarks.
Scrap	51	0					
Pig	27	4					
			5.05 a.m.	Premelt Sample Slag Sample.		0.840	
			5.45	Bath Sample	1520	0.605	
				Bomb Sample 7(1) Slag Sample		0.605	
			5.53				10 cwt. Lime charged.
			5.55				7 cwt. scale charged.
			6.10	Bath Sample Slag Sample		0.470	
			6.30	Bath Sample Slag Sample	1552	0.407	
			6.35				12 cwt.Scale and 10 cwt.Burnt Lime. charged.
			6.50	Bath Sample Slag Sample		0.270	1½ cwt. Fluorspar.
			7.00				5 cwt. Lime and 5 cwt.scale fed.
			7.10	Bath Sample Slag Sample	1568	0.195	
			7.10	Bomb Sample 7(2) Slag Sample.			Bad sample.
			7.30	Bath Sample Slag Sample	1605	0.142	
			7.40	Bath Sample Slag Sample		0.117	1 cwt. Fe Mn. 2 cwt. Fe Si.
			7.50				TAPPED.

HEAT LOG B.O.H. HEAT 8.

Charge composition.	Tons.	Cwt.	Time	Sample	Temperature °C.	[C]	Remarks.
Scrap	50	15					
Pig	26	8					
			5.35p.m.	Premelt Sample Slag Sample		1.08	
			6.00				1 cwt. Fluorspar fed.
			6.30	Bath Sample (melt out)		0.631	
				Bomb Sample 8(1) Slag Sample.	1525		
			6.40				12 cwt. Scale fed.
			7.00	Bath sample Slag Sample	1565	0.421	
			7.05	Bomb sample 8(2) Slag Sample.			Bad sample.
			7.10				6 cwt.burnt lime and 5 cwt.scale fed.
			7.12				1 cwt. Fluorspar fed.
			7.25	Bath sample Slag sample	1590	0.245	7 cwt. burnt lime.
			7.45	Bath sample Slag sample	1603	0.181	
			7.45	Bomb sample 8(3) Slag sample		0.172	
			7.50				1 cwt. Fluorspar.
			8.05	Bomb sample 8(4) Slag sample.		0.123	
			8.10	Bath sample Slag sample.			1 cwt. Fe Mn and 2 cwt. FeSi charged.
			8.20		1610		
			8.27	Tapping Sample		0.097	

HEAT LOG B.O.H. HEAT 9.

Charge composition.	Tons.	Cwt.	Time	Sample	Temperature °C.	[C]	Remarks.
Scrap	50	6					
Pig	27	1					
			3.42 a.m.	Premelt Sample Slag Sample.			
			4.20	Bath Sample Slag Sample		0.365	9 cwt. Burnt Lime charged.
			4.40				Box of pig charged.
			4.57				1 cwt. Fluorspar fed.
			5.15	Bath sample Slag Sample		0.450	
			5.20				Box of Pig added.
			5.35	Bath sample Slag Sample.		0.505	
			5.36	Bomb Sample 9(1) Slag Sample	1530	0.505	
			5.40				1 cwt. Fluorspar fed.
			5.55	Bath Sample Slag Sample.		0.480	1/2 box lime added.
			6.20	Bath Sample		0.308	3 cwt. lime.
				Bomb Sample 9(2) Slag Sample	1594	0.308	
			6.40	Bath Sample Slag Sample		0.195	
			7.00	Bath Sample		0.128	
				Bomb Sample 9(3) Slag Sample			
			7.10	Bath Sample Slag Sample.		0.120	2 cwt. Fe Si charged.
			7.15				TAPPED.

VIIA.

HEAT LOG B.O.H. HEAT 10.

Charge Composition.	Tons.	Cwts.	Time	Sample	Temperature °C.	[C]	Remarks.
Scrap	48	7					
Pig	28	0					
Soft Billet B498			2.15 p.m.	Premelt Sample Slag Sample		0.980	
			2.45	Bath Sample Slag Sample		0.747	Clear melt.
			2.52	Bomb Sample 10(1) Slag Sample	1520	0.702	
			2.55				10 cwt.burnt lime and 20 cwt.scale fed.
			3.20	Bath Sample Slag Sample		0.446	
			3.23		1550		
			3.25	Bomb Sample 10(2) Slag Sample		0.405	10 cwt. lime fed.
			3.30				12 cwt. scale fed.
			3.45	Bath Sample Slag Sample		0.255	
			3.46				10 cwt.burnt lime, 3 cwt.fluorspar
			4.00	Bath Sample Slag Sample	0	0.210	[charged.
			4.01				10 cwt.lime, 3 cwt.scale added.
			4.10	Bath Sample Slag Sample		0.181	
			4.13	Bomb Sample 10(3) Slag Sample	1580	0.175	
			4.15				10 cwt.lime, 2 cwt.fluorspar added.
			4.20	Bath Sample Slag Sample		0.160	
			4.25		1575		2 cwt. Fluorspar.
			4.40	Tap Sample		0.134	1 cwt. Fe Mn, 2 cwt. Fe Si added.
			4.41				TAPPED.

HEAT LOG B.O.H. HEAT 11.

Charge Composition.	Tons.	Cwts.	Time	Sample	Temperature °C.	[C]	Remarks.
Scrap	48	6					
Pig	28	5					
Soft Billet C501			11.30 p.m.				Foaming strongly but boil breaking through.
			12.15 a.m.				Much better. Boiling quite strongly.
			12.30	Premelt Sample Slag Sample.		0.78	
			12.47				Cleared quite nicely, foaming almost gone.
			12.52	Bath Sample Slag Sample.			
			1.00	Bomb Sample 11(1)	1550	0.576	
				Bath Sample		0.576	
				Slag Sample			
			1.07				10 cwt. lime charged. Burnt.
			1.10				8 cwt. scale fed.
			1.25	Bath Sample Slag Sample		0.434	
			1.30		1580		10 cwt. burnt lime.
			1.35				6 cwt. scale.
			1.55				4 cwt. Fluorspar.
			2.10	Bath Sample		0.237	
				Bomb Sample 11(2)	1600	0.237	
				Slag Sample			
			2.16				5 cwt. Lime, 2 cwt. scale charged.
			2.30	Bath Sample Slag Sample		0.142	
			2.34				3 cwt. Scale fed.
			2.45	Bath Sample Slag Sample		0.101	
			2.52	Bomb Sample 11(3) Slag Sample		0.075	
			2.55	Tap Sample		0.068	

HEAT LOG. B.O.H. HEAT 12.

Charge Composition.	Tons.	Cwts.	Time	Sample	Temperature °C.	[C]	Remarks.
Scrap	48	17					
Pig	27	19					
Soft Billet C504							Foaming commenced at 8.20 a.m. and continued until 10.30.
			9.00 a.m.				3/4 cwt. high grade FeSi
			9.45	Premelt Sample Slag Sample.		1.20	Still light foam.
			10.05				Unmelted scrap still present. Attempt to break down with charger. Foam down.
			10.25				Foaming started again.
			10.40				Foam down.
			10.50				Almost clear melt.
			10.55	Bath Sample Bomb Sample 12(1) Slag Sample	1540	0.720 0.720	
			11.10				Boil coming through.
			11.15				Steady boil.
			11.25	Bath Sample Bomb Sample 12(2) Slag Sample		0.589	Bad sample rejected.
			11.27				14 cwt. lime fed.
			11.44	Bath Sample Slag Sample		0.329	
			11.51	Bomb Sample 12(2) Slag Sample	1573	0.300	
			11.57				7 cwt. lime charged.
			12.00				3 cwt. spar fed.
			12.05 p.m.	Bath Sample Slag Sample		0.213	
			12.10				Lime Boil.
			12.11				10 cwt. lime fed.
			12.12				2 cwt. Fluorspar fed.
			12.20	Bath Sample Bomb Sample 12(3) Slag Sample	1593	0.196 0.196	

XI.

HEAT LOG B.O.H. HEAT 12 (Cont'd).

Charge Composition.	Tons.	Cwts.	Time	Sample	Temperature °C.	[C]	Remarks.
Scrap	48	17					
Pig	27	19					
Soft Billet C504							
			12.29				5 cwt. lime fed.
			12.50	Bath Sample	1608	0.117	
				Bomb Sample 12(4)			
				Slag Sample			
			12.55	Bath Sample		0.104	1 cwt. FeMn, 2 cwt. FeSi charged.
				Slag Sample			
			1.05				TAPPED.

HEAT LOG B.O.H. HEAT 14.

Charge Composition.	Tons.	Cwts.	Time	Sample	Temperature °C.	[C]	Remarks.
Scrap	46	16					
Pig.	29	5					
			6.15 a.m.	Premelt Sample		0.705	Boiling vigorously but still bank of unmelted material.
				Slag Sample			
			6.50	Bath Sample		0.355	Slag thin and watery.
				Slag Sample		check 0.352	
			7.00				1 Box Pig Iron charged.
			7.10				Slag thickening up.
			7.20				1 Box Pig Iron, 10 cwt.lime charged.
			7.25				Clear melt.
			7.40	Bath Sample	1545	0.406	
				Bomb Sample 14(1)			
				Slag Sample			
			7.45				10 cwt. burnt lime.
			8.00				Boiling freely.
			8.15	Bath Sample		0.273	
				Bomb Sample 14(2)		0.273	
				Slag Sample			
			8.23		1586		
			8.25				5 cwt. scale fed.
			8.30				4 cwt. burnt lime.
			8.43	Bath Sample	1586	0.183	
				Bomb Sample 14(3)		0.177	
				Slag Sample			
			9.00				4 cwt. burnt lime.
			9.10	Bath Sample		0.136	
				Slag Sample			
			9.20	Bath Sample		0.125	
				Slag Sample			
			9.25	Bomb Sample 14(4)	1597	0.115	1 cwt. FeMn, 2 cwt. FeSi charged.
				Bath Sample		0.115	
				Slag Sample			
			9.34				TAPPED.

HEAT LOG A.O.H. HEAT A.

Charge Composition.	Tons.	Cwts.	Time	Sample	Temperature °C.	[C]	Remarks.
Scrap	34	7					
Pig	13	7					
Shafting.			8.30 a.m.				Melt Out.
			9.20				11.5 cwt. lime fed.
			10.00	Bath Sample Bomb Sample A(1) Slag Sample.	1620	0.740 0.740	
			11.00				End of Ore addition (15 cwt.) started at 8.30.
			11.30	Bath Sample Bomb Sample A(2) Slag Sample.	1630	0.330	6 cwt. Ore added between 11.00 and 11.30.
			12.30 p.m.	Bath Sample Bomb Sample A(3) Slag Sample.	1635	0.224	4 cwt. ore fed between 11.30 and 12.30
			13.30	Bath Sample Bomb Sample A(4) Slag Sample.	1625	0.170	TAPPED AFTER ADDITIONS.

HEAT LOG A.O.H. HEAT B.

Charge Composition.	Tons.	Cwts.	Time	Sample	Temperature °C.	[C]	Remarks.
Scrap	42	6					
Pig	21	4					
Foundry Heat			11.45 a.m.				Melt out.
			12.05 p.m.	Bath Sample Bomb Sample B(1) Slag Sample.	1615	0.960	
			12.10				16.25 cwt. lime charged.
			12.40				12 cwt. ore between 11.45 and 12.40
			14.00				20 cwt. ore between 12.40 and 14.00 .
			14.40	Bath Sample Bomb Sample B(2) Slag Sample.	1645	0.405	
			15.00				12 cwt. ore between 14.00 and 15.00.
			15.30	Bath Sample Bomb Sample B(3) Slag Sample.	1645	0.250	
			15.50				1 cwt.ore between 15.00 and 15.55
			16.20	Bath Sample Bomb Sample B(4) Slag Sample.	1645	0.123	TAPPED AFTER ADDITIONS.

HEAT LOG A.O.H. HEAT C.

Charge Composition.	Tons.	Cwt.	Time	Sample	Temperature °C.	[C]	Remarks.
Scrap	41	16					
Pig.	21	4					
Foundry Heat.			10.00 a.m.				Melt out.
			11.30	Bath Sample Bomb Sample C(1) Slag Sample.	1618	0.669	
			12.10 p.m.				16¼ cwt. lime fed.
			12.30	Bath Sample Bomb Sample C(2) Slag Sample.	1630	0.360	50 cwt. ore added between 10.00 and 12.30
			13.30	Bath Sample Bomb Sample C(3) Slag Sample.	1644	0.220	TAPPED AFTER ADDITIONS.

HEAT LOG A.O.H. HEAT E.

Charge Composition.	Tons.	Cwt.	Time	Sample	Temperature °C.	[C]	Remarks.
Scrap	47	1					
Pig	22	14					
Shafting.			8.00 a.m.	Bath Sample Bomb Sample E(1) Slag Sample.	1590	1.100	
			8.30				17.75 cwt. lime added.
			10.15				46 cwt. ore added between 8.00 and 10.15.
			10.45	Bath Sample Bomb Sample E(2) Slag Sample.	1634	0.515	6 cwt. ore added between 10.15 and 10.45
			11.40				8 cwt. ore added between 10.45 and 11.40.
			11.50	Bath Sample Bomb Sample E(3) Slag Sample.	1636	0.393	
			12.30	Bath Sample Bomb Sample E(4) Slag Sample	1630		2 cwt. ore added between 11.40 and 12.30 TAPPED AFTER ADDITIONS.

HEAT LOG. A.O.H. HEAT F.

Charge Composition.	Tons.	Cwt.	Time	Sample	Temperature °C.	[C]	Remarks.
Scrap	43	11					
Pig	29	14					
Marine Rotor			13.00	Meltout Sample	1580		
			13.55				19 cwt. lime charged.
			16.30				55 cwt. ore fed between 13.00, and 16.30
			16.40	Bath Sample Bomb Sample F(2) Slag Sample.	1640	0.620	
			17.30	Bath Sample Bomb Sample F(3) Slag Sample.	1650	0.390	8 cwt. ore added between 16.30 and 17.30.
			18.05	Bath Sample Bomb Sample F(4) Slag Sample.	1630	0.360	
			18.35	Bath Sample Bomb Sample F(5) Slag Sample.	1600	0.350	TAPPED AFTER ADDITIONS.